UNIVERSITY OF SOUTHAMPTON

FACULTY OF PHYSICAL AND APPLIED SCIENCES

Electronics and Computer Science

Dynamic and game theoretic modelling of societal growth, structure and collapse

by

Sabin Roman

Thesis for the degree of Doctor of Philosophy

January 2018

UNIVERSITY OF SOUTHAMPTON

ABSTRACT

FACULTY OF PHYSICAL AND APPLIED SCIENCES
Electronics and Computer Science

Doctor of Philosophy

DYNAMIC AND GAME THEORETIC MODELLING OF SOCIETAL GROWTH, STRUCTURE AND COLLAPSE

by Sabin Roman

The dynamics and structure of societies have long been a puzzle to archaeologists, historians and social scientists in general. In particular, increases in social inequality and the possibility of societal collapse are two deeply distressing prospects for any society. In this three paper thesis we provide two contributions to the literature of societal collapse and one regarding the emergence of social inequality.

In the first article we present a mathematical model of Easter Island and show that the collapse can be modelled as a supercritical Hopf bifurcation where the critical parameter is the harvesting rate of resources. This suggests an universal mechanism by which societal collapse can be understood quantitatively. In addition, we show that societies coupled together can be more robust against collapse, which means that, within a larger region of parameter space, a sustainable outcome can occur for both societies than in the case when the societies are isolated. In particular, if at least one society has a harvesting rate below the critical value, then collapse can be prevented for the entire system.

In the second article we build a dynamical system model of the Maya civilisation taking into account the main specialisations of the population: swidden and intensive agriculturalists, and monument builders. The archaeological record for population growth and monument construction is accurately reproduced, with the model calibration close to archaeologically determined values for the parameters. We show that if, after the year 550 CE, a significant part of each new generation moved from swidden to using intensive agricultural methods, then this would explain the rapid population growth and the subsequent collapse. This conclusion is reached irrespective of the impact of drought. Furthermore, the model is shown to also undergo a supercritical Hopf bifurcation when the harvesting rate is high. An extensive sensitivity analysis indicates that the model predictions are robust under parameter changes, which means that the period around the year 550 CE played a key role in the collapse.

In the third article we address the issue of social inequality by considering games on networks. In contrast to large parts of the literature, we investigate for what network structure a system of linked agents can exhibit maximally rational strategic behaviour. The agent's strategies are quantified through the quantal response equilibrium, and the network is optimised so that the strategies are as close as possible to the Nash equilibrium. Previous work has argued that a scale-free topology maximises system rationality. In contrast, we show that a core-periphery structure emerges, where a small set of nodes enjoy higher degrees than the majority, which are leaf nodes. In symmetric games the difference in degrees between the two node types are stark, whereas in asymmetric games the difference is less notable.

Taken together, the different parts of this thesis highlight and explain dynamical and large-scale structural features in societies as seen throughout the history of the world. Thus, this work can help deepen our understanding of complex social phenomena.

UNIVERSITY OF Southampton

Academic Thesis: Declaration Of Authorship

I, Sabin Roman

declare that this thesis and the work presented in it are my own and has been generated by me as the result of my own original research.

Dynamic and game theoretic modelling of societal growth, structure and collapse

I confirm that:

1. This work was done wholly or mainly while in candidature for a research degree at this University;
2. Where any part of this thesis has previously been submitted for a degree or any other qualification at this University or any other institution, this has been clearly stated;
3. Where I have consulted the published work of others, this is always clearly attributed;
4. Where I have quoted from the work of others, the source is always given. With the exception of such quotations, this thesis is entirely my own work;
5. I have acknowledged all main sources of help;
6. Where the thesis is based on work done by myself jointly with others, I have made clear exactly what was done by others and what I have contributed myself;
7. Either none of this work has been published before submission, or parts of this work have been published as:

    - Coupled Societies are More Robust Against Collapse: A Hypothetical Look at Easter Island, Ecological Economics, Volume 132, Pages 264-278, 2017, Sabin Roman, Seth Bullock and Markus Brede
    - The Dynamics of Human-Environment Interactions in the Collapse of the Classic Maya, Ecological Economics, Volume 146, Pages 312-324, 2018, Sabin Roman, Erika Palmer and Markus Brede
    - Topology-dependent rationality and quantal response equilibria in structured populations, Physical Review E 95, 052310, 2017, Sabin Roman and Markus Brede

Signed:

Date: 8 January 2018

Acknowledgements

Thank you to my supervisors, Dr. Markus Brede and Prof. Seth Bullock, for their guidance throughout the doctoral program. I appreciate and thank the Institute for Complex Systems Simulation (ICCS) for offering an environment where novel ideas can be pursued. Thanks to my collaborator from the University of Bergen, Erika Palmer for her help and support. And thank you to Iulia-Tania Andronache and Garvin Haslett for help in proof reading the document.

Preface

The thesis is structured according to the three paper format. Each paper represents an independent contribution but they all address long-standing problems regarding societal structure and function.

The introduction highlights the themes of the three papers and provides a literature review of the main topics addressed in the thesis, as recommended by the official guidelines. The conclusion summarises the main findings and outlines possible future research directions.

Appendix A provides a review of the most common theories regarding the collapse of societies. The other appendices complement the papers with analytical and numerical results that strengthen the main findings of the papers. All the appendices are places at the end of thesis, as stipulated by the official guidelines.

List of publications and conferences

First authored papers

- Coupled Societies are More Robust Against Collapse: A Hypothetical Look at Easter Island, *Ecological Economics, Volume 132, Pages 264-278, 2017*, Sabin Roman, Seth Bullock and Markus Brede
- The Dynamics of Human-Environment Interactions in the Collapse of the Classic Maya, *Ecological Economics, Volume 146, Pages 312-324, 2018*, Sabin Roman, Erika Palmer and Markus Brede
- Topology-dependent rationality and quantal response equilibria in structured populations, *Physical Review E 95, 052310, 2017*, Sabin Roman and Markus Brede

Conferences

- *Conference on Complex Systems*, Cancun, Mexico, September 2017, delivered two presentations: "Topology-dependent rationality and Quantal Response Equilibria in structured populations" and "Dynamical system modelling of human-environment interactions: the case of the Classic Maya collapse"
- *International Conference on Statistical Physics (SigmaPhi)*, Corfu, Greece, July 2017, delivered two presentations: "Topology-dependent rationality and Quantal Response Equilibria in structured populations" and "Dynamical system modelling of human-environment interactions: the case of the Classic Maya collapse"
- *Workshop on Economic Science with Heterogeneous Interacting Agents*, Milan, Italy, June 2017, delivered presentation: "Topology-dependent rationality and Quantal Response Equilibria in structured populations"
- *Conference on Complex Systems*, Amsterdam, Netherlands, September 2016, delivered two presentations: "Coupled societies are more robust against collapse: a hypothetical look at Easter Island" and "Topology-dependent rationality and Quantal Response Equilibria in structured populations"
- *60th anniversary of Robert MacKay Conference*, Warwick University, UK, May 2016, presented poster: "Resilience of Networked Societies"
- *Winter School on Complex Systems*, Madrid, Spain, January 2016, delivered tutorial: "Modelling the Macro-dynamics and Collapse of Societies"
- *Student Conference on Complex Systems*, Granada, Spain, September 2015, delivered presentation: "Resilience of Networked Societies"

- *International Conference on Computational Social Science*, Helsinki, Finland, June 2015, presented poster:"Resilience of Networked Societies"
- *Student Conference on Complex Systems*, Brighton, UK, August 2014, presented poster: "Intersocietal extensions of the Human and Nature Dynamics (HANDY) model"

Contents

Chapter 1

Introduction

1.1 Motivation and aims

1.1.1 Modelling of societal dynamics

The large scale dynamics of societies has presented many questions for historic and scientific inquiry, in particular the phenomenons of societal collapse and the emergence of social inequality. History provides us with a multitude of examples where societies have failed to solve the problems they faced and collapsed, e.g., Easter Island, the Lowland Classic Maya, the Western Roman Empire, the Egyptian Old Kindom, the Minoan and Mycenaean civilisations (Tainter, 1988; Butzer and Endfield, 2012). Hence, societal collapse is a recurrent phenomenon that has been taking place at least since the agricultural revolution (Diamond, 2005) and the archaeological record provides accounts of these historical "experiments".

The collapse of past societies is associated with a loss of economic functions, of centralised control, of trading relations, of investment in cultural property such as literary, artistic or architectural work, and is also often accompanied by a significant loss of life (Tainter, 1988). Thus, it represents a traumatic process that a society can undergo and, given its characteristics, is generally undesirable. The topic of societal collapse is highly relevant to the contemporary world, as the modern, global society is pushing environmental boundaries and leaving the safe operating space it once found itself in (Rockström et al., 2009). Climate change, resource depletion (of oil, phosphorus, water etc.), deforestation and species extinction pose great challenges to modern society that make us question its long-term sustainability and give us reasons to worry about a potential collapse (Turner, 2012). Given that a collapse would entail a loss of life, culture and modern amenities, it is a worthwhile pursuit to seek and understand the phenomenon through past cases of societies that have collapsed.

Understanding why and how the collapse of past societies takes place can provide unique insights into our present condition (Costanza et al., 2007b). Past societies that have collapsed offer test cases in geographically restricted and temporarily limited conditions that allow us to quantify and understand their socio-environmental relationships. The aim of the research presented here is to construct mathematical and computational models of societal structure and dynamics, focusing in particular on two historical cases of collapse: Easter Island and the Classic Maya.

There have been numerous studies that address societal collapse within the field of archeology, see the work of Tainter (1988) and references therein, but also from an ecological perspective (Costanza et al., 2007b). But, with few exceptions, the topic has been approached from a mostly qualitative perspective, which presents arguments in a narrative form without a mathematical understanding of the underlying dynamics. In some cases, even an aversion to quantitative models has been manifested (Tainter, 2004). The argument invoked by Tainter (2004) says that quantitative models are inadequate to capture the full scope of societal complexity and the underlying drivers of its evolution. Turchin (2003b, p. 1) disagrees and argues that "a discipline usually matures only after it has developed mathematical theory", especially if the discipline deals with dynamical quantities. Informal verbal models are appropriate if the underlying mechanisms are sufficiently simple (acting in a linear and additive manner), but generally misleading if the system exhibits non-linear feedbacks and time lags (Turchin, 2003b; Sterman, 2000).

Casting hypotheses into quantitative models can thus help in illuminating uncertainties regarding the system, expose prevailing wisdom as incompatible with available data, guide data collection or discover new questions (Epstein, 2008). Mathematical models can thus be "indispensable when we wish to rigorously connect the set of assumptions about the system to predictions about its dynamics behavior" (Turchin, 2003b, p. 4). The use of quantitative models to test the validity of hypotheses has not been common in the historical social sciences, and in recent years a new field called "cliodynamics" has emerged to tackle this issue (Turchin, 2008). The work presented here on societal collapse is an application of quantitative methods, in particular dynamical systems modelling, to encapsulate simple hypotheses about the drivers of collapse. Specifically, we capture some key socio-environmental feedbacks that prove sufficient in explaining the long-term behaviour of the societies we investigate. Thus, if simpler hypotheses are enough to explain the archaeological record, this then challenges or at least questions the complex narratives that have been put forth by archaeologist or historians regarding the societies in question.

In cases where quantitative models have been developed, such as world integrated models (Costanza et al., 2007a) or agent based models (Axtell et al., 2002; Heckbert, 2013), there has been a tendency to develop very complex models that capture as many environmental and social features as possible. Prominent models include the IPCC models on climate change (Flato et al., 2013), the World3 model of Limits to growth (Meadows et al.,

2004), the GUMBO model (Boumans et al., 2002) and several others (Costanza et al., 2007b). Human behaviour and the multitude of relationships and processes the models attempt to capture are, arguably, not well understood individually either and, given the complexity of the systems, separating the different parts and effects might not be feasible or possible (Corning, 1998). Thus, these efforts again run against problems with validation, as disentangling the different effects is prohibitive.

Much simpler mathematical models have also been employed to explain societal dynamics and collapse, such as in the work of Hamblin and Pitcher (1980) on the Maya civilisation and of Brander and Taylor (1998) on Easter Island. But these models can fail to meaningfully capture societal structure (Lowe, 1982) or do not reproduce known historical trends (Erickson and Gowdy, 2000). Thus, searching for models at a mesoscopic scale of intermediate complexity can be advantageous, as sufficient societal elements can be accounted for to reproduce known data but also keeping the model manageable to understand analytically and communicate more easily.

Furthermore, most models of societal dynamics focus on one particular system in isolation. The literature that addresses how multiple societies can interconnect and interact is scarce (Roman et al., 2017). The issue of how the sustainability of multiple, connected regions is affected by their individual characteristics has been rarely explored, and in cases where such a study was undertaken (Anderies and Hegmon, 2011) no noticeable deviation from the independent case was seen. Also, no previous study has analysed the most basic coupling of socio-environmental systems, namely through simple diffusion.

Our models for the Easter Island and the Maya societies have been developed with the goals of tractability and realism in mind. The models incorporate sufficiently many details of the societies in question that the existing archaeological record can be reproduced. But, they are also simple enough to be analytically tractable and general insights on the nature of societal collapse can be obtained. In addition, we have explored how two coupled socio-environmental systems can evolve depending on their resource extraction rates. We analysed two different types of coupling, including simple diffusion, and we found significant differences compared to when the societies are isolated.

1.1.2 Games on networks

Another common pattern observed throughout time for many societies has been the existence of social structure manifesting a high degree of inequality between individuals. Understanding how social (in particular economic) inequality appears and persists has been a long-standing problem in the social sciences (Kuznets, 1955). Recent decades have seen a increase in social and economic inequality worldwide (Piketty, 2014). Societies with high degrees of inequality also have higher death rates (Wilkinson, 2002), less social cohesion as measured by the civic participation score (Lancee and Van de Werfhorst,

2012) as well as more mental health problems; examples in the latter case include status anxiety (Layte and Whelan, 2014), depression (Layte and Whelan, 2014) and a rise in narcissistic tendencies (Wilkinson and Pickett, 2017). While these associations are not necessarily causal, they are sufficient to warrant concern if inequality (e.g., as measured through the Gini index) is increasing. Thus, understanding how inequality can arise is important to be able to manage or decrease it within society.

Applying game theory on complex networks can give insights into the large scale structure of the relationships between socio-environmental agents. In particular, it has provided a variety of mechanisms by which inequality can emerge between agents (Gross and Blasius, 2008), but this literature has yet to consider agent rationality explicitly, at least in the context of the quantal response equilibrium (McKelvey and Palfrey, 1995). We build on previous work to investigate social structure through game theory on networks, looking at the quantal response equilibrium for agents that posses a quantified degree of rationality, and we develop an optimisation procedure by which highly unequal states can emerge. More generally, we can obtain insights into the emergence of heterogeneous social structures and hierarchy through the modelling of both network features and peer to peer interactions.

Methodologically, our work falls in the network optimization literature (i Cancho and Solé, 2003), but similar results to our own have also been found in the context of adaptive coevolutionary networks (Gross and Blasius, 2008; Perc and Szolnoki, 2010). The appearance of division of labour and of class structures is a common pattern observed in the network optimisation literature (Holme and Ghoshal, 2006; Brede, 2010a; Guttenberg and Goldenfeld, 2010; Peixoto and Bornholdt, 2012; Mahault et al., 2017) and coevolutionary networks (Ito and Kaneko, 2001, 2003; Zimmermann et al., 2004; Zimmermann and Eguíluz, 2005; Eguíluz et al., 2005), but the research up to now has not dealt with quantifying rationality on networks. By assigning varying degrees of rationality to agents depending on their status in the network, we are able to see how the topology of the network evolves to facilitate higher (or perfect) rationality. Previous work (Kasthurirathna et al., 2016b) has argued that scale-free networks maximise the system's rationality. In contrast with this result, but more consistent with the general literature, we show that a network that admits two classes of nodes (of higher and lower connectivity) maximises the system's rationality.

1.1.3 Common themes and chapter outline

The research presented here focuses on the topics of societal collapse and the emergence of social inequality. Both topics naturally refer to large-scale social organisation and behaviour. Methodologically, Chapters 2 and 3 use dynamical systems to specify the models for the collapse on Easter Island and the Maya civilisation. The analysis of the models is also carried out according to dynamical system's theory. Quantifying the

effect of network structure on internal node dynamics is another common theme in our work. The Easter Island model is extended to consider the simplest possible network, consisting of one edge. Despite the simplicity of this network structure, the effects on the internal dynamics of the nodes are significant. Chapter 4 is dedicated to exploring an optimisation algorithm applied on networks, wherein the topology of the network directly affects the node behaviour.

Another unifying theme of the present work is the subject of rationality (or lack thereof) of human behaviour. In our game-theoretic network model of Chapter 4, the degree of rationality (or irrationality) of the different agents is explicitly modelled, whereas in the dynamical models of Chapter 2 and Chapter 3 the issue of rationality is implicit but nevertheless important. Despite the unsustainable path past and present societies can find themselves on, a certain inertia in changing the course of their evolution can be seen, e.g., the case of shifting from fossil fuel for our modern world, also known as carbon lock-in (Unruh, 2000). This phenomenon highlights a potentially high degree of irrationality found in larger social systems, commonly referred to as the sunk-cost fallacy (Janssen et al., 2003; Janssen and Scheffer, 2004).

The rest of this chapter provides a literature review of mathematical models that pertain to societal growth and collapse, and of the game theoretic results on networks regarding class formation. The literature on modelling societal dynamics can be further divided into models of high or low complexity, and we dedicate a section for each category. The work pertaining to games on networks also falls in two categories: coevolutionary networks, where the topology adapts in response to local dynamics, and optimisation, where the network structure is changed to minimise or maximise a certain objective function. In the final section we provide a synopsis of the main contributions of the thesis.

1.2 Dynamic modelling of societal growth and collapse

The large-scale, long-term development of numerous complex societies, such as the Lowland Classic Maya civilisation, the Western Roman Empire, The Egyptian Old Kingdom, The Minoan civilisation, the Mesopotamian civilisations and the Anasazi, ended in collapse. Thus, any study that aims to understands and model the long-term dynamics of societies should account for the recurrent historical phenomenon of societal collapse. In this section we review the literature that models the long-term developments of societies and, in particular, their collapse.

According to Tainter (1988), collapse is a rapid and significant loss of an established level of socio-political complexity of a society. A complex society usually exhibits (Tainter, 1988): a degree of social stratification and differentiation, specialisation of economic

functions and occupations at the individual, group and territorial level, centralised control i.e. elites that regulate and integrate economic and political activity, regimentation and behavioural control (e.g., rule of law), investment in cultural property (e.g., monumental architecture, literary and artistic creation etc.), information flow between individuals (e.g., education), between economic and political groups, and between centralised structures and the periphery, trading and redistribution of resources, general coordination and organisation of individuals and groups and a single political unit which integrates an extended territory. Practically, collapse is signalled by (or has been associated with) the disappearance or significant decline in these indicators of complexity. Within the scope of our present research we identify societal collapse with a significant decline in the population of a society within a short timespan. A population crash is not a necessary condition for a society to collapse, as can be seen in the case of the Roman Empire (Van der Leeuw and de Vries, 2003), but it is a sufficient condition due to the loss of the underlying support structure of the more complex social constructs.

Our treatment of the topic is not archaeological in focus, but rather mathematical and computational. We detail some of the main archaeological theories regarding collapse in Appendix A. Hence, we focus mostly on the research that pertains to the quantitative analysis of long-term societal development and collapse. The quantitative modelling literature can be divided into the following areas of inquiry:

1. Large-scale models that attempt to capture multiple socio-environmental factors in a fine-grained fashion. These models fall in two broad classes:

   (a) Agent based models (ABMs), which represents individuals (or communities) as agents with set attributes and behavioural rules, such that a realistic rendering of relevant behaviour is desired with the aim of obtaining larger scale emergent phenomena. Often, they explicitly also model the spatially-extended features, such as terrain.

   (b) Integrated world models, which employ a wide variety of modelling techniques (dynamical systems, econometrics etc.) and aim for an accurate, detailed representation of the system under study. So, they are complex models that use a large number of variables and parameters.

2. Low-dimensional dynamical system models that consists of a set of coupled ordinary differential equations which represent in an aggregated way the dynamics of the system. The models generally fall into one of two methodological approaches:

   (a) Economic based models, in which individuals of the society are modelled as rational, utility-maximising agents. Typically, a utility function is chosen dependent on labour and land, and maximised under certain constraints. The relations that are obtained later inform the choice of dynamical system and parameters that give the societal dynamics.

(b) Ecologically inspired models, which employ functional forms used in ecology to build the dynamical system and do not rely on neo-classical assumptions of consumer behaviour. The choice of dynamical system in this case is made by attempting to match the model structure to a theoretical framework (sociological or archaeological) along with empirical observations and measurements.

Agent based models provide an alternative framework to the one we employ in the present work and it is worthwhile to contrast the different approaches. Integrated world models are some of the most ambitious attempts at comprehensively capturing socio-environmental factors, and their achievement thus form an important benchmark for our own work. Low dimensional models have most in common with our research, and represent a direct counterpart to our work in the present literature. In the next two sections we outline in detail the quantitative modelling literature.

1.2.1 Large-scale models

1.2.1.1 Agent based models

Early agent based models were formulated and implemented in the 1970's and 80's, of which we mention Schelling's model of racial segregation (Schelling, 1971), the iterated prisoner's dilemma (Axelrod and Hamilton, 1981) and Reynolds boids (Reynolds, 1987). In the 1990's the method expanded significantly and become widely applied to modelling social and economic phenomena. Of particular interest is the Sugarscape model (Epstein and Axtell, 1996) that is build up gradually, grows increasingly complex and more realistic phenomena start to emerge, like wealth inequality, trade relations and conflict. This example is an excellent illustration of the general, non-trivial and useful insights ABMs can provide by building social structure from the bottom-up.

There are several notable examples of agent based models (Kohler and van der Leeuw, 2007; Barceló and Del Castillo, 2016) that address the dynamics of past societies and human activity (trade, migration etc.). Arguably, the first significant effort in this sense is by Dean et al. (2000), Axtell et al. (2002) and Gumerman et al. (2003) who modelled the Kayenta Anasazi that lived in the Long House Valley in the Black Mesa area of north-eastern Arizona (U.S.) from about 1800 B.C. to 1300 A.D. The area is bounded topographically and there is ample geographical and historical data, which makes it well suited for multi-agent modelling. An agent is taken to be a typical household with five people on average. The model predicts well the population growth, the change in spatial settlement patterns and the collapse of the society. The fit of the model output to the archaeological record has helped popularise the work (Diamond, 2002; Janssen, 2009). But, Janssen (2009) reproduces the main findings of Axtell et al. (2002) and shows that the endogenous model dynamics make little contribution to the fit of

the aggregated archaeological record. Rather, the model mostly acts as a smoothing function for the input. Janssen (2009) finds that if the carrying capacity approximates the population levels this determines a good fit to the data, while parameters regarding the demographics are not so important. Janssen (2010) provides an alternative model for populations in ancient arid environments to investigate the role of climate variability. In contrast to Axtell et al. (2002), the different assumptions in the model of Janssen (2010) have a marked effect on temporal and spatial population dynamics. Janssen (2010) concludes that higher climate variability increased the resilience of ancient societies, which would have been more vulnerable to collapse otherwise.

Another agent-based model focuses on the Mayan civilisation (Heckbert, 2013) and proceeds in similar fashion to the above. It incorporates geographical and archaeological information and produces a spatial model of the south-west Yucatan peninsula, which we discuss in more detail in Chapter 3. Beyond the case of the Anasazi and the Maya civilisations, agent based models that aim to reproduce the archaeological records of complex, past societies are scarce. Effort in this area is directed more towards understanding prehistoric social dynamics and organisation (Barceló and Del Castillo, 2016).

Given the large number of parameters and the many specific modelling choices that have to be made when designing such a high-resolution model, the problem of validating it is quite difficult. How many other parameter values and design decisions are compatible with the output of the model? To what extent are these possible models equivalent and insightful about the actual historical behaviour, decisions and events? These questions cannot be answered in general and despite the significant effort put into developing a realistic ABM, the whole endeavour can be at risk of being a very sophisticated curve fitting exercise and provide little historical insight. Still, a variety of empirical approaches have been applied to ABMs and this has led to a continued debate regarding their validation (Windrum et al., 2007; Moss, 2008).

ABMs have been a relatively recent addition to the literature on modelling societal dynamics. Models formulated as dynamical systems (ODEs) have been the predominant type within the literature, starting with the "Limits to Growth" model, which is also the first instance of a integrated world model.

1.2.1.2 Integrated world models

The first major example of a mathematical model developed to account for collapse has not been for an ancient society, but actually for modern society. During the sustainability movement of the 1960's, the Club of Rome was established in 1968 by a group of economists and scientists with the goal to pursue a holistic understanding of and solutions to the world's major social and environmental problems (Ozbekhan, 1976). In

the mid 1950's, Prof. Jay Forrester at MIT developed system dynamics, a diagrammatic method to aid in developing large scale models consisting of differential equations (Forrester, 1961).

At the request of the Club of Rome, Forrester developed the World1 and World2 models (Forrester, 1971), which showcased some of the complex feedbacks that characterise modern industrial society. Eventually, the World3 model was developed which led to the "Limits to growth" (LTG) study (Meadows et al., 1972) that attempted to understand the development of society by taking into account a wide range of phenomena, including food production, pollution, economic well-being, population growth and industrial output. "Limits to growth" is based on the World3 model which consists of 16 state variables (e.g., population, pollution, arable land) and 80 fixed parameters. The time frame the model is concerned with is of 200 years, between 1900 and 2100. The study focused on 3 scenarios: a base case which used parameters that fitted best to historical data, an environmentally sustainable case and a technological driven, industry-intensive scenario. The first and latter cases led the a peak in industrial output sometime in the 21st century and subsequent decline in economic activity and demographic numbers. The sustainable case manages to reach a steady state for the system with little loss of life, but it required parameter choices that in the real world would correspond to drastic action to curtail pollution and population growth. Given its dire outlook, the LTG study has received significant amount of criticism from economists (Bardi, 2011), but in recent years the standard run of the model has been found to match well historical trajectories (Turner, 2008).

Since LTG was published several other models have been developed and aimed at integrating social, ecological and technological factors into a coherent whole to provide policy recommendations (Costanza et al., 2007b). The model by Mesarovic and Pestel (1974) is an extension of World3 and disaggregates the world into 10 regions, thus accounting for regional variation of parameters and dynamics. Despite the higher level of spatial resolution, the model had a much shorter time horizon that World3, only 50 years. The results mostly show upward curves in key variables and no decline in the short-term, very similar to World3 within the same timespan. Other world models, like IMAGE (Rotmans, 1990), IMAGE-2 (Alcamo et al., 1998) and TARGETS (Rotmans and de Vries, 1997) are significantly focused on ecological modelling and so, their emphasis is misaligned with our main concerns. Models such as IFs (Hughes, 1993) and GUMBO (Boumans et al., 2002) are formidable with regard to the amount of data inputs they require and their level of detail. They are comprehensive in the representation of the world but their level of complexity hinders their communication and use. In our work we aim to model long-term societal behaviour using low-dimensional mathematical structures that can accurately capture aggregate features. Of the above models, World3 is closest to our desired aims because it is the simplest of the world models and is built only using coupled sets of ordinary differential equations. Nevertheless, the number

of parameters and the complexity of the World3 model are still high, which make it counterproductive to understand its behaviour.

The modelling methodology of LTG, namely system dynamics, was also applied to the case of ancient Maya (Hosler et al., 1977). The model of Hosler et al. (1977) is by no means a world model but with 40 variables, it is comparable to World3 in complexity. The main result of the model is predicting a complete demographic collapse of the Lowland Classic Maya in the year 800. Nevertheless, the time-scales and specific dynamics in the model are questionable (Sharer, 1977). After the year 800, the model predicts a population of 10^{-36}, which is essentially zero, clearly at odds with the historical record that shows a rapidly decreasing, but still present population. As noted by Sharer (1977), the timescales and dynamics in the model output are not consistent with the actual data. Nevertheless, the model does capture certain relevant feedback mechanisms within the system and reproduces a rapid demographic decline. Its drawbacks, rather than discrediting the model, could just as well indicate contradictions in the understanding of the scientific community about the Maya at the time the model was proposed. Potential contradictions might not have otherwise been observed without the use of a quantitative model that tries to integrate several strands of knowledge.

Most other models focused on modelling societal structure and process have employed a more conservative approach in model scope and size. We detail these models next, with particular emphasis on work related to Easter Island and the Maya civilisation.

1.2.2 Low-dimensional dynamical systems

After the model by Hosler et al. (1977), a set of one-equation models was built by Hamblin and Pitcher (1980) to test the class-conflict hypothesis of the Maya collapse and alternative theories. The models are a drastic simplification from the previous modelling effort by Hosler et al. (1977) and attempted to gradually built a quantitative understanding of Maya civilisation (Lowe, 1982).

A broader trend started in the late 1990's to develop simple dynamical systems to model societal evolution. Renewed interested in the mathematical modelling of societal development (and collapse) was sparked by the work of Brander and Taylor (1998). The general premise is to represent humans as predators and resources (palm trees in this case) as prey, and develop a Lotka-Volterra type of system to model an isolated historical example of collapse, namely Easter Island. Two stocks are considered: the resources and the population. Resources are assumed to regenerate logistically. The rate at which the resources are harvested is determined based on neoclassical economic principles, in which the individuals of the society are seen as utility maximising, rational agents. The utility function of an individual is considered to be a Cobb-Douglass function of individual consumption of resources and manufactured goods, and is maximised under

certain budget constraints. Only the current utility is maximised, with no foresight assumed on the part of the agents. The optimal harvesting rate is determined to be proportional to the population and resource stock, i.e. the law of mass action as in a typical Lotka-Volterra model.

The modelling effort does have some shortcomings, one of which is that the minimum population levels that Brander and Taylor (1998) predict for the year 1500 A.D. actually corresponds closer to a maximum population in the archaeological record, according to Flenley and Bahn (2003). More details regarding the model and its fit to the archaeological record for Easter Island are provided in Chapter 2.

1.2.2.1 Economic based models

Several papers appeared following Brander and Taylor (1998) also employed the economic methodology and analysed how different factors, such property rights, technology or growth, could have impacted and possibly modified the outcome on Easter Island. These papers do not focus on improving the fit between the model prediction and the archaeological record, such as reconstructed by Flenley and Bahn (2003). Rather, they represent thought experiments on how different extensions of the model by Brander and Taylor (1998) behave. The models we review below study the effects of different institutional settings, of technical progress, what would happen if agents had foresight, of different resource dynamics and of conflict.

Dalton and Coats (2000), Pezzey and Anderies (2003) and Chakraborty (2007) have considered the effects of different institutional settings. Dalton and Coats (2000) introduce a parameter that models people's response to changes in expectations of future prices. A positive (negative) parameter implies that the society's institutions encourage people to harvest less (more) intensely in anticipation of higher future (lower) prices, which in turn has the effect of avoiding (intensifying) the collapse. Pezzey and Anderies (2003) considers four different institutions: one that taxes the collective resource consumption and three that cap the total extraction. In all cases, if the subsistence resource consumption in utility is small enough, then the collapse is prevented. Chakraborty (2007) introduces a tax to the extraction supply price and finds that a tax of 54% would suffice to avert the collapse.

Reuveny and Decker (2000) consider a different avenue to possibly avoiding the "Malthusian trap" on Easter Island, namely technical progress. The effect of this is to spur exponential growth in one of three aspects: the carrying capacity, the extraction rate of resource or the regeneration rate of renewable resources. They find that only the latter effect can avert collapse. Decker and Reuveny (2005) carry out similar research but with technical progress spurred on by resource scarcity, as expected by Boserup's theory (Boserup, 1965). Nevertheless, there is no significant difference from the findings of

Reuveny and Decker (2000). Anderies (2003) introduces a growth model incorporating Hicks neutral technical progress, but concludes that technological change is not as important in avoiding collapse as are demographic processes. Dalton et al. (2005) analyse Easter Island by taking into account the possibility of economic growth. Pre-modern societies experience little economic growth and were subject to feast-famine Malthusian cycles (Gailor and Weil, 2000). The model shows that economic growth in combination with strong property-rights institutions can help mitigate Malthusian cycles. Case in point, "property-rights regimes that favour biological growth rates over harvest rates tend to dampen feast-famine cycles, while those that favour harvest efficiency worsen such cycles" (Dalton et al., 2005, p. 31).

Good and Reuveny (2006) were the first to consider agents with foresight, that optimise taking into account future utilities. What they conclude is that even if the people of Easter Island had a complete assignment of property rights, implemented optimal resource management with infinite horizon, or had a social planner to perform such a task, a boom-bust cycle would still occur due to natural resource limitations, which could not have been fully substituted by capital. Good and Reuveny (2009) also introduce a social welfare function (SWF) given by the society's total utility. They conclude that, even with modern institutions, foresight and SWFs similar to today, it "... seems reasonable to assert that these collapses were socially optimal" (Good and Reuveny, 2009, p. 877). Good and Reuveny (2012) consider foresight along with technical progress but reach conclusions similar to Reuveny and Decker (2000).

Anderies (2000) argues that in the Brander and Taylor (1998) model the Cobb-Douglas utility function allows for unlimited substitution between goods without affecting utility, which is unrealistic in case of resource scarcity. To address this, Anderies (2000) introduces a subsistence requirement in the utility function which has the desired effect of reducing manufacturing when resources are low. Nagase and Mirza (2006) also tackle the issue of substitutability of natural and man-made goods and find that a decrease in the elasticity of substitution has negative effects on the population, resource stock and welfare. Janssen and Scheffer (2004) extend the model of Anderies (2000) by introducing a stock of manufactured goods, meant to measure the extent of sunk-costs effects of the society. The general finding is that large boom-bust cycles occur in the presence of sunk-costs. D'Alessandro (2007) investigates what happens when two different renewable resources are present and which can irreversibly disappear under a critical threshold. What is found is that multiple equilibria exist and there is a greater sensitivity to parameter changes than seen in previous literature. Similarly, but only considering one resource, Taylor (2009) extends Brander and Taylor (1998)'s model by adding a minimum resource threshold which, if it exceeds 30% of the carrying capacity, then extinction occurs.

Beyond the impact of different institutional settings, technical progress, foresight or various assumptions regarding resource dynamics, there has been considerable research

into economic models incorporating negative social change, such as fighting for resources (Maxwell and Reuveny, 2000; Reuveny and Maxwell, 2001; Prskawetz et al., 2003; Maxwell and Reuveny, 2005; Reuveny et al., 2011) or demographic rivalry (Faria, 2000; Horan et al., 2007; Ruseski and Quinn, 2007; de la Croix and Dottori, 2008). Given that war and conflicts are not the main focus of our research, we point the interested reader to the review by Reuveny (2012).

With regard to economic models of societal dynamics we can identify three weakness: (i) the fundamental assumption of rational human behaviour is not justified empirically (Janssen and Scheffer, 2004; Nell and Errouaki, 2013), (ii) the literature did not aim to improve the archaeological fit of the initial model by Brander and Taylor (1998) and (iii) the models have increased in complexity over time with no discernible, testable features, e.g., more parameters were added or more complicated objective functions were proposed. Models developed on ecological and archaeological ground, which we detail next, do not share these difficulties.

1.2.2.2 Ecologically inspired models

Some models have not employed an economic approach to modelling societies, but rather develop the dynamical systems more heuristically, from either ecological considerations or society specific features consistent with the archeology. All the models borrow elements from population biology, hence we choose to label them as "ecologically inspired". Such extensions of Brander and Taylor (1998)'s model dynamics include the addition of a capital stock (Erickson and Gowdy, 2000), modification of the Lotka-Volterra dynamics (Basener and Ross, 2004; Bologna and Flores, 2008), the introduction of a rat population (Basener et al., 2008) or the incorporation of several factors, including rodents and disease (Brandt and Merico, 2015). These models are reviewed in more depth in Chapter 2.

The models we address in this section can be very diverse in their scope, ranging from modelling specific societies (Anderies, 1998), to quantifying the impact of a cognitive bias (Janssen et al., 2003), accounting for the impact of inequality on collapse (Motesharrei et al., 2014) to modelling dynamics between different regions (Anderies and Hegmon, 2011). We have selected only a few models to specify in more detail, so as to both give an idea of this type of modelling and to contrast it with to the economic approach discussed earlier. The rationale for our selection is as follows: Anderies (1998) presented one of the earliest smaller-scale models of societal dynamics, Janssen et al. (2003) analyse the impact of sunk-costs effects which play a key role in collapse dynamics, Motesharrei et al. (2014)'s model was a starting point in developing our own Easter Island model and Anderies and Hegmon (2011) is one of the few papers that address multi-regional dynamics.

Beyond Easter Island, other societies have also been modelled, such as in the work of Anderies (1998), who captures the social dynamics of the Tsembaga of New Guinea. The Tsembaga have domesticated animals, predominantly pigs. There is a ritual activity called the Kaiko, a year-long pig festival that is meant to end a 5-25 year-long cycle that couples pig husbandry and warfare. When the pig population becomes too high, the number of garden invasions will likely increase as well, leading to more tension in the community. If a garden is invaded, there is a chance that the person who's garden was invaded will kill the owner of the pigs (Anderies, 1998). Records of these incidents are kept so that they are avenged in the next ritualistic outbreak of warfare. To lower the pig population and repair the community ties, the Kaiko starts and all but a few of the pigs are slaughtered. Thus, pig husbandry is deeply rooted in the traditions of the Tsembaga and it implies the existence of periodic social dynamics. The model of Anderies (1998) reproduces these cycles. If the pig population is low, their maintenance is unproblematic and the work level required is low. The dynamics in this case leads to a steady state. Otherwise, when pig numbers grow, a bifurcation boundary is passed and the ritualistic cycle begins.

Janssen et al. (2003) introduces a model that aims to illustrate what are called sunk-cost effects. Humans take into consideration prior investments when deciding what course of action to take, a phenomenon commonly referred to as sunk-cost effects. Research on sunk-cost effects has been mostly focused on the individual level, but the effect is even more pronounced in groups. Reaching consensus is critical to group cohesion and activity, and often constitutes an explicit, key goal of political processes. Once consensus is reached there is an inbuilt bias and the group "may not suggest abandoning an earlier course of action because this might break the existing unanimity" (Janssen et al., 2003, p. 722). So, the groups tends to commit to the decision taken, even though negative results are obtained. The model only features a resource variable and the human population is taken as an adjustable parameter. The bifurcation diagram for the system shows that at higher population levels (and hence higher sunk-costs) the critical level of resource that is tolerated tends to be smaller. A point is reached where the resource collapses and the population abandons the settlement.

Motesharrei et al. (2014) proposes a model of societal dynamics that attempts to capture the relation of economic inequality to collapse. To do this they introduce a new variable, specific to human activity: wealth, that serves as a stock of refined/preserved resources, e.g., food reserves. This helps distinguish humans from other factors that could impact nature, and clarifies the interpretation of the model. The population is separated into commoners and elites, which differ in the intensity of their wealth (reserves) consumption. Also, it is only commoners that extract resources. The model suggests inequality can be a significant factor leading to collapse due to the rapid consumption of wealth by the elites, which limits the access its availability to commoners and leads to an increase in the death rate.

Anderies and Hegmon (2011) aim to develop a model of the Mimbres River Valley in New Mexico, USA, to explain why the richer area was significantly more degraded than the less rich eastern area. As such, the model consists of three patches: a hinterland with low resource availability and two areas with different resource abundance (one area has more resources and higher regeneration rates). The resources regenerate according to logistic growth and are consumed through a Lotka-Volterra predation term, with humans acting as "predators". The human population growth rate depends on the resource levels in its patch. If the resources are above a certain threshold then the growth rate is positive, otherwise it is negative. Net migration occurs towards a patch if its resource levels are sufficiently large compared to neighbouring patches. Using the model, they conclude that a richer region that also requires less harvesting effort will show greater degradation, which is consistent with empirical observations. Furthermore, they analyse the effect of migration between patches but find that it is has no significant effect on the long-run configuration of the system. The equilibrium states in the two regions with and without migration are found to be very similar, even when the regeneration rate of natural resources for one of the regions is varied.

As we can see from the above examples, the topics and aims of what we labelled as "ecologically inspired models" are diverse, and the methodology of building the models is not as unified as it is for economic models. What these models have in common is the goal of translating certain real-world dependencies and feedbacks regarding human societies into appropriate functional forms that accurately represent the dynamics in question. In building models such as those of Anderies (1998), Janssen et al. (2003), Motesharrei et al. (2014) or Anderies and Hegmon (2011) we must question if the proposed equations indeed convey the idea they intend, or if alternative formulations are preferable. Without reference to a specific real system, some models might not be possible to validate, such as that of Janssen et al. (2003) or Motesharrei et al. (2014).

In mathematical ecology, similar to economics, an adequate representation of a system by a model is achieved by following certain general modelling principles (Turchin, 2003a). But, with regard to historical processes, there has not yet to be a consensus on the appropriate modelling techniques. A new field, called "cliodynamics" (Turchin, 2008), seeks to provide such a common framework for modelling historical processes, but the field is still in its infancy.

Nevertheless, certain ecologically inspired models do share a common modelling methodology, namely system dynamics (Forrester, 1961). Models of Maya society have been largely developed in the system dynamics methodology and share many features with the ecologically oriented models discussed above. There has been a recent renewal in interest in the modelling the Maya, but despite capturing structural features of the societies, some models (Forest, 2007, 2013) are deficient in recovering known population developments. Models that fare better in the population modelling (Bueno, 2011; Kuil

et al., 2016) neglect monument construction and show high sensitivity to parameter changes. More details on these models are provided in Chapter 3.

1.3 Network and game theoretic modelling of social structure

In this section we review game-theoretic literature that addresses class formation in networks of agents. Game theory provides a framework for modelling strategic decision making, while network theory allows us to capture social structure and interaction. Naturally, we can expect their combination to give insight into the different social phenomena, such as cooperation and, the subject we are concerned with, the emergence of different class structures.

There are two broad categories of models that have provided insights into class formation: one that is methodologically similar to our approach, namely network optimisation (i Cancho and Solé, 2003), and the other is adaptive or coevolutionary networks (Gross and Blasius, 2008), where the topology of the network can adapt depending on the local dynamics. Certain models, with an economic focus (Mahault et al., 2017), lie at the junction between the two approaches, with the network optimisation algorithm acting as the topological evolution of the network. Our own work is methodologically aligned to the network optimisation literature but, given that our results show a type of class emergence, we detail both types of models.

1.3.1 Coevolutionary networks

Adaptive networks are defined by a feedback mechanism that exists between the local dynamics and the topology of the network. The local interaction between agents determines the overall state of the system, which then affects the topological evolution. Concomitantly, the emerging topology influences the local dynamics between agents. The emergence of different classes of nodes, that manifested a type of "division of labour" with certain nodes acting as leaders, was first reported by Ito and Kaneko (2001) and Zimmermann et al. (2001).

Ito and Kaneko (2001) propose a model of a temporally evolving, directed network where the state of a node is given by a logistic map coupled to all other nodes, and the connection weights vary depending on the current state. The weights update such that they increase between similar states, but the total indegree of each node is kept constant. By letting the network evolve, Ito and Kaneko (2001) find that the nodes form two distinct groups: a first group whose nodes posses many connections (i.e., large weights) towards the second group, and a second group with few outward connections to the first. Thus,

a core-periphery structure is manifest in the network. Further work (Ito and Kaneko, 2003) reveals the dynamical regimes that the system undergoes in different regions of parameter space. In a certain region a temporally stable core-periphery structure emerges due to a positive feedback that exists between node dynamics and the weights, which reinforces the separation of the nodes into the two groups.

Zimmermann et al. (2001) considers a network where each node represents an agent playing a Prisoner's Dilemma game against his neighbours. If the payoff collected by a node is not the largest in its neighbourhood then (with a certain probability) it rewires its links to new nodes. Cooperator nodes of high degree emerge that help sustain cooperation in the network. Under a perturbation of the cooperator "leader" nodes the network oscillates between states with low and high numbers of cooperators, before stabilising again to a cooperative state. Zimmermann et al. (2004) and Eguíluz et al. (2005) consider a variant of this model and modify the selection rule for a new node such that (with a certain probability q) it is selected from the neighbourhood of a neighbour. Even for $q = 1\%$, the emerging network has the small world property. Zimmermann and Eguíluz (2005) perform a more detailed analysis of the model and discover an uneven wealth distribution between cooperators and defectors. While cooperators are more numerous, they are on average poorer than defectors. After the finding of Zimmermann et al. (2001), that cooperation can dominate in a adaptive network, significant efforts were invested in developing models of coevolutionary networks that can maintain cooperation; for a review, see Perc and Szolnoki (2010).

In the model of Ito and Kaneko (2001) the network does not freeze in a given configuration but the weights continue to grow or decrease, whereas in the model of Zimmermann et al. (2004), Eguíluz et al. (2005) and Zimmermann and Eguíluz (2005) the network evolution stops at a certain point, achieving what is called a network Nash equilibrium (Gross and Blasius, 2008).

As we can see from the above summarised work, the different rules governing the dynamics of nodes and network evolution give rise to core-periphery networks, wherein a set of nodes enjoy a high degree and the rest are poorly connected. The highly connected nodes are associated a leadership status in the network, due to their influence in the network that helps maintain the disaggregated topology.

The emergence of leadership structure has also been reported beyond core-periphery networks, e.g., scale-free networks (Anghel et al., 2004; Zhang et al., 2014). In other studies (Kianercy and Galstyan, 2013; Lipowski et al., 2014; Allahverdyan and Galstyan, 2016), we can see a common pattern among the different models, namely that most admit at least two different phases: one where the structure and interaction of agents can be considered egalitarian, and another phase where leaders distinguish themselves and the topology becomes centralised.

1.3.2 Network optimisation

Network structure optimisation follows the same pattern of other optimisation problems, namely that a certain objective function is chosen which is either minimised or maximised. In certain cases, a structure manifesting class differentiation emerges. We highlight some studies that have had notable results in this regard.

Holme and Ghoshal (2006) model agents on a network that aim to maximise centrality while keeping a low degree. The simulations show that no stable configuration is arrived at, but there are long periods of stability where a certain rewiring strategy dominates. Between these periods of stability the network undergoes transitions that can manifest a wide diversity of topologies. Holme and Ghoshal (2006) highlight a specific topology where a small set of elite nodes achieve both high centrality and a low degree.

Guttenberg and Goldenfeld (2010) build an abstract model of information exchange to capture key features of political organisation. Agents need to allocate time between producing resources and information, and each agent makes decisions by combining information observed from other agents with its own. A score is computed for each agent which depends on guessing the environmental state correctly, and the goal is to optimise the average score obtained over many trials. There are three phases that are observed for the system: a state with disconnected independent agents, or a homogenous cooperative state or a cooperative state with a leader.

Peixoto and Bornholdt (2012) aim to find an optimal topology robust to random failures and intentional attempts. They build a block-model that is general enough to contain arbitrary degree distributions, block correlations and different types of links (for connectivity and interdependence). If the percolation properties of the network are optimised, then resulting network is a core-periphery network where the core consists of a small number of nodes of large degree.

Mahault et al. (2017) proposes a model wherein a network of agents have certain quantified amounts of wealth, power, frustration and initiative. In topologies optimised for maximum power (which a quadratic function of wealth) the wealth inequality is extreme. If a trade-off between power and frustration is sought, then three social classes emerge (lower, middle and upper class) and above a certain initiative level, the system no longer converges but shows cyclical regimes of equality and inequality.

Finally, we consider the model of Kasthurirathna and Piraveenan (2015), who model agents on a network playing different games (Prisoner's Dilemma, Stag Hunt, Battle of the Sexes or Matching Pennies) with their neighbour. The quantal response equilibrium (QRE) (McKelvey and Palfrey, 1995) is computed for every pair of interactions (or link in the network) with the rationality of a node being taken to be a monotonous function of its degree. The network is rewired such that the QRE is as close as possible to the Nash equilibrium, i.e., the rational outcome. Kasthurirathna and Piraveenan (2015)

claim that a scale-free topology with a power law distribution in the degree maximises the rationality in the system. We show in Roman et al. (2017) and Chapter 4 that the model proposed by Kasthurirathna and Piraveenan (2015) actually leads to the formation of core-periphery topologies.

The core-periphery topology is ubiquitous in the real-world, having been found in social relations (Bourgeois and Friedkin, 2001; Boyd et al., 2006), financial networks (Vitali et al., 2011; Lux, 2015; Barucca and Lillo, 2016), online social networks and collaboration networks (Yang and Leskovec, 2014) and the structure of scientific outputs (Zelnio, 2012). Given their predominance, several techniques have been developed to detect such structures (Borgatti and Everett, 2000; Holme, 2005; Rombach et al., 2014; Zhang et al., 2015).

As we have seen, the literature on theoretical models that aim to capture the emergence of social structure is rich with mechanisms that lead to the emergence of leaders, and the core-periphery topology is a frequent pattern that forms in these cases. But, with the exception of Kasthurirathna and Piraveenan (2015), no research has considered modelling agent rationality as an explicit factor that depends on the network topology. Furthermore, the research of Kasthurirathna and Piraveenan (2015) is questionable in several regards: no analytic arguments are provided for the results, the optimisation that is performed for the network does not reach a minimum and it is claimed that the results do not dependent on the type of games played. We address these problems in Chapter 4 by showing numerically and analytically that core-periphery topologies optimise the network structure for maximum system rationality, and that there is marked difference between the features of the core-periphery topologies for symmetric and asymmetric games.

1.4 Synopsis

In this chapter we have looked at modelling techniques employed to capture large-scale societal growth and collapse, as well as the use of network theory and game theory to model social interactions.

Agent based models offer a bottom-up approach to understanding a system's structure and behaviour. The insight these models can provide is how basic building blocks of the system in question behave. The difficulty lies in matching underlying agent behaviour with large scales features in the data and discriminating between alternative assumptions regarding the agent's characteristics.

Integrated world models have a high degree of complexity (many variables, equations, mechanisms and sub-models) that hinder understanding and communication. Nevertheless, due to their complexity and comprehensiveness they are also the most realistic models and are used in policy making.

Low-dimensional dynamical systems models have been widely used to capture societal mechanisms from a top-down approach. There are different schools of thought on how to develop these type of models: economically or ecologically focused, which different emphases and strengths. The advantage of these type of models is that they can capture a specific idea or theory on how societal evolution takes place. This, plus their smaller number of variables, allows for comparison with the archaeological record. The main shortcomings of these models is the potential over-simplifications they make in describing the systems under study.

Overall, we identify the following gaps and largely unaddressed issues in the literature:

- A lack of an explicit and precise match between model prediction and archaeological data (where available). This is the bare minimum that any model attempting to capture real world behaviour should aim for. The model of Brander and Taylor (1998) for Easter Island does not fit well with the data by Flenley and Bahn (2003), and no better fit was attempted by any subsequent paper building on their work. While Hosler et al. (1977) aim to reproduce the collapse of the Maya, it does so with unrealistic time-scales and model behaviour. Notable examples where a good fit with empirical data has been achieved is the work by Anderies (1998) and the World3 model (Meadows et al., 1972), with the comparison done by Turner (2008).

- Models tend to be either complex or of very low dimensionality, most often 1 or 2 dimensional. There is a lack of models between these two extremes, which is problematic because justifying the features, calibrating and communicating a complex model is challenging, while getting valuable real insights from very low-dimensional models is unlikely. Complex models include the agent-based and integrated world models. The models of Hamblin and Pitcher (1980) and the economic-based models of Easter Island (Reuveny and Decker, 2000; Dalton and Coats, 2000; Pezzey and Anderies, 2003; Dalton et al., 2005; Good and Reuveny, 2006) fall in the very low-dimensional category, while giving questionable insight (Lowe, 1982; Janssen and Scheffer, 2004). Ecological-type models like (Turchin, 2009; Motesharrei et al., 2014) are 3 or 4 dimensional and capture sufficient features for their aims.

- Even when a model makes an explicit fit with the archaeological record and aims for a high-enough level of detail to warrant a meaningful interpretation, like that of Bueno (2011), the behaviour of the model can be too sensitive to changes in parameters to provide robust conclusions.

- While some integrated world models dissagregate the world into distinct regions to capture regional effects, such as Mesarovic and Pestel (1974) have done, there is a lack of low-dimensional models that aim to understand the dynamics of multiple coupled socio-environmental systems.

We provide two contributions to the literature on modelling societal growth and collapse. The first paper, found in Chapter 2, focuses on Easter Island and offers a dynamical system model of the island society. The model is the first to aim for a match with the archaeological record (Flenley and Bahn, 2003) and provides mathematically precise conditions under which a sustainable outcome or a collapse can occur. Specifically, the collapse of the island society corresponds to a supercritical Hopf bifurcation, where the critical parameter is the harvesting rate of resources.

Furthermore, we extend the model by coupling two societies together under different assumptions. The framework in which we formulate the two-society model is that of coupled dynamical oscillators. This is appropriate because, in the unsustainable regime, a society behaves like a dynamical (limit cycle) oscillator with a large amplitude. The two-society model is the first of its kind to study coupling of socio-environmental oscillators representing human societies. We establish under what conditions two coupled societies can be both sustainable and when mutual collapse occurs. Surprisingly, as long as one society had a sufficiently low harvesting rate, then the overall system could reach a steady state. Steady states of such coupled oscillators are thus more prevalent in the parameter space, making the system more robust to collapse.

The second paper, that constitutes Chapter 3, is on the Maya collapse. Again, we build a dynamical system model that is the first to match fine-grained archaeological data on the growth rates and population levels of the Lowland Classic Maya (Folan et al., 2000), and the data on monument building rates (Erickson, 1973). To validate the model, an extensive sensitivity analysis is performed which shows that the best-fit parameters lie at a minimum in parameter space, and also correspond to archaeologically determined values. Given the excellent fit to the data and the consistency of the determined parameters with the broader literature, the model is validated and suggests that a drastic increase in the practice of intensive agriculture can account for the collapse. The model also offers the possibility to assess the role of drought in the collapse of the ancient Maya, which is a commonly invoked reason for their demise. We find that, as long as a significant shift to intensive agriculture takes place, the archaeological record is reproduced irrespective of the effects of precipitation. Specifically, the models shows that the archaeological record is recovered only if after 550 CE a fraction of around 70% of each new generation undertakes intensive agricultural practices. A mathematical analysis shows that this system also undergoes a supercritical Hopf bifurcation when the harvesting rate increases beyond a critical point.

In the network and game theoretic literature we have seen a wide variety of models that give rise to social structure, manifested in particular through the emergence of leaders and core-periphery topologies. In the literature applying game theory on networks we can identify two gaps:

- The quantal response equilibrium has been extensively used in economics and provides a way to quantify a graded notion of rationality (McKelvey and Palfrey, 1995). But, it has been sparsely used in adaptive network models despite allowing a natural link between topological properties and game parameters, such as in the work of Kasthurirathna and Piraveenan (2015).
- There are certain shortcomings in the work by Kasthurirathna and Piraveenan (2015): the optimisation of network structure did not reach a local minimum (no plateau observed), a lack of analytic arguments and an erroneous conclusions regarding the nature of the optimal topology and the fact that it is independent of the type of game played.

In the third paper, which is Chapter 4, we employ the framework of Kasthurirathna and Piraveenan (2015) to quantify the rationality of players and to measure the distance of an agent's strategy from perfectly rational outcomes. Instead of computing the Nash equilibrium, we allow for a range of rationalities (given by the degree of a node) and determine the quantal response equilibrium (QRE). In the limit of perfect rationality (or infinite degree in our case) the QRE coincides with the Nash equilibrium. Hence, we compute the quantal response equilibrium and measure the deviation of the resulting probability distribution from the Nash equilibrium using the Jensen-Shannon divergence. We address the problems with Kasthurirathna and Piraveenan (2015) treatment and provide numerical and analytic arguments that in symmetric games (Prisoner's Dilemma and Stag Hunt) the optimal network configuration to maximise rational behaviour is that of core-periphery graph with small number of hubs of high degree that form a complete subgraph, and a periphery consisting of nodes of degree one. In asymmetric games (Battle of the Sexes and Matching Pennies) a core-periphery topology also emerges, but the core consists of a regular subgraph and the degrees of the hubs are smaller.

Chapter 2

Coupled societies are more robust against collapse: A hypothetical look at Easter Island

Abstract

Inspired by the challenges of environmental change and the resource limitations experienced by modern society, recent decades have seen an increased interest in understanding the collapse of past societies. Modelling efforts so far have focused on single, isolated societies, while multi-patch dynamical models representing networks of coupled socio-environmental systems have received limited attention. We propose a model of societal evolution that describes the dynamics of a population that harvests renewable resources and manufactures products that have positive effects on population growth. Collapse is driven by a critical transition that occurs when the rate of natural resource extraction passes beyond a certain point, for which we present numerical and analytical results. Applying the model to Easter Island gives a good fit to the archaeological record. Subsequently, we investigate what effects emerge from the movement of people, goods, and resources between two societies that share the characteristics of Easter Island. We analyse how diffusive coupling and wealth-driven coupling change the population levels and their distribution across the two societies compared to non-interacting societies. We find that the region of parameter space in which societies can stably survive in the long-term is significantly enlarged when coupling occurs in both social and environmental variables.

2.1 Introduction

Modern society is pushing beyond the safe operating boundaries of its global environment (Rockström et al., 2009). Resource depletion, species extinction, deforestation and climate change are symptoms associated with passing these boundaries. A starting point for managing modern societies response to these these problems is understanding the dynamics governing human-environment interactions, and studying past societies offers the possibility of gaining insight into these dynamics. There are many examples throughout history of societies that have collapsed: Mesopotamia, the Minoan and Mycenaean Civilisations, the Western Roman Empire, the Lowland Classic Maya and the Chacoans to name a few (Tainter, 1988). Understanding and quantifying the conditions which lead to collapse can provide a guide for present society concerning how to cope with resource constraints and environmental challenges, and avoid a potential collapse.

Societal collapse can be defined as a "rapid, significant loss of an established level of sociopolitical complexity" (Tainter, 1988, p. 4). Under what conditions do human societies face a collapse or, in particular, a population crash? This question has been a recurrent issue in the history of mathematical and computational modelling. Arguably, the earliest study addressing it can be considered to be the work of Malthus (1798) which raised wide concerns over population growth and land availability. Much later, a more sophisticated model was developed in Limits to Growth (Meadows et al., 1972) that showed a decline in population levels in the second half of the 21st century. Both works were misunderstood and faced harsh criticism (Neurath, 1994), mostly because the quantitative reasoning and modelling they employed were unfamiliar at the time to large portions of the educated population, especially in the case of Limits to Growth (Bardi, 2011). In recent times, interest in the mathematical modelling of societal dynamics has revived (Anderies, 2000; Turchin, 2008), with several models quantifying historical cases of societies that have experienced collapse (Brander and Taylor, 1998; Axtell et al., 2002; Heckbert, 2013).

The focus of most recent models has been on the dynamics of single societies, most prominently Easter Island (Brander and Taylor, 1998; Dalton and Coats, 2000; Reuveny and Decker, 2000; Pezzey and Anderies, 2003; Good and Reuveny, 2006). While, like Easter Island, many cases of collapse occurred in isolation, the dynamics of multiple coupled societies is no less important to historical knowledge and understanding. Given the highly interconnected nature of the modern world, studying the behaviour of a network with many coupled, interacting socio-environmental systems is of much interest for the present environmental debate (Rockström et al., 2009). Furthermore, it is likely that it can shed light on past cases of collapse. The movement of populations, along with the products they carry, have had a significant effect on social dynamics throughout human history (Manning and Trimmer, 2013). Historically, commerce and the establishment of trade routes proved crucial to the growth and development of many complex societies, in

particular the Roman empire (Van der Leeuw and de Vries, 2003). The building of road networks and the development of exchange systems contributed to its growth (Dowdle, 1987). Subsequently, the migration of Germanic tribes had a large impact on the later stages of the empire (Halsall, 2007). Seafaring has been equally important to migration and trade, e.g., the Roman Empire with Egypt, but also in the society of the Maya (McKillop, 1996). The systematic movement of people and goods over large distances and the building of the necessary infrastructure (roads, bridges etc.) to facilitate transit and transport are characteristic signs of high levels of societal complexity (Tainter, 1988).

In this paper we present a dynamical systems model of societal development, which we apply to Easter Island. Then, we take a first step in the direction of quantifying the dynamics of networks of societies by starting with the simplest possible case, namely two coupled societies interacting by various forms of movement of people, goods or resources. To add historical context to our study, we again parametrise the model for Easter Island. By investigating the situation of interacting societies, we are essentially addressing the hypothetical situation: What if Easter Island was not an isolated island? What if people migrated and traded goods with an adjacent island? Would such interactions have prevented, alleviated or accelerated the collapse?

The paper is organised as follows. In Section 2.2 we review the recent literature on models of the long-term dynamics of societies. We find that the modelling methodology regarding dynamical systems is separated into two schools of thought, one focusing on economic principles underlying societal dynamics, while the other uses a more heuristic ecological approach to model building.

In Section 2.3 we propose a model aligned to the ecological methodology for the dynamics of a single society. In Subsection 2.3.1 we describe the model and apply it to reproduce the archaeological data of Flenley and Bahn (2003) about the collapse of Easter Island. Furthermore, a comparison is made between the results of the proposed model and the model of Brander and Taylor (1998), that also focuses on Easter Island. In Subsection 2.3.2 we analyse the critical transitions in the model when important parameters are changed. Appendix B contains a more detailed mathematical treatment.

Having validated the model for a single society, we proceed in Section 2.4 to investigate scenarios of two societies coupled together through exchanges of population, resources or goods under different conditions. We initially investigate simple diffusion in Subsection 2.4.1, and then in Subsection 2.4.2 we study targeted, wealth-driven migration, in which migration occurs from poor to rich societies driven by a difference in the wealth per capita. The results pinpoint when the coupling is beneficial or not for the sustainability of the entire system.

2.2 Related literature

The earliest arguments regarding long-term societal sustainability or collapse that were amenable to quantitative modelling were in the work of Malthus (1798). Concerns regarding human-environment interactions started to re-emerge in the 1960s, when sustainability science was born, arguably through the publication of the work of Carson (1962). A work that sparked intense debate and interest in mathematical modelling was Limits to Growth (LTG) (Meadows et al., 1972), which proposed an aggregated world model formulated in terms of a set of equations describing the dynamics and time evolution of several key aspects of society. Such a set of equations constitutes a dynamical system that attempts to capture important feedbacks present in socio-environmental systems. Recent research by Turner (2008) has compared the trajectories from Meadows et al. (1972) with real data over a span of 30 years. The comparison shows a reasonably good fit despite the initial modelling effort not aiming to be predictive but only precautionary.

In recent times, modelling the long-term development of societies, in particular the possibility of their collapse, has received renewed attention. The paper that re-sparked interest in this topic was by Brander and Taylor (1998). By appealing to neo-classical utility maximisation arguments, along with a set of functional forms widely used in ecology (e.g., logistic growth) Brander and Taylor (1998) arrive at a set of predator-prey type equations used to describe the evolution of the human population and renewable resources on Easter Island. Following this work a stream of papers appeared that adopted the methodology of Brander and Taylor (1998), expanded on it or applied it to other cases. We can broadly categorise these models as "economic type models", meaning that they represent people as utility maximising, rational agents.

There is a second class of models that aim to capture societal development that we label "ecologically inspired models." In this case the choice of dynamical system is made heuristically to capture the observed real-world dynamics of the society, while respecting modelling principles of population biology (Turchin, 2003a), but rationality of individuals is not enforced. An early model following this approach was developed by Anderies (1998) to capture the social dynamics of the Tsembaga of New Guinea. The wider diversity of assumptions that underlie the ecological style of modelling means that the endeavour tends to lack the conceptual unity of economic models. The theoretical appeal of the more unified economic framework is understandable, with modelling efforts that that were initially ecological in style (Anderies, 1998; Janssen et al., 2003), soon joining the economic camp (Anderies, 2000; Janssen and Scheffer, 2004). Nevertheless, the reliability of the rationality hypothesis has been questioned many times (Nell and Errouaki, 2013), including by Janssen and Scheffer (2004).

The underlying difference between the two modelling schools is in the theoretical framework from which they start the modelling process. The economic type models use a

narrower set of assumptions, typically including utility maximisation as a driver of human behaviour along with a decision on the global institutional policy. The ecologically flavoured models are less restrictive in their theoretical underpinnings, more attentive to characteristic features of the society and try to account for emergent social phenomena that can contrast with or even contradict economic rationality, e.g. sunk-cost effects (Janssen et al., 2003) or war rituals (Anderies, 1998).

We proceed to give a short overview of the different strands of literature that deal with societal modelling, starting with the economic type models. Dalton and Coats (2000) extends the model of Brander and Taylor (1998) for Easter Island to account for possible institutional reforms and how these could effect feast-famine cycles. Reuveny and Decker (2000) investigates other possible solutions to the "Malthusian Trap" for Easter Island in the form of technological progress and population management. Pezzey and Anderies (2003), along with considerations of institutional adaptation, also adds a resource subsistence requirement to preferences. Dalton et al. (2005) analyses Easter Island by taking into account the possibility of economic growth. Good and Reuveny (2006) look at limits to resource management institutions and conclude that even if the people of Easter Island had a complete assignment of property rights, implemented optimal resource management with an infinite horizon, or had a social planner to perform such a task, a boom-bust cycle would still occur. D'Alessandro (2007) investigates what happens when two different renewable resources are present which cannot recover once below a critical threshold. A comprehensive survey of these type of models is to be found in Nagase and Uehara (2011) and Reuveny (2012).

We now turn to the ecological strand of models which have arguably received less attention. Anderies (1998) modelled the social structure of the Tsembaga, which employ a simple swidden (slash-and-burn) agricultural system that also features domesticated animals, predominantly pigs which are part of a periodic war ritual called the Kaiko. Other research attempts to quantify conceptual theories of societal dynamics, such as the work of Turchin (2003b) who, among several ideas, also develops models reflecting Ibn Klaldun's theory of collective solidarity ("asabiya"). Janssen et al. (2003) introduces a model that aims to illustrate what are called sunk-cost effects, which refer to people taking into consideration prior investments when deciding what course of action to take. A group "may not suggest abandoning an earlier course of action because this might break the existing unanimity" (Janssen et al., 2003, p. 722). Turchin (2009) takes into account the demographic-structural theory proposed by Goldstone (1991) in developing a model that reproduces the dynastic cycles seen in many societies. Motesharrei et al. (2014) propose the Human and Nature Dynamics (HANDY) model for societal dynamics that attempts to capture the relation of economic inequality to collapse. The model suggests inequality can be a significant factor leading to collapse.

Regarding Easter Island, Erickson and Gowdy (2000) point out discrepancies between Brander and Taylor (1998) and the archaeological record for Easter Island reconstructed

by Bahn and Flenley (1992) and propose the addition of a capital stock to account for continued population growth despite resources being depleted. While a more abrupt collapse is observed than compared to Brander and Taylor (1998), the overall trajectories for the population and resources levels do not match the quoted historical record. Basener and Ross (2004) build a two-dimensional model that aims to reproduce a discrete set of data points of the population levels, particularly around the population peak. While the model achieves the desired fit, the results show a near instantaneous collapse of the population after 1700 which is unrealistic. Bologna and Flores (2008) develop a very similar model to Basener and Ross (2004) but with a Lotka-Volterra term for resource extraction. While no instant collapse occurs, the results of Bologna and Flores (2008) show a much earlier peak in the population compared to data Flenley and Bahn (2003), similar to Brander and Taylor (1998).

Basener et al. (2008) extends the model from Basener and Ross (2004) to account for rat infestation on Easter Island, while Brandt and Merico (2015) also considers rat infestation along with an epidemic component. With the higher dimensional model, Brandt and Merico (2015) investigate multiple scenarios regarding the collapse that reflect different theories regarding it. Plausible results are obtained under each scenario and none can be ruled out, which is not a surprinsing fact given the large number of parameters of the model and their uncertainty. We aim for a simpler treatment and propose a three dimensional model, that uses a similar parametrisation to Brander and Taylor (1998), provides analytic insights and has results that match very well with the time series by Flenley and Bahn (2003).

The examples in the above categories develop dynamical systems that describe a single, isolated society. Follow up studies by Quirin et al. (1977) and Mesarovic and Pestel (1974) extended the model in LTG by disaggregating the world into two and ten regions, respectively. The finer resolution allows for an analysis of societal development that moves past the homogeneity assumption that went into building the model behind LTG. For example, both Quirin et al. (1977) and Mesarovic and Pestel (1974) take into consideration the differences in internal development between the various regions, the imports and exports among them and variation in industrial activity.

While the work of Mesarovic and Pestel (1974) increased spatial resolution, it decreased the temporal horizon to 50 years and shows increasing trends in population and resource usage and no global collapse, much like the results of Meadows et al. (1972) up to the middle of the 21st century. Quirin et al. (1977)'s standard run also shows steadily increasing production of services, industrial output and population but for the next 300 years, completely disagreeing with Meadows et al. (1972). A significant role in this outcome is likely played by the annual rate of technological growth, which Quirin et al. (1977) assumed to be at least 5% and has a beneficial effect on all aspects of the model.

Instead of using a model of high complexity such as the one in LTG, here we opt for lower dimensional models and focus on systematically understanding their dynamics. Research on (relatively) simple models of coupled dynamical oscillators has a rich history in theoretical ecology, the closest related literature to our purposes being the Lotka-Volterra (LV) predator-prey models that explore diffusion between two patches. Early research on the topic was pursued by Levin (1974), who finds predator and prey can co-exist provided the migration rate is sufficiently low, while higher rates make the system act like a single patch and co-existence is no longer possible. Nisbet et al. (1992) and Jansen (1995) find that, for identical patches linked together by dispersal at a constant rate, the only possible equilibrium is symmetric with equal densities on each patch, which is a general result highlighted in a review by Briggs and Hoopes (2004). On two heterogeneous patches with LV predation, Murdoch et al. (1992) finds that different prey birth rates have a stabilising effect, while Jansen (1995) concludes that temporal variability in predator death rates decreases the amplitude of fluctuations in the system when it is perturbed by noise.

While the ecological literature provides us with useful mathematical tools, there are nevertheless specific features that predator-prey models do not capture when applied to societal dynamics. Examples of this include the building and use of products derived from natural resources (such as tools, food reserves and infrastructure) or specific incentives regarding migration, like economic prosperity, both of which are key aspects that we are modelling. However, methods from population biology modelling have been used to asses the impact of human population growth and migration on the carrying capacity of the environment, and to understand the feedbacks associated with these processes. In particular, the Prehistoric U.S. Southwest has been researched from this perspective, with early work on the problem by Zubrow (1971), and a more recent study by Anderies and Hegmon (2011) who proposes a heterogenous, three-patch model that captures population and resource dynamics, with net migration occuring towards a region if its resource stock is sufficiently large compared to neighbouring patches. Anderies and Hegmon (2011) finds that the equilibrium states of regions with and without migration are very similar.

In the present work we present a thought experiment where-in two regions similar to Easter Island interact through diffusion or through targeted migration due to differences in wealth per capita. The regions not only exchange people, but also resources and manufactured goods can interchange between patches. The coupling of the patches significantly changes the equilibrium states obtained in the regions, a result which is in opposition to the findings of Anderies and Hegmon (2011).

Societal dynamics has also been explored with agent based models. Representative examples for the work done in this area are Axtell et al. (2002), who develop a model of the Anasazi in north-eastern Arizona (U.S.), Heckbert (2013), who focuses on the Maya civilisation and Turchin et al. (2013), who aim to understand how intense competition,

in particular warfare, contributed to the emergence of large-scale complex societies. Agent based models, like the examples mentioned, incorporate detailed features such as spatially extended terrain and multiple forms of social interaction, and account for heterogeneity in agent behaviour and in the environment. The focus of this paper is, instead, to obtain a description of the time evolution of aggregate measures of societal macro-features, such as the population and resource consumption. Following previous research in the area (Brander and Taylor, 1998; Erickson and Gowdy, 2000; Basener and Ross, 2004; Bologna and Flores, 2008; Brandt and Merico, 2015), dynamical systems are an adequate tool for our purposes, which we use to formulate and specify our model.

2.3 Easter Island model

2.3.1 Model specification

Here, we opt for an ecological type of model for the dynamics of a single society that we apply to Easter Island. Using, where possible, the same parameter choices as Brander and Taylor (1998), we compare the solution of the model to the historical data provided by Flenley and Bahn (2003), who present an exhaustive review of the archaeological research of Easter Island. For comparison with an economic approach, we also show the model of Brander and Taylor (1998) and its solution. Subsequent papers, that extended the treatment of Brander and Taylor (1998), did not attempt to match the historical data, hence, our focus for comparison is on the original model.

By matching model output to real data we, at least partially, validate the proposed model. This means that by reproducing the observed historical trends, we can consider the relationships that the model describes to be plausible mechanisms at play within the socio-environmental system. Hence, the model moves beyond a thought experiment, and makes a better connection to reality which lends validity to later extensions of the model for coupled societies. However, it is beyond the scope of this paper to explain the collapse of Easter Island or quantify all relevant factors that led to it, such as rats (Hunt, 2007) or European contact (Stevenson et al., 2015).

We propose the following model for the dynamics of a society:

$$\begin{aligned} \dot{x} &= (b - de^{-z/(\rho x)})x \\ \dot{y} &= ry(1 - y/K) - \alpha xy \\ \dot{z} &= \alpha xy - sx(1 - e^{-z/(\rho x)}) - cz \end{aligned} \tag{2.1}$$

We regard the x variable as a stock of population, y as a stock of renewable natural resources and z as the cumulated goods produced from extracting natural resources, which we also refer to as wealth. In more concrete terms we could think of y as crops,

Symbol	Meaning	Typical values
b	Maximum birth rate	0.002
d	Maximum death rate	0.012
r	Resource regeneration rate	0.004
K	Maximum stock of resources	12,000
s	Subsistence requirement	0.004
ρ	Wealth per capita threshold	0.1
α	Resource extraction rate	10^{-6}
c	Decay rate of goods	0
β	Fraction of population harvesting	0.4 or 1.
ϕ	Effect of consumption on fertility	4 or None

Table 2.1: Parameters for model (2.1) and the model of Brander and Taylor (1998) for Easter Island. The time unit is taken to be one year.

wood, animal stock, etc., and z as products derived from these, like food stocks, shelter, tools, etc.; these are characteristic elements of past agricultural societies.

The dynamics governing the population change is consistent with the early phases described by demographic transition theory: in a developing society (which has relatively low, but growing levels of wealth per capita) the death rates drop quickly due to improvements in food supply and material conditions (Landry, 1934; Kirk, 1996). Data for modern societies indicates that infant death rates have fallen significantly over time (Chesnais, 2001), sometimes exponentially. We do not include a mechanism for the reduction of birth rates because the maximum net birth rate in the model is 0.2% per year, comparable to net growth rates in the High Middle Ages in Europe (Russell, 1972), which we judge to already be quite low.

The demographic mechanism is implement as follows: if the wealth per capita z/x is high compared to a threshold ρ then the population grows exponentially at the (maximum) rate b, while if z/x is close to 0 then the population decreases exponentially at the (minimum) rate $b - d$, where d is the maximum raw death rate. The presence of material wealth lowers the death rate, hence it has a positive impact on net growth rates, consistent with the first stages hypothesised by demographic transition theory.

As has been common in many models of societal dynamics, we consider natural resources to recover logistically at a rate r, with a maximum capacity of K. Another classical feature is that the resource extraction is governed by a predator-prey term αxy, with people acting as predators and resources as prey. The extraction rate α is the fraction of the resource base that can be extracted by one person over a year. Thus, the equation for the rate of change of resources is analogous to that used by Brander and Taylor (1998).

Material goods, i.e. the wealth z, are produced at the same rate as the resources are extracted, which reflects conservation of matter. The consumption of goods is proportional

to the population and the rate of consumption per capita is equal to the subsistence requirement s when wealth per capita is high. We expect that, if the average wealth per capita decrease, then the average consumption per capita also decreases. Hence, the consumption per capita tends to zero when z/x is low, which is similar to the dynamics proposed by Motesharrei et al. (2014). To account for wear-and-tear, manufactured products decay exponentially at a rate c, a feature previously considered by Erickson and Gowdy (2000). A summary of the parameters and their values is found in Table 2.1.

We show that by solving the equations of model (2.1) it is possible to reproduce to high accuracy the archaeological record for Easter Island as presented in Flenley and Bahn (2003). To achieve this, the choice of parameters in (2.1) is made to coincide with the values (and notation) used in the model (2.2) proposed by Brander and Taylor (1998):

$$\begin{aligned} \dot{L} &= (b - d + \phi\alpha\beta S)L \\ \dot{S} &= rS(1 - S/K) - \alpha\beta SL \end{aligned} \tag{2.2}$$

where L is the population and S is the renewable resource stock. We set most of the parameters in (2.1) to have the same values as the choices Brander and Taylor (1998) made for model (2.2). The maximum birth rate is $b = 0.002$, while the maximum death rate is $d = 0.012$, so that $b - d = -0.01$ as in (Brander and Taylor, 1998). The regeneration rate (per year) of resources is $r = 0.004$, the maximum resource level is $K = 12000$ and the extraction rate is $\alpha = 10^{-6}$ (per person, per year).

Some parameter choices for model (2.1) differ from model (2.2) of Brander and Taylor (1998). We choose the subsistence requirement per person per year to be $s = 0.004$. Despite being mentioned, no explicit value is quoted by Brander and Taylor (1998) for the subsistence requirement. The largest difference between equations (2.1) and (2.2) is how the resource extraction is modelled and how this impacts birth rates.

For Brander and Taylor (1998), the parameter β is the fraction the population involved in resource extraction, so $\alpha\beta$ is the effective extraction rate per capita in model (2.2). The parameter α was assigned the value 10^{-6} so that at maximum resource levels a "household could provide its subsistence requirements in about 20 percent of available labour time ... A value of 0.4 for β is probably in the reasonable range" (Brander and Taylor, 1998, p. 128). In model (2.1) we eliminate the redundancy of the extra β parameter and take the effective extraction rate per capita to be $\alpha = 10^{-6}$, such that at maximum resource levels a person can meet his subsistence requirement in 33% of available time. While debatable, this value for the extraction rate allows the solution of (2.1) to match the archaeological record, see Fig. 2.1.

The parameter $\phi = 4$ scales the effect of resource consumption on birth rates in model (2.2). Resources do not directly impact birth rates in model (2.1) so, there is no ϕ

parameter in our case. We made the assumption in (2.1) that wealth per capita affects demographic rates and the parameter $\rho = 0.1$ sets the scale at which the impact of wealth cumulation on population growth is significant, corresponding to $\rho/s = 25$ years of material requirements (food reserves, tools etc.). There is no equivalent parameter for the decay rate c in model (2.2) so, we take $c = 0$ in model (2.1) if we are considering Easter Island. By choosing $c = 0$, we are assuming that wealth decreases mainly through human consumption.

Fig. 2.1(a) shows the historical evolution of population and resource levels on Easter Island according to Flenley and Bahn (2003). For initial conditions of 1100 people, 12000 units of natural stocks and no wealth, the output of model (2.1) is shown in Fig. 2.1(b). The initial conditions for model (2.2) are set to 40 people, while resources are at 12000 units, with trajectories in Fig. 2.1(c).

The population peak in Fig. 2.1(c) occurs several centuries earlier than in the data of Fig. 2.1(a), as noted by Erickson and Gowdy (2000). Also, the decline in population and resource levels in Fig. 2.1(c) is much less abrupt than Flenley and Bahn (2003) show in Fig. 2.1(a). Furthermore, the initial population value of 40 is much lower than estimates of the minimum viable population sizes, which are placed between 100s and 10,000s for humans (Smith, 2001). A higher initial population leads to an even earlier population peak in model (2.2).

Model (2.1) does not suffer from these shortcomings and its output in Fig. 2.1(b) fits Fig. 2.1(a) visibly better, both in population and aggregate resource trajectories, while using almost identical parameter estimates to Brander and Taylor (1998). The population peak, its timing, the collapse profile and the significant decline in resources, as indicated in Fig. 2.1(a) are accurately reproduced in Fig. 2.1(b). Thus, the results in Fig. 2.1 partially validate model (2.1). The resource level in Fig. 2.1(b) should be seen as an aggregated mean of renewable stocks (trees, livestock etc.) which are not all included in Fig. 2.1(a). This explains why the minimum resource level in Fig. 2.1(b), which occurs close to the time when the population reaches its maximum level, does not precisely match the resource minima in Fig. 2.1(a).

(a)

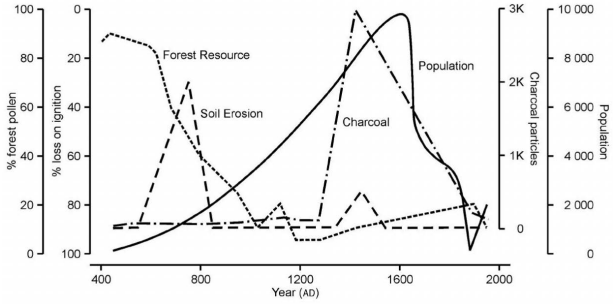

(b)

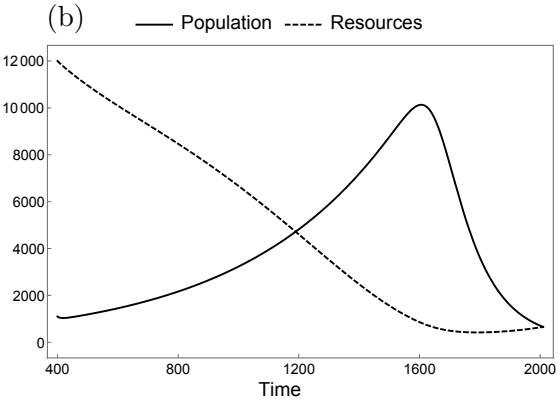

(c)

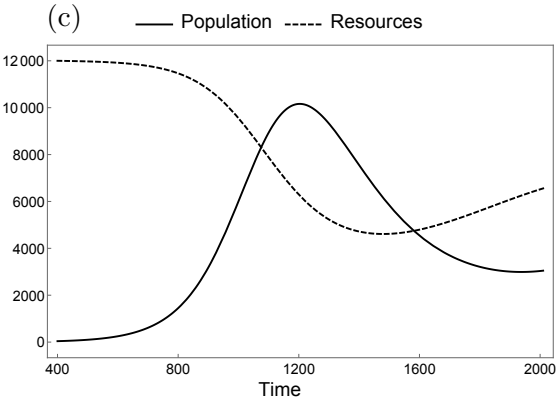

Figure 2.1: (a) Figure showing the archaeological record of Easter Island from collected data and estimates (Flenley and Bahn, 2003, p. 201). We see the population reaches a peak of approximately 10,000 people around the year 1600 AD. The resources were continually declining as the population was increasing.

(b) The population and resource levels for Easter Island as determined by model (2.1) from the year 400 AD to 2000 AD assuming no outside influence. The predictions are valid up to the late 19th century when significant interaction between Easter Island and the outside world started taking place. We see a good fit between the output of (2.1) and the real data.

(c) The solution of the model by Brander and Taylor (1998) shown for comparison. The timing of the population peak as well as the overall shape of the model output is inconsistent with the data in Fig. 2.1(a). The initial population value is below the lower bound for the minimum viable population size for humans.

Why do we obtain a better fit using the model (2.1)? Part of the reason lies in the delay induced by the additional equation describing the accumulated amount of manufactured

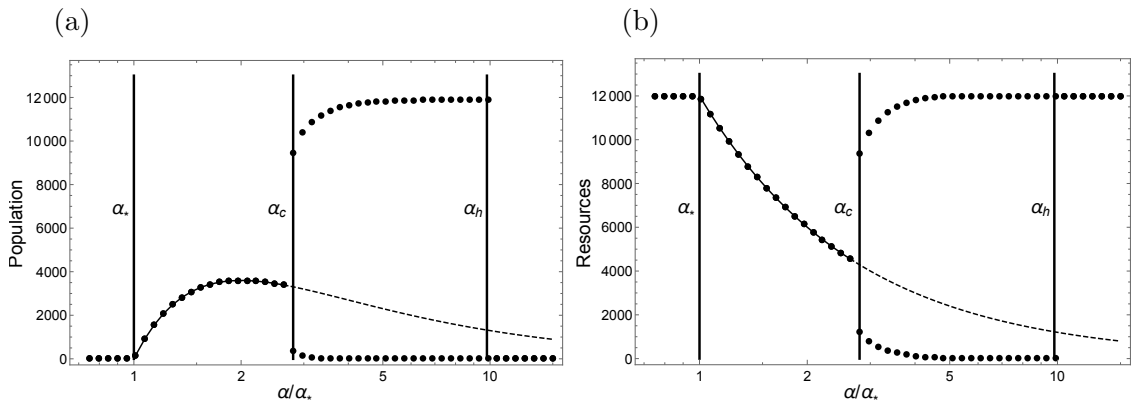

Figure 2.2: Bifurcation diagram for (a) population level, and (b) resource level. The vertical solid lines show the bifurcation points. The curved solid line indicates the analytically computed stable inner fixed point E, while the dashed line shows when E becomes unstable. The dotted lines highlight the maximum and minimum population on the numerically determined stable attractors. For $\alpha < \alpha_c = 2.8\alpha_\star$ the inner fixed point E is attracting while for $\alpha > \alpha_c$ a stable limit cycle emerges. When $\alpha \gtrsim 10\alpha_\star$ the system equilibrates to the saddle point N with no population and maximum resources.

products (wealth), which leads to a longer feedback loop within system (2.1) compared to other models.

The fit between the output of model (2.1) and the historical record shows us that the structure of the model and the feedbacks captured by it are viable choices to describe the dynamics of a simple agricultural society. Moreover, by fitting the model to a real world-case, we obtain reasonable parameter estimates, which can inform further modelling efforts and make them more realistic. Given this, the model can serve as a starting point to explore new dynamics, like that of multiple interacting societies. Nevertheless, it is worth pointing out that the results do not fully explain or quantify the scope of the collapse of Easter Island, as many more factors were at play in the collapse and model (2.1) does not incorporate all the complexities of reality.

2.3.2 Critical transitions

In this section we focus on the critical transitions that model (2.1) exhibits. Fig. 2.2 shows the bifurcation diagram for system (2.1) when varying the extraction rate α. The critical transition points are highlighted through vertical lines that separate the different regimes. The different regimes correspond to different long-term outcomes for our model society.

The mathematical analysis of the equilibrium points and transitions undergone by the system (2.1) is provided in Appendix B. The model has a single interior equilibrium

point that we denote by $E = (x_e, y_e, z_e)$ where:

$$\begin{aligned} x_e &= \frac{r}{\alpha}\left(1 - \frac{y_e}{K}\right) \\ y_e &= \frac{1}{\alpha}\left(s\left(1 - \frac{b}{d}\right) + \rho c \log\frac{d}{b}\right) \\ z_e &= \rho x_e \log\frac{d}{b} \end{aligned} \tag{2.3}$$

The first transition occurs at $\alpha_\star = (s(1 - b/d) + \rho c \log d/b)/K$, which we take as a reference value for the other transitions. When the extraction rate α is varied beyond $\alpha_\star$ it leads to a stable steady state (at the point E) or to oscillations, see Fig. 2.2. This indicates the presence of a critical transition (a Hopf bifurcation) in the system at a certain threshold value of the extraction rate, which we denote as α_c. That value separates regimes with long-term stable outcomes from boom-bust cycles. The precise determination of the transition point is of interest, as it dictates the eventual state of the system. The structure of system (2.1) allows for the exact analytic determination of the critical value α_c at which the Hopf bifurcation occurs:

$$\alpha_c = \frac{B + \sqrt{B^2 + 4AC}}{2A}\alpha_\star \tag{2.4}$$

where

$$\begin{aligned} A &= bdr\rho\left(ds - bs + cd\rho\log\frac{d}{b}\right) \\ B &= bdrs\rho(2c + d) + c^2d^2r\rho^2 + b^2rs(s - d\rho) \\ &\quad + bdr\rho(2bs + 3cd\rho)\log\frac{d}{b} + b^2d^2r\rho^2\log^2\frac{d}{b} \\ C &= dr^2\rho\left(bs + cd\rho + bd\rho\log\frac{d}{b}\right). \end{aligned} \tag{2.5}$$

In case of $\alpha < \alpha_\star$ the equilibrium population is zero, which means that the extraction rate is too low for any human population to meet their subsistence requirements. For $\alpha_\star < \alpha < \alpha_c$ there exists an attractive fixed point E, as the single branch of the bifurcation diagram in Fig. 2.2 indicates. This regime corresponds to a sustainable society in the sense that it equilibrates to a long term steady state. For $\alpha > \alpha_c$ the system oscillates and we can interpret this as a sequence of boom-bust cycles the society goes through.

For very large extraction rates, exceeding a threshold we call α_h, the natural resources are depleted quickly and they reach low enough levels for long enough that the population dies off and all wealth disappears. Without population pressure, natural resources recover and the system stabilises at a fixed point with no human population or wealth,

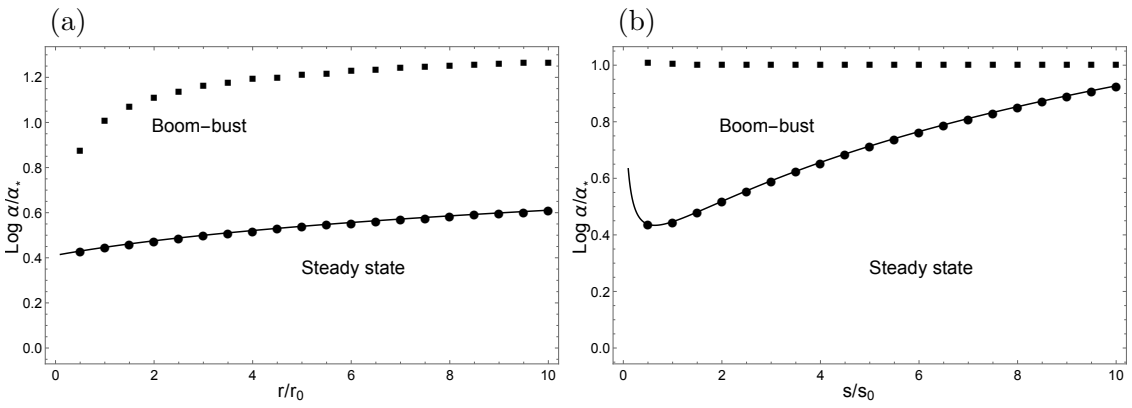

Figure 2.3: Plots depicting how regime boundaries vary with (a) resource regeneration rate, r, and (b) subsistence rate, s. Solid lines indicate the analytically computed value of the critical extraction rate α_c using equation (1). Above this critical rate the system exhibits oscillation, while below it the system equilibrates to a steady state with positive population. Dots indicate numerically determined values of α_c. Squares indicate numerically determined values of α above which the system equilibrates to the maximum resource state, N. The reference values r_0 and s_0 are equal to the corresponding values in Table 2.1.

but with maximum amount of natural resources. In practice, if $\alpha > \alpha_c$, the larger amplitude cycles would likely manifest as a collapse due to the low population values that are reached at the lower bound of the periodic orbit.

Relation (2.4) allows us to determine the behaviour of the critical threshold α_c when varying other parameters. In particular, we notice that the relative extraction rate $\alpha_c/\alpha_\star$, at which the transition to the boom-bust regime occurs, has no dependence on the maximum resource level K. The dependence of $\alpha_c/\alpha_\star$ on the value of r, the regeneration rate of natural resources, is shown in Fig. 2.3(a), while the dependence on s, the subsistence requirement, is presented in Fig. 2.3(b). As we see, the higher the regeneration rate r the higher the critical ratio $\alpha_c/\alpha_\star$ at which the transition to the unsustainable regime takes place. A similar trend is seen for the subsistence rate s. Also, with increasing values of the regeneration rate r, the threshold $\alpha_h/\alpha_\star$ is shifted upwards, whereas for the case of subsistence requirement s it is roughly constant.

With an increasing regeneration rate r we would expect an upward shift in the points of critical transition as the natural resources replenish faster. An increase in the subsistence requirement means goods are consumed at a higher rate which tends to lower the cumulated wealth, and hence the wealth per capita which leads to lower birth rates. We would thus expect the system to reach a steady state over a wider range of extraction rates, which is what Fig. 2.3(b) confirms.

In the case of Easter Island we have that $\alpha_0/\alpha_\star = 3.6$ which is larger than the critical ratio $\alpha_c/\alpha_\star = 2.8$ so, the system is in a boom-bust regime that in real terms translates into a collapse. Thus, the critical value α_c of the extraction rate serves to separate

the sustainable regime (that leads to a steady state) from unsustainable regimes (where collapse can occur).

We can give model (2.1) and its behaviour a more concrete interpretation by identifying the feedbacks at play. If the extraction rate is above the critical value than the feedback loop dominance in the model changes between two competing mechanisms: resource extraction and wealth consumption. Initially, the resource extraction is the dominant feedback (an increasing population leads to a decrease in resources and an increase in wealth, which implies an increase in wealth per capita and, thus, a further increase in the population). Once the resources are depleted, the cumulated wealth reserves are no longer produced but only consumed, which leads to a decrease in wealth per capita, which implies a decrease in the population. A smaller population means a slower rate of wealth consumption. As can be seen, resource extraction is part of reinforcing feedback loop, while wealth consumption is in a negative feedback loop. The feedback loops balance out when $\alpha < \alpha_c$, while if $\alpha > \alpha_c$ the feedbacks alternate in strength.

2.4 Coupled societies

2.4.1 Diffusive coupling

Having established and understood a model that reproduces the historical development of Easter Island, we now proceed with an analysis of two coupled socio-environmental systems. This is a first step at trying to quantify and understand the dynamics of networks of multiple, interacting societies, which is a situation that characterises the modern, industrial world but was also typical of many ancient societies. We aim at obtaining general insights on what new features the coupling of two socio-environmental systems gives rise to.

Human settlements and their surrounding environment, e.g. islands, form a natural partition of the overall socio-environmental landscape. Flows between different regions, such as migration or trade, provide additional sources (or sinks) for the respective stocks within regions. Accounting for these flows adds an important degree of realism to any model that tries to quantify inter-societal interactions.

There are many different types of possible interactions, and hence flows, that can occur between two systems. We start by considering possibly the simplest of such interactions, namely we model flows between systems through the mechanism of diffusion. If we assume people, resources and goods move or are moved randomly and unguided between different regions then a coarse description of such flows is given by a diffusion term in the equations. A further motivation for our choice is that diffusion is one of the most common types of coupling employed in the study of coupled dynamical systems (Pikovsky et al., 2001). Also, diffusion terms are widely used in spatial ecology to represent population

dispersal from one region to another (Briggs and Hoopes, 2004). We do not model the geographical structure behind the flow of people, resource or goods. Here we are only considering how the average flows between two regions (or land masses, islands) impact the stocks levels within the different systems.

More specifically, we consider two instances of the system (2.1) which we couple by adding diffusion terms to all variables. The equations for the first socio-environmental system (referred to as $S1$) are given by:

$$\begin{aligned} \dot{x}_1 &= (b - de^{-z_1/(\rho x_1)})x_1 + \sigma_x(x_2 - x_1) \\ \dot{y}_1 &= ry(1 - y_1/K) - \alpha_1 x_1 y_1 + \sigma_y(y_2 - y_1) \\ \dot{z}_1 &= \alpha_1 xy - sx_1(1 - e^{-z_1/(\rho x_1)}) - cz_1 + \sigma_z(z_2 - z_1) \end{aligned} \tag{2.6}$$

where the first terms are from model (2.1) and the additional terms represent the diffusive coupling, with $\sigma_x, \sigma_y, \sigma_z$ acting as coupling constants. The equations for x_2, y_2, z_2 of the second system (called $S2$) are analogous to (2.6). For concreteness and mathematical convenience, the two societies share all the same parameter values except for the extraction rate and initial conditions. $S1$ has the same initial conditions (x_0, y_0, z_0) as Easter Island, while $S2$ has half those values, namely $(x_0/2, y_0/2, z_0/2)$. Hence, we can think of the second society as a sister island to Easter Island, which shares most of its features but starts off with fewer people and resources.

The diffusion in the population x can be interpreted as migration. If $x_1 > x_2$ there will be a net influx of people from $S1$ into $S2$. A similar mechanism holds for the other diffusion terms. The diffusion of wealth z along with migration can be seen as people moving with their share of goods. A value of 0.1 for a diffusive coupling constant is quoted with respect to one year, just like the rest of the parameters in model (2.1). So, if $\sigma_x = 0.1$ then 10% of population difference can move between the societies (or islands) in the span of one year, e.g., if one island has 10,000 people and the other 5000, this means roughly 500 people moving per year between the two landmasses. We consider natural resources to be less mobile and when they do diffuse, only 1% of their difference is allowed to move between the regions in a year.

As we saw in the case of one society, the factor determining the long-term behaviour (steady state or collapse) is the critical value of the extraction rate α_c. We are interested in investigating if coupling societies can expand the volume of the parameter space that leads to sustainable outcomes. Hence, we will focus on the equilibrium states of the system rather than the transient dynamics.

To help us identify the bifurcation boundary we first quantify the decline in the population by looking at the relative change in the population over the long term, i.e., the relative distance between the maximum and the minimum of the oscillations with the amplitude measured in the population variable.

Thus, we define:

$$\delta = 1 - \frac{\liminf_{t\to\infty} x(t)}{\limsup_{t\to\infty} x(t)} \tag{2.7}$$

where $\liminf_{t\to\infty} x(t)$ is the smallest value the population reaches in the long term and $\limsup_{t\to\infty} x(t)$ is the largest. If a system reaches a steady state (sustainable outcome) then the relative change is 0%, with no decline in the population. On the other hand, if there are large amplitude oscillations (collapse) the relative change in the population is close to 100%. The use of the measure (2.7) allows us to represent the 3-dimensional bifurcation diagram for the population of $S1$ on a 2-dimensional diagram, see Fig. 2.4.

Other relevant measures are the long-term average population μ of a system:

$$\mu = \lim_{T\to\infty} \frac{1}{T} \int_0^T x(t)dt, \tag{2.8}$$

and the average population relative to the uncoupled regime, which we write as η:

$$\eta = \frac{\mu_{\text{coupled}}}{\mu_{\text{uncoupled}}}. \tag{2.9}$$

An index indicates what society we are referring to, e.g. δ_1 for $S1$, while no index refers to both societies.

We are interested in the long-term behaviour of the system for relative extraction rates above and below the critical ratio $\alpha_c/\alpha_\star = 2.8$ for a single society. To explore the parameter space we take the relative extraction rates of the two societies $\alpha_1/\alpha_\star$ and $\alpha_2/\alpha_\star$, and vary them in the range 1 to 5. No population exists for an isolated society if $\alpha/\alpha_\star < 1$, which sets a natural lower bound for the interval of exploration. The choice of the upper bound forms an almost symmetrical interval around the critical ratio.

Figs. 2.4(a)-2.4(d) shows the relative change in the population of $S1$ when diffusion occurs in progressively more dimensions of the system. Similarly, Figs. 2.4(e)-2.4(h) shows the long-term average population of $S1$. The corresponding figures for $S2$ are given by reflecting the graphs in the two top rows of Fig. 2.4 with respect to the second diagonal.

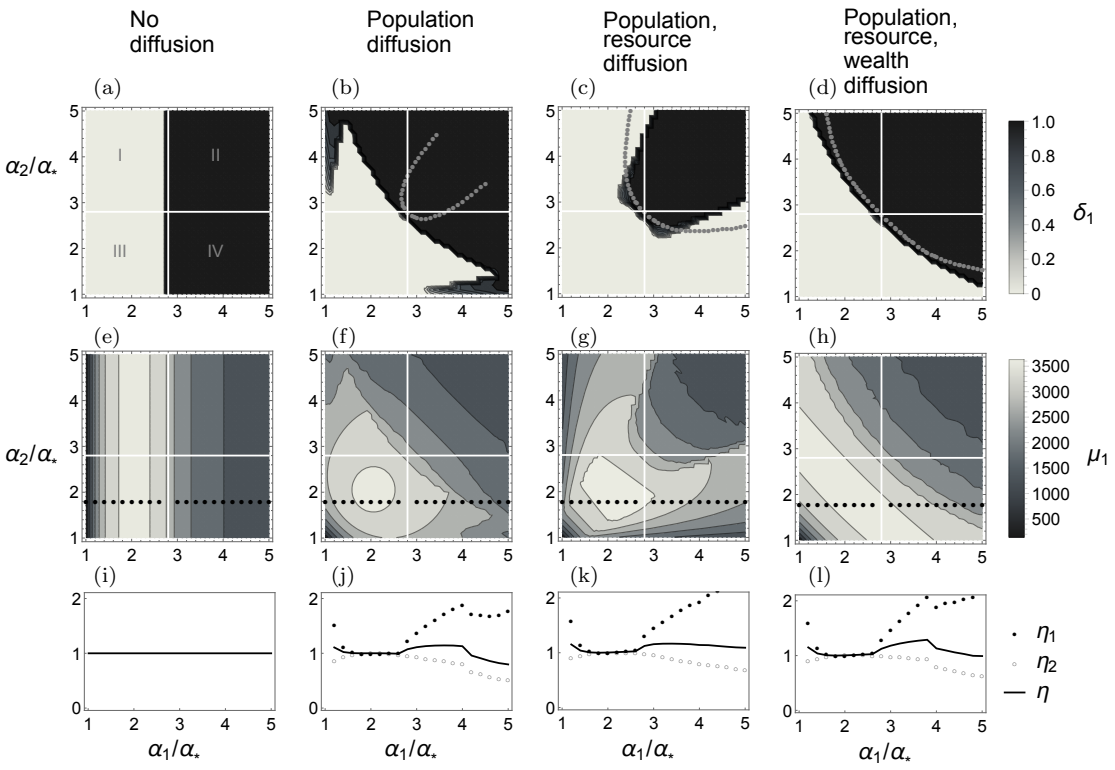

Figure 2.4: Graphs for two societies coupled via simple diffusion. Horizontal and vertical (white) lines at the critical ratios divide panels into quadrants, labelled from I to IV. Top: The relative population change in population for system 1 ($S1$) when: (a) uncoupled from system 2 ($S2$), with $(\sigma_x, \sigma_y, \sigma_z) = (0, 0, 0)$, or coupled via: (b) migration, with $(\sigma_x, \sigma_y, \sigma_z) = (0.1, 0, 0)$, (c) migration and resource diffusion, with $(\sigma_x, \sigma_y, \sigma_z) = (0.1, 0.01, 0)$ and (d) migration with wealth and resource diffusion, with $(\sigma_x, \sigma_y, \sigma_z) = (0.1, 0.01, 0.1)$. The gray dotted curves indicate the bifurcation boundary determined using the first-order approximation of the interior equilibrium point for the coupled system, see Appendix C. Middle (e)-(h): The average population for $S1$ in the same regimes as above. Bottom (i)-(l): The ratio between the average population in $S1, S2$ and overall system in the coupled and uncoupled regimes along the black dotted line where $\alpha_2/\alpha_\star = 1.8$. The mesh size in the numerical simulations is $\Delta\alpha/\alpha_\star = 0.1$.

Horizontal and vertical (white) lines divide the panels into 4 quadrants, such that both relative extraction rates are above the critical ratio in quadrant II and below it in quadrant III. Only one of the extraction rates is above the critical ratio in quadrants I ($S2$) and IV ($S1$).

Figs. 2.4(i)-2.4(l) indicate the ratio between the average population size of $S1, S2$ and the overall system to its value in the uncoupled regime along the dotted black line, where $\alpha_2/\alpha_\star = 1.8$. Figs. 2.4(a), 2.4(e) and 2.4(i) show the relative population change, the average population and the relative population (along the black dotted line) in the uncoupled case and can be taken as a reference to compare the results in the coupled regime. We can see that Fig. 2.4(a) reflects the critical transition seen in Fig. 2.2(a) that separates the steady state and oscillatory regimes.

The gray dotted line in Figs. 2.4(a)-2.4(d) represents the bifurcation boundary computed using an approximation of the stable equilibrium point of the system, see Appendix C. The determination of the boundary become more accurate due to better mixing of the system when more couplings are present, as can be seen in Fig. 2.4(d) that includes diffusion in all the variables.

A steady state is a sustainable outcome, hence we refer to the region of parameter space where the relative population change is 0% as the sustainability region. By contrast, the region with a 100% change in the population is the collapse region. In all cases of Figs. 2.4(a)-2.4(d) quadrant III lies in the sustainability region and quadrant II in the collapse region. So, when both societies have a low extraction rate the overall system reaches a steady state, whereas if both societies intensively extract resources we have a case of mutual collapse. Figs. 2.4(b)-2.4(d) are symmetric along the second diagonal, so we only need to discuss quadrant IV. In contrast to Fig. 2.4(a) all coupled regimes show the sustainability region extending to quadrant IV, where $\alpha_1/\alpha_\star$ is above the critical threshold. In Figs. 2.4(a) and 2.4(d) the sustainability area is similar, occurring below the main diagonal but in Fig. 2.4(c) it extends to most of quadrant IV.

When $\alpha_1 = \alpha_2$, which occurs along the second diagonal in Fig. 2.4(b)-2.4(d), the societies share the exact same parameters and they follow identical trajectories in the long run. Thus, they synchronise completely. The populations of the two societies continue to synchronise throughout most of the parameter space that we consider, which is consistent with the symmetrical stable equilibria seen in predator-prey patch models with diffusion (Briggs and Hoopes, 2004). For the sustainability region, synchronisation is illustrated by the population levels in Figs. 2.5(c) and 2.5(d), 2.5(e) and 2.5(f), 2.5(g) and 2.5(h) that match closely. For the collapse region, synchronisation implies that the collapse occurs in both societies simultaneously.

The region with the highest average population in Figs. 2.4(e)-2.4(h) is shown in white and, in all cases, it occurs within the sustainability region. The average population then gradually decrease in the direction of the collapse region. In case of migration in Fig. 2.4(f), the region with the highest average population does not change significantly from the uncoupled case of Fig. 2.4(e). By adding couplings in more dimensions the area increases noticeably, as seen in Figs. 2.4(g), 2.4(h).

Figs. 2.4(j)-2.4(l) show that, on the black dotted line where $\alpha_2/\alpha_\star = 1.8$, the long-term average population of each society in the coupled regime is equal to its population in the uncoupled regime, provided $\alpha_1/\alpha_\star$ is smaller than the critical ratio $\alpha_c/\alpha_\star = 2.8$. For values above the critical ratio, the average population of $S1$ is higher in the coupled regime than when isolated, while for $S2$ it is lower. Along the black dotted line, the population of the overall system of coupled societies is greater or equal to the sum of the populations of the isolated societies, with the only exception occurring in Fig. 2.4(j) when $\alpha_1/\alpha_\star \simeq 5$ and diffusion takes places only in the population variable.

Repeated numerical simulations show that the results in Figs. (2.4)(a)-2.4(k) are robust over changes in initial values and coupling constants. If the coupling constant for product diffusion is greater than that for population diffusion, namely $\sigma_z > \sigma_x$, the results are similar to those in Figs. 2.4(d), 2.4(h).

We next look at a specific scenario: we take $\alpha_1/\alpha_\star = 3.6$ which corresponds to the case of Easter Island and $\alpha_2/\alpha_\star = 1.8$. The results are shown in Fig. 2.5(a)-2.5(h) for the different couplings. We see that in the uncoupled case in Figs. 2.5(a), 2.5(b) $S1$ collapses and $S2$ reaches a steady state.

In the coupled regimes both systems stabilise so, Easter Island could potentially have been saved provided an almost identical sister island was present where the population extracted resources at a smaller rate. The most rapid approach to equilibrium occurs in Figs. 2.5(e), 2.5(f) where migration and resource diffusion take place but no wealth is transported between the two societies. In the case of population diffusion in Figs. 2.5(c), 2.5(d) and full diffusion in Figs. 2.5(g), 2.5(h) there is a long-term, oscillatory transient until equilibrium is reached.

The increased sustainability regions and the new areas of higher population that occur in the coupled regime compared to the uncoupled one, allows us to conclude that diffusive coupling makes societies more robust against collapse. By this we mean a larger area of the parameter space can be explored without the risk of collapse or significant loss of population. We can broadly interpret these results as follows: the diffusion of people alleviates the demographic pressure from the more populous society, while the diffusion of goods lowers the wealth per capita and hence the birth rate in the society with higher overall wealth. This allows both societies to reach a steady state as long as one of the societies has a low enough extraction rate of natural resources.

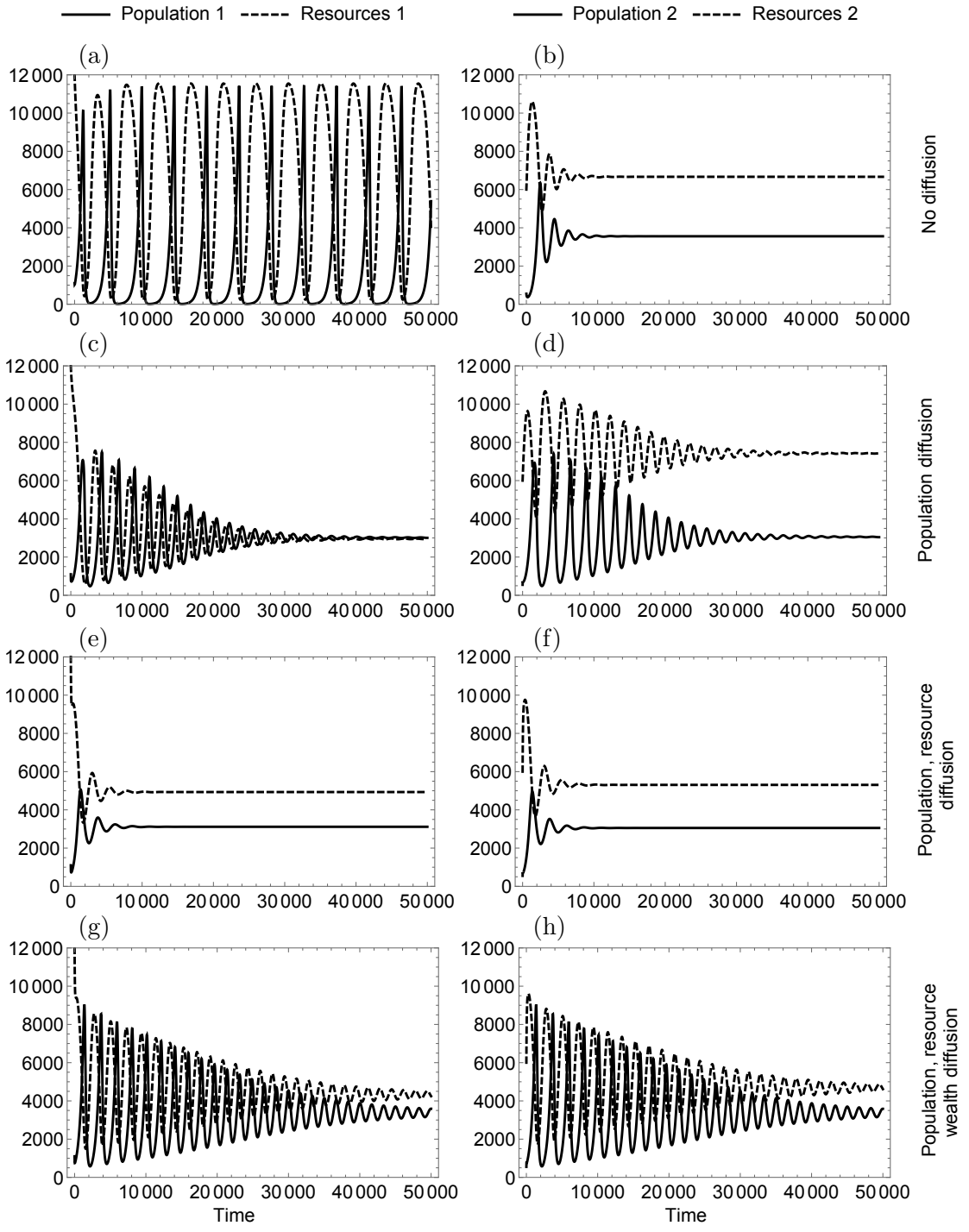

Figure 2.5: Graphs for two societies coupled via simple diffusion. Trajectories for system 1 (left) with $\alpha_1/\alpha_\star = 3.6$ and system 2 (right) with $\alpha_2/\alpha_\star = 1.8$ in the regimes: uncoupled (a) and (b), only migration (c) and (d), migration and diffusion of resources (e) and (f), and coupling in all variables (g) and (h).

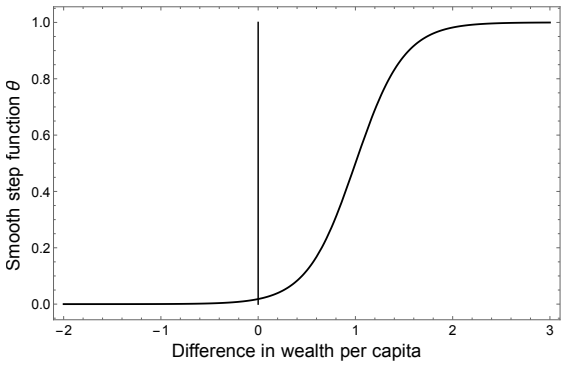

Figure 2.6: The graph of the step function θ in terms of the difference in wealth per capita. As a reference, we indicate the zero point with a vertical line.

2.4.2 Wealth-driven coupling

In the previous section we explored what happens when two societies are coupled in a simple, diffusive manner. We can explore alternative ways to couple societies and this is the goal here. What if people decided to move from poor to rich societies, i.e., from low to high wealth per capita?

We can write a dynamical system that captures this possibility as follows:

$$\begin{aligned}
\dot{x}_1 &= \cdots + \sigma_x \left(\theta \left(\frac{z_1}{\rho x_1} - \frac{z_2}{\rho x_2} \right) x_2 - \theta \left(\frac{z_2}{\rho x_2} - \frac{z_1}{\rho x_1} \right) x_1 \right) \\
\dot{y}_1 &= \cdots + \sigma_y (y_2 - y_1) \\
\dot{z}_1 &= \cdots + \sigma_z \left(\theta \left(\frac{z_1}{\rho x_1} - \frac{z_2}{\rho x_2} \right) z_2 - \theta \left(\frac{z_2}{\rho x_2} - \frac{z_1}{\rho x_1} \right) z_1 \right)
\end{aligned} \tag{2.10}$$

where $\ldots$ represent the source terms from system (2.1) for $S1$ and $\theta(x) = 1/(1 + e^{-2n(x-h)})$ is a smooth step function, with $n = 2$ and $h = 1$. Analogous equations hold for $S2$.

The function θ is a smoothed out step function shifted to the right by one unit, as seen in Fig. 2.6. If $z_1/x_1 \leq z_2/x_2$ then there will be no movement of people from $S2$ to $S1$. The greater z_1/x_1 is relative to z_2/x_2 the greater the influx to $S1$, which is shown in the monotone increase of the function θ. So, if the wealth per capita in $S1$ is greater than in $S2$, then there will be an influx of people from $S2$ into $S1$ which corresponds to the intuition that people will move to the society with higher wealth per capita.

Fig. 2.7 shows the same analysis as performed previously in Fig. 2.4 but now for the case of the system (2.10).

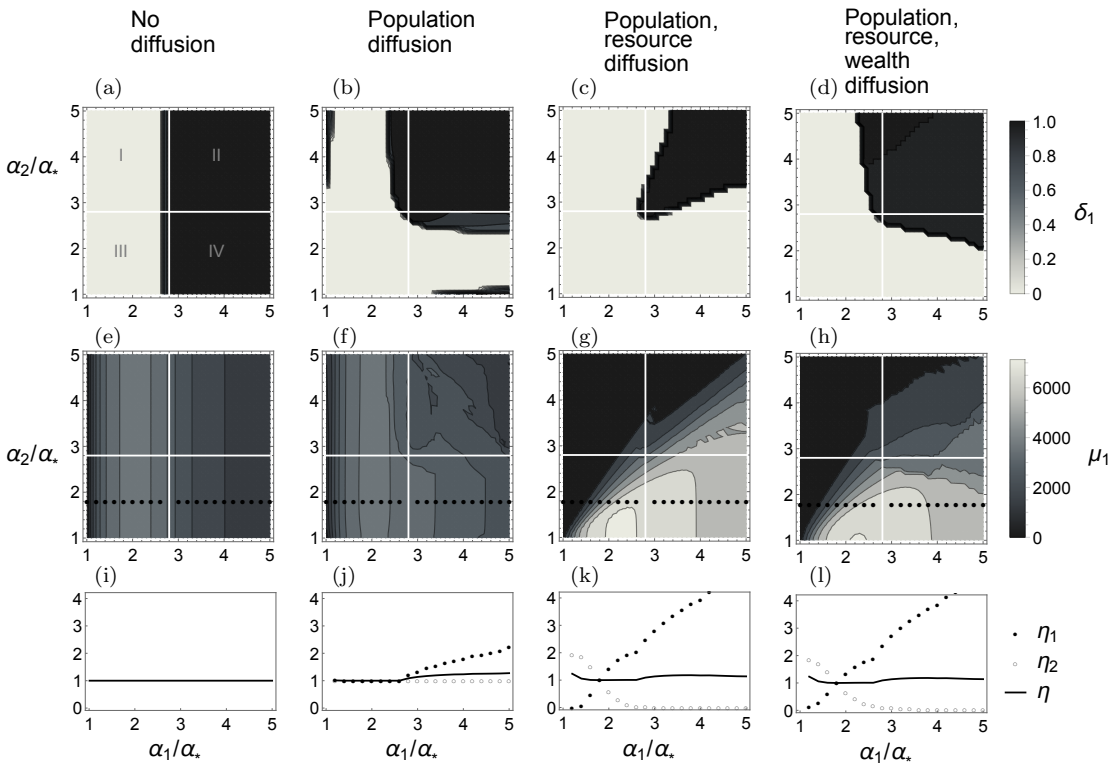

Figure 2.7: Graphs for two societies coupled via wealth-driven diffusion. Horizontal and vertical (white) lines at the critical ratios divide panels into quadrants, labelled from I to IV. Top: The relative population change in population for system 1 ($S1$) when: (a) uncoupled from system 2 ($S2$), with $(\sigma_x, \sigma_y, \sigma_z) = (0, 0, 0)$, or coupled via: (b) migration, with $(\sigma_x, \sigma_y, \sigma_z) = (0.1, 0, 0)$, (c) migration and resource diffusion, with $(\sigma_x, \sigma_y, \sigma_z) = (0.1, 0.01, 0)$ and (d) migration with wealth and resource diffusion, with $(\sigma_x, \sigma_y, \sigma_z) = (0.1, 0.01, 0.1)$. Middle (e)-(h): The average population for $S1$ in the same regimes as above. Bottom (i)-(l): The ratio between the average population of $S1, S2$ and the overall system in the coupled and uncoupled regimes along the black dotted line where $\alpha_2/\alpha_\star = 1.8$. The mesh size in the numerical simulations is $\Delta\alpha/\alpha_\star = 0.1$.

For convenience, Figs. 2.7(a) and 2.7(e) again show the relative population change and average population of $S1$ in uncoupled regime, which is to be taken as a reference case. We see that in all cases of Figs. 2.7(b)-2.7(d) quadrants I to III are predominantly in the sustainability region, whereas quadrant II is mostly in the collapse region. Again, if $\alpha_1 = \alpha_2$ the two societies synchronise completely but, in contrast to the case of diffusive coupling, synchronisation no longer extends beyond the second diagonal, as is shown by the asymmetry in the average population levels in Figs. 2.7(f)-2.7(h).

The average long-term population of $S1$ is increased in the new sustainability regions of the population diffusion case, as Fig. 2.7(f) shows. Compared to the other graphs, we notice some new features present in Figs. 2.7(g) and 2.7(h) regarding the long-term average population of $S1$. The novelty of these scenarios consists in the very low (almost zero) population in $S1$ above the second diagonal, and the clustering of almost the entire population of both societies into $S1$ when $2 < \alpha_1/\alpha_\star < 3$ and $\alpha_2/\alpha_\star$ is close

to 1. Both cases Figs. 2.7(g), 2.7(h) have in common the coupling of population and natural resources. The diffusion of resources clearly plays a role in the emergence of the new features as they are not present in the case of only population diffusion. The equivalent diagrams for $S2$ are obtained by reflecting the figures in the top two rows of Fig. 2.7 along the second diagonal.

We can see that resource diffusion is important because in the region of parameter space with the highest population of Figs. 2.7(g), 2.7(h) essentially most of the population moves into $S1$ and lowers the level of natural sources. In $S2$ on the other hand, the population is low while the resource level is high and this ensures a high influx of resources into $S1$, allowing it to maintain a higher population.

Figs. 2.7(i)-2.7(l) show the ratio of the average population in $S1, S2$ and the overall system to its population in the uncoupled regime for the subset of the parameter space that lies along the black dotted line in Figs. 2.7(e)-2.7(h). For diffusion occurring only between populations, the average population of $S1$ is equal to that of the uncoupled case if its relative extraction rate is below the critical ratio $\alpha_c/\alpha_\star = 2.8$, after which the population increases, as Fig. 2.7(j) shows. For $S2$, the population is fairly similar to the uncoupled regime.

In Figs. 2.7(k), 2.7(l) at low extraction rates the population of $S1$ is 0, but then steadily increases at higher extraction rates. In $S2$ the situation is reversed, with the population high at low extraction rates (for $S1$) and then decreasing to 0 at higher rates. This contrast is to be expected from the asymmetry in Figs. 2.7(g), 2.7(h). The overall average population of the system in the coupled regimes in Figs. 2.7(j)-2.7(l) matches the average population in the uncoupled case.

We again look at the specific scenario when $S1$ has the extraction rate corresponding to Easter Island, namely $\alpha_1/\alpha_\star = 3.6$ and $S2$ has half that value, $\alpha_2/\alpha_\star = 1.8$. The results are presented in Fig. 2.8 and we see that the coupling again stabilises both systems. In the case of migration in Figs. 2.8(c), 2.8(d) both societies reach the same population level in the steady state. In the other coupled regimes of Figs. 2.8(e)-2.8(h) the population of $S2$ is 0, having moved completely into $S1$.

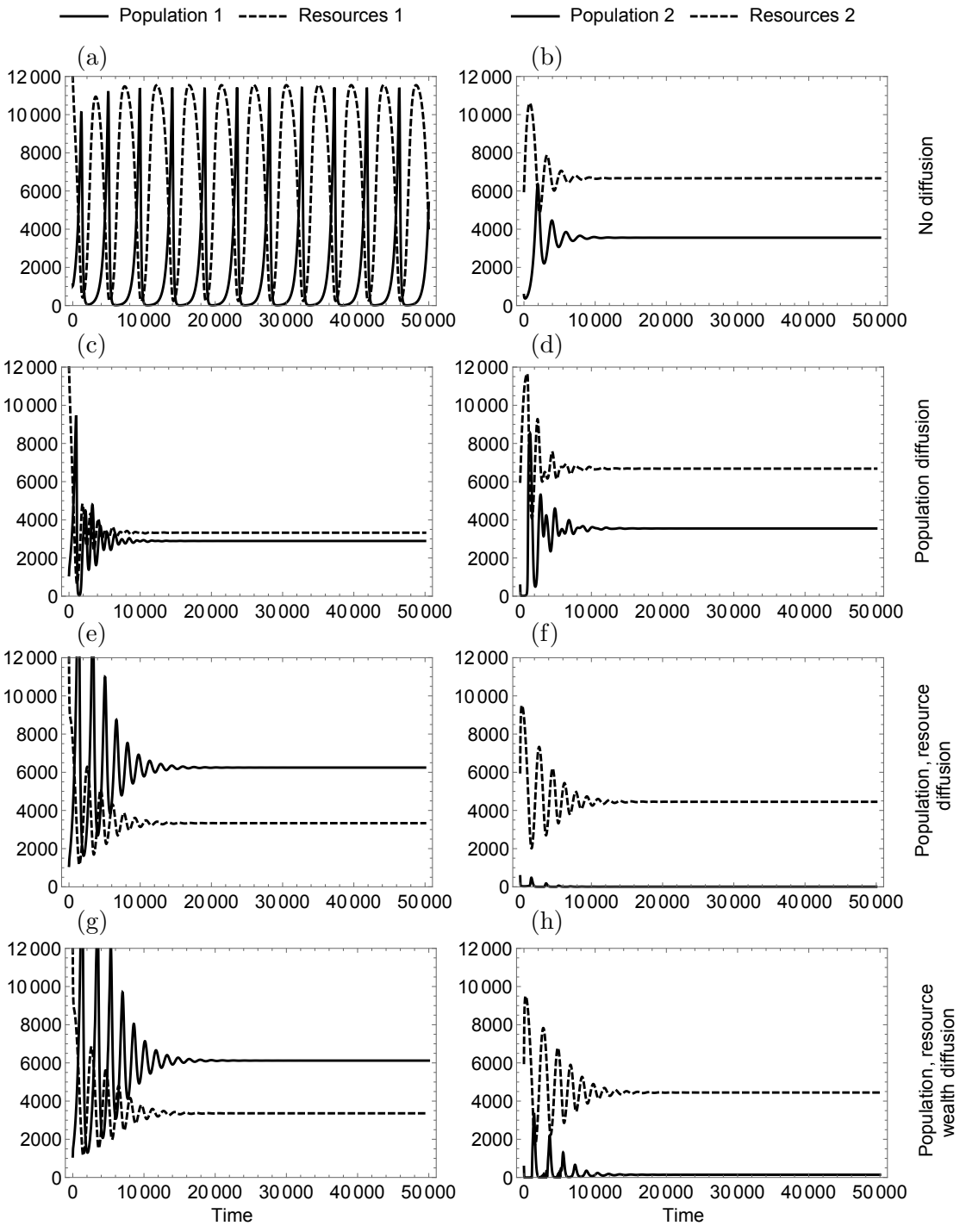

Figure 2.8: Graphs for two societies coupled via wealth-driven diffusion. Trajectories for system 1 (left) with $\alpha_1/\alpha_\star = 3.6$ and system 2 (right) with $\alpha_2/\alpha_\star = 1.8$ in the regimes: uncoupled (a), (b), only migration (c), (d), migration and diffusion of resources (e), (f) and coupling in all variables (g), (h).

In all coupled cases we see an increased sustainability region in Fig. 2.7, noticeably larger than the corresponding simple diffusion cases of Fig. 2.4. Why is this the case? Whenever one of the societies has a higher wealth per capita than the other, people will migrate to it. The influx of people increases demographic pressure in the richer

society but lowers its wealth per capita. The lower wealth per capita leads to a decreased population growth rate that helps stabilise the system. This different operating principle makes wealth-driven diffusion more effective at generating sustainable outcomes than simple diffusion, while maintaining similar overall levels of the population. Similarly, we can conclude that the coupling via wealth-driven diffusion makes the overall system of societies more robust against collapse.

2.5 Conclusion

In this paper we proposed and analysed a model to describe the simultaneous dynamics of the population, resources and manufactured goods of a society. We can match most of the parameters in the model with a well-known model of Easter Island by Brander and Taylor (1998) and by using similar values we obtain a faithful reproduction of the archaeological record provided by Flenley and Bahn (2003). The model captures crucial feedbacks present in most ancient agrarian societies, making it more general than the case of Easter Island.

We found the equilibrium points of the system along with the critical transitions (bifurcations) it undergoes when the rate of resource extraction is varied. At values below a particular extraction rate α_c the system reaches a steady state (sustainable outcome), whereas for value above it the system displays oscillatory behaviour (unsustainable outcome). Large amplitude oscillations can be identified with collapse, and this is the regime that Easter Island is found to be in. It is important to mention that for ecological systems, fold bifurcations provide a general mechanism by which ecosystem transitions can be understood and modelled (Scheffer et al., 2001). Given the prevalence of persistent oscillations in data and models of societal dynamics (Anderies, 1998; Turchin, 2009; Turchin and Nefedov, 2009), we can hypothesise that Hopf bifurcations, as the one illustrated by the model we propose, could serve a similar role when modelling critical transitions, such as collapse.

We then investigated the case of two societies coupled through simple diffusion or wealth-driven diffusion. We set up experiments with two societies parametrised to match Easter Island, except for the extraction rates which we systematically varied. In contrast to the results of Anderies and Hegmon (2011), we generally found that population migration, along with resource and wealth diffusion, makes a significant change to the equilibrium states the subsystems reach compared to uncoupled, non-interacting societies.

In particular, coupling leads to new or extended regions of parameter space where sustainable outcomes occur. This means that societies that would have undergone large amplitude fluctuations and collapsed if they were isolated, can now reach a stable steady

state, provided they are coupled with other societies with less resource intensive practices. The differences in resource extraction rates between the two societies helps stabilise the overall system, which echoes findings that heterogeneity in two patch predator-prey models is stabilising (Murdoch and Oaten, 1975; Murdoch et al., 1992; Briggs and Hoopes, 2004). Furthermore, the regions of parameter space where a given society achieved the highest average population increased. The more couplings are added (in population, resource etc.) the stronger the effect.

The present world is in a similar situation where, because of competing power centres of comparable strength, any collapse that could occur is more likely to be simultaneous and global (Tainter, 1988). These results indicate that a coupled network of societies could prove more robust against collapse provided that at least some societies maintain lower extraction rates of natural resources to dampen the oscillations in the rest of the system. Precisely quantifying the regime in which overall system sustainability is achieved is of obvious importance and is the future focus of our research efforts.

Acknowledgements

This work was supported by an EPSRC Doctoral Training Centre Grant (EP/G03690X/1). The models were implemented and all results were obtained using the Wolfram Research software Mathematica 10. No new data was collected by this research.

Chapter 3

The dynamics of human-environment interactions in the collapse of the Classic Maya

Abstract

In this study we investigate the societal development of the Maya in the Southern Lowlands over a span of approximately 1400 years and explore whether societal dynamics linked to the depletion of natural resources can explain the rise and fall of the Classic Maya. We propose a dynamical systems model that accounts for the state of the land, population and workers employed in swidden and intensive agriculture and monument building. Optimisation of model output to fit empirical data fixes biometric parameters to values consistent with the literature and requires that a shift from swidden to more intensive agriculture took place at around 550 CE. The latter prediction is consistent with the dating of the beginning of the Late Classical period. Thus, our model offers an explanation of the collapse of the society of the Maya and suggests that the role of droughts may have been overestimated. Consistent with previous work, the collapse can be modelled by a critical transition (supercritical Hopf bifurcation), where the critical parameter is the harvesting rate per capita of intensive agriculture. Furthermore, an extensive sensitivity analysis indicates that the model and its predictions are robust.

3.1 Introduction

The collapse of the Classic Maya has been the subject of considerable focus in the published literature, with many different hypotheses having been proposed regarding the underlying causes and drivers for the collapse (Tainter, 1988; Aimers, 2007; Turner and Sabloff, 2012). It is important to check to which degree these narratives are consistent with the historical record, which requires mathematical or computational modelling (Turchin, 2003b). Beyond this, Occam's razor needs to be applied, which means checking if simple hypotheses are enough to explain collapse. If the simple hypotheses are enough, this then helps to put more complex explanations into perspective.

The aim of this study is to explore whether a nonlinear dynamical system focused on socio-environmental feedbacks can account for the observed data about the Maya civilisation. In the present study, we identify and quantify some key feedback mechanisms of the socio-environmental system of the Lowland Classic Maya by building a model that captures the different specialisations of the majority of the population, and links them to the resource abundance in the environment and the number of monuments built over time.

We show that, if less intensive (e.g., swidden) agriculture would have remained the dominant method of food production, then the rapid increases in population levels that occurred around 700 CE and the concomitant extent of monument construction would not have taken place. We numerically determine that a match of the model's outputs to the archaeological record requires assumptions about a change in farming practices from less to more intensive agriculture around the year 550 CE. This change eventually leads to a severe depletion of agricultural resources and largely accounts for a steep drop in population numbers around the year 900 CE.

Hence, we find that, from 550 CE onward, an increased spread of intensive agricultural practices can account for the observed archaeological record of the Maya society as reconstructed in the demographic data of Folan et al. (2000) and monument building rates reported in Erickson (1973). In similar fashion to the work of Anderies (2003), by carrying out extensive sensitivity testing, we ensure the robustness of our findings. In addition to this, by changing assumptions about precipitation levels, we can also analyse the impact of droughts and find that the dynamical model can reproduce historical data with and without assuming reductions in precipitation.

To the best of our knowledge, the present work provides the first robust mathematical model of the Maya society that accurately reproduces the historical trends regarding population growth, as presented by Folan et al. (2000), and the building rate of monuments, as found in the work by Erickson (1973), and also available in Tainter (1988, p. 165). The collapse can be understood as driven by a critical transition in the system (a supercritical Hopf bifurcation), where the critical parameter is the harvesting rate

per capita of intensive agriculture. Importantly, this is consistent with previous findings regarding Easter Island (Roman et al., 2017) and generalises its conclusion that collapse can be modelled as a certain type of critical transition. The collapse is thus understood as an endogenous process in the socio-environmental system and questions the importance of contingent events, such as catastrophic droughts. Our modelling thus suggests that a socio-cultural process might have led to the widespread, permanent adoption of intensive agriculture, which has been a key driver of the rapid growth and expansion of the Maya civilisation starting in the Late Classic Period, as well as the cause of their later decline.

It is important to note that, given the vast array of potential aspects that can be studied regarding the Classic Maya, we do not aim for a model that gives an accurate representation of each potential factor. Furthermore, the definition of societal collapse and how it applies to the Maya has been a issue of ongoing debate (Aimers, 2007). Rather, we address an Occam's razor-type question, and investigate if a small set of interlocking factors could potentially account for the available data about the Maya society, in particular the significant decline in population and monument construction that occurred after 800 CE.

The paper is organised as follows. In section 3.2 we highlight some of the main theories regarding the collapse of the Classic Maya and provide a review of the quantitative (mathematical or computational) modelling regarding it. Following on, in section 3.3 we present a parsimonious model of the Maya society and their human-environment interaction. The results of the model, which are analysed in section 3.4, demonstrate an excellent match to empirical data for the evolution of the crude growth rates, population levels and building rates. Finally, we provide a summary of results in section 3.5. The results are complemented by two appendices: Appendix D includes a simplified mathematical treatment of the critical transitions undergone by the model we propose, and in Appendix E we present a detailed sensitivity analysis.

3.2 Literature review

Hypotheses for the the collapse of the Maya can generally be separated into two categories: (i) socio-political, such as class conflict (Hamblin and Pitcher, 1980; Chase and Chase, 2005), inter-site warfare (Webster, 2000; Inomata, 2008), changes in trade routes (Demarest et al., 2014) or pathological ideological systems (Dornan, 2004; O'Mansky and Dunning, 2004); and (ii) environmentally related, which includes soil erosion (Beach and Dunning, 2006; Anselmetti et al., 2007), volcanic activity (Gill and Keating, 2002; Tankersley et al., 2011), deforestation (Oglesby et al., 2010; McNeil et al., 2010), diseases (Acuna-Soto et al., 2005) and climate change induced drought (Hodell et al., 2001; Haug et al., 2003; Hodell et al., 2005; Gill et al., 2007; Webster et al., 2007; Medina-Elizalde

et al., 2010; Medina-Elizalde and Rohling, 2012; Kennett et al., 2012; Douglas et al., 2015).

Concomitant with present day concerns with climate change, the drought hypothesis for the Maya collapse has received significant attention in recent years. A strong case has been made for climate change and drought as the main contributing factors towards the collapse of the Lowland Classic Maya; however, single-factor explanations of the collapse can misrepresent the underlying complexities of the Maya socio-environmental system, which shows a wide range of diverse features over space and time (Aimers, 2007; Dunning et al., 2012; Turner and Sabloff, 2012).

Some researchers have been more skeptical with regard to the significance of drought episodes in the context of the Maya collapse; Robichaux (2002); Aimers and Hodell (2011); Dunning et al. (2012) argue for the need of a more integrated understanding of the socio-cultural processes along with environmental constraints. This view is supported by Robichaux (2002) who highlights that the initial signs of collapse are also present in water-advantaged areas.

Rosenmeier et al. (2002) distinguish two possibilities for explaining observed isotope concentrations in Lake Salpetén, Guatemala: either greater aridity or decreased water intake by the lake due to forest recovery (which implies previous deforestation). Aimers and Hodell (2011) points out that some climate data has been highly localised, and this prohibits us from generalising across length scales of several thousand miles. Also, even though some experimental methods provide annual resolution in the data collection, this does not guarantee annual accuracy.

Furthermore, the calibration between proxies and actual rainfall is not necessarily exact. Luzzadder-Beach et al. (2012) show that site abandonment occurred even in wetlands where effects of drought are not as significant. Carleton et al. (2014) reassess the conclusions of Hodell et al. (2001) and Hodell et al. (2005) and determine that they are methodological artefacts, which casts doubt on the drought cycle hypothesis. While drought and water scarcity certainly played a role in the dynamics of the Maya society, socio-cultural processes are at least equally important and should be quantified (Aimers and Hodell, 2011).

3.2.1 Numerical models of the dynamics of the Maya society

Quantitative modelling of the dynamics of the Maya society has had a sparse history and began with an early model proposed by Hosler et al. (1977), developed within the framework of system dynamics (Forrester, 1961). The model attempts to capture in mathematical form the best of historical knowledge and understanding at the time about the Maya (Coyle, 2000). The model manages this using 40 variables but, despite it's complexity, the model's realism is debatable as it predicts an average life span of

13 years for the Maya, many of whom were building monuments despite the lack of available food. As noted by Sharer (1977), the timescales and dynamics in the model output are not consistent with the actual data.

Hamblin and Pitcher (1980) incorporate different hypotheses into one-equation models regarding monument building at Maya sites and find that the class conflict hypothesis of collapse fits the data best. Compared to Hosler et al. (1977), the models of Hamblin and Pitcher (1980) are much simpler and "the attempt to cast explanations of collapse into mathematical form points the way for the next generation of collapse models" (Lowe, 1982, p. 643). Despite a good fit to data, the models lack a good fit between their conceptual and mathematical elements because the same mathematical relationship can be used to support completely different views of the collapse (Lowe, 1982). Furthermore, the models lack any feedback between their variables and are therefore too simple to capture enough systemic features of Maya society to provide an accurate description of it or at least allow for a univocal interpretation.

Several system dynamics models, similar in spirit to Hosler et al. (1977), have recently been developed. The focus of these models is the demographical evolution of the Maya (Forest, 2007; Bueno, 2011; Forest, 2013). While all these models attempt to capture societal feedbacks and features of the Maya society, their validity is questionable. The models of Forest (2007) and Forest (2013) conclude that either involvement in warfare or climatic variations are sufficient to account for the collapse. However, the model of Forest (2007) shows that population is close to maximum before 600 CE and that the population levels undergo a boom-bust cycle of 800 years, while the results of Forest (2013) show a collapse before 800 CE and population cycle of 600 years. Both outcomes are inconsistent with reconstructed time series of the archaeological record (Folan et al., 2000, p. 12). In contrast, the model of Bueno (2011) shows qualitative agreement with the archaeological data on the overall trend of population levels. However, the model proposed by Bueno (2011) is highly sensitive to parameter changes. A critical parameter is the fraction of population engaged in warfare. Above a certain threshold, not enough people would be available to harvest and produce food, leading to a collapse. Such high sensitivity of behaviour based on a single parameter is unrealistic, as it suggests that the society could have averted collapse by slightly reducing its army.

More recently, Kuil et al. (2016) developed a dynamical socio-hydrological model to examine the impact of water scarcity on the Maya in the Classic Period (400-830 CE). A main result of the simulations is that a modest reduction in precipitation could have led to an 80% reduction in the population. Nevertheless, they point out that the population density and sensitivity of crops to variations in precipitation may have had an equally important role. The model has findings consistent with the archaeological record of population growth and decline. However, Kuil et al. (2016) recognises that the model outcomes show sensitivity to its parameters and inputs to an extent to which reliable predictions are difficult to make.

In addition to ODE-based models assuming large well-mixed populations, spatially resolved agent-based models (ABMs) are an alternative approach, which might be more suitable to account for the diversity in Maya society (Lucero, 1999). Heckbert (2013) makes an ambitious attempt at integrating and quantifying many features of the environment and Maya society. Settlements are represented as agents that develop in a spatial landscape, which itself evolves in response to climate and anthropogenic effects. The richness of the model allows many elements of physical and social reality to be explored, but there is little empirical evidence to validate all the features of the model (Heckbert, 2013). The calibration, verification and validation of ABMs are troublesome, and insights into the real system are not straightforward (Crooks et al., 2008). Ideally, the complexity of a model should rise in proportion to gains in explanatory power. It is not clear if ABMs offer the best balance in this regard when considering the Maya society, and given the sparsity and uncertainty of empirical data, we prefer a more parsimonious modelling framework.

None of the studies mentioned above perform an explicit comparison to historical data; hence, our discussion is based on our own independent comparison between the model output presented in the articles and the data from Folan et al. (2000). The model we propose is specified as a dynamical system. As we have seen, early models of this type (Hosler et al., 1977) did not match known demographic developments from the archaeological record. More recent models (Bueno, 2011; Kuil et al., 2016) agree to a good extent with data on overall population trends over time. However, they all show a sensitivity to changes in parameters that precludes robust prediction making. Furthermore, they do not address the issue of monument construction, which could prove important in constraining model dynamics. In contrast to previous approaches, we explicitly compare our model output with the archaeological record for population growth (Folan et al., 2000) and monument construction (Erickson, 1973) and find a very good fit to data. Furthermore, we show that the collapse can be understood to be driven by a supercritical Hopf bifurcation and we provide a comprehensive sensitivity analysis which shows that the modelling outcomes are robust under changes in parameters.

3.3 Quantifying Maya society and environment

We provide a concise model of Maya society and their human-environment interaction. We capture portions of the population engaged in mainly agricultural and monument building activities, undertaken within a representative site of 1000 $\text{km}^2 (\simeq 32 \times 32\ \text{km}^2)$ of agriculturally productive land.

The model consists of the set of ordinary differential equations (3.1). Table 3.1 lists all the parameters of the model and their values. We divide the population into three occupations: workers in swidden agriculture x_s, intensive agriculture x_i and monument

building x_b. The environment is modelled simply as one stock, namely the food production capacity of the land, labelled y, and the number of monuments built in the region is z. At least 70% of the Maya population was involved in agriculture (Diamond, 2005). Given the scope of the model, this is the part of the population of highest interest because the agricultural activity and related practices likely had the largest impact on the environment (Turner, 1974; Webster, 2002).

Beyond agriculture,Becker (1973) identifies six specialisations of the Classic Maya at Tikal, four of which are directly related to stone work (or likely so) and the other two are woodworking and pottery. Hence, by considering agricultural and monument related practices we cover most of the activities the Maya were involved in.

We do not try to capture the administrative, military or artisan aspects of the society. Compared with the segments of the population we do include, these occupations made up a much smaller part of the demography. Assuming that the environmental impact of the people in these professions derived mainly from food requirements, the model can easily be extended to account for these parts of the population, though their roles would otherwise remain inert within the model's scope. The above considerations can be taken as forming the model's boundary, and while they do limit the internal dynamics of the model, the choice of boundary is informed by the data we have and the time series we aim to explain/reproduce.

Concretely, the dynamical model we propose is given by

$$\begin{aligned}
\dot{x}_s &= [(1-\tau)+\tau p_s]\beta n x - \beta n^{-\delta} x_s + \sigma[(1-\theta(n))x_b - \theta(n)x_s] \\
\dot{x}_i &= \tau p_i \beta n x - \beta n^{-\delta} x_i \\
\dot{x}_b &= -\beta n^{-\delta} x_b - \sigma[(1-\theta(n))x_b - \theta(n)x_s] \\
\dot{y} &= w_t r y(1 - y/(w_t K)) - s d n x \\
\dot{z} &= b x_b - m z
\end{aligned} \tag{3.1}$$

where x, n, and $\theta(n)$ are given by:

$$\begin{aligned}
x &= x_s + x_i + x_b \\
n &= w_t \frac{x_s + \alpha x_i}{x_s + x_i + x_b}(1 - e^{-y/(w_t c K)}) \\
\theta(n) &= \frac{1}{1 + e^{-2k(n-n_b)}}
\end{aligned} \tag{3.2}$$

Above, x represents the total size of the population, n is the food available per capita and $\theta(n)$ is a smooth approximation of the step function ($k = 1.5, n_b = 2$), where n_b parameterises the required minimum food availability for people to change their activity towards monument building and k controls the steepness of the step function $\theta(n)$.

Type	Symbol	Meaning	Values
Population parameters	β	Natality scale factor	0.0014
	δ	Death rate exponent	0.08
	p_s	Prevalence (popularity) of swidden agriculture	1 or 0.27
	p_i	Prevalence (popularity) of intensive agriculture	0 or 0.73
	t_T	Year of transition	550
	τ	Transition switch	0 or 1
Resource parameters	r	Land recovery rate (1/yr)	0.045
	K	Maximum available land (ha)	100,000
	c	Threshold fraction of land	0.2
	w_t	Relative precipitation at time t	1 ± 0.5
	d	Land depletion rate	0.007
	α	Relative productivity of intensive agriculture	20
	s	Swidden productivity (ha/pers/yr)	0.5
	t_P	Year when precipitation changes	800
Monument parameters	b	Builder productivity (monum/pers/yr)	0.00006
	m	Monument decay rate (1/yr)	0.00015
	σ	Diffusion coefficient (1/yr)	0.1
	k	Step function stepness	1.5
	n_b	Minimum food availability for monument building	2

Table 3.1: Parameters for the Maya model (3.1). The values of β and K set the scales in the model and are chosen to simplify presentation and analysis; r, α, s are set to match values from the literature (Turner, 1976), and similarly for w_t, t_P (Haug et al., 2003; Medina-Elizalde et al., 2010; Medina-Elizalde and Rohling, 2012). Other parameters are subject to constraints: literature on soil management suggests a lower bound for $1/rd$ of 7 (USDA Survey, 1962, pp. 20-21), the parameter c signals scarcity of food, so we expect it to be below 40%, the diffusion coefficient σ has at most a value of 1 and monument building would not occur if food per capita would not be sufficiently high, so we estimate $n_0 \geq 2$. The values of d, c, σ and n_b were chosen to satisfy the constraints but also numerically optimised. The parameters δ, b, k are determined solely by numerical optimisation, see Appendix E. The parameters p_i, t_T are optimised but also consistent with values in the literature, see section 3.4.

The model can be interpreted as follows: People are born into certain agricultural specialisations, determined by fractions given by p_s and p_i. They then harvest resources at a rate specific to their specialisation, i.e. proportional to s for swidden or αs for intensive agriculture. The harvested amount provides food which, if in surplus, positively affects the population growth rate. If the harvest is insufficient to meet basic requirements per capita, then the population will start to decrease. Left alone, the land's productive capacity regenerates within a characteristic time of $1/r \simeq 22$ years, but a given patch can only be harvested up to 7 consecutive years using intensive practices before crop failure.

Thus, there exists a negative feedback loop between population and environment, reflecting a Malthusian mechanism. A higher availability of resources leads to higher population, which leads to a more rapid depletion of the resource base that later impacts the growth rate of the population. As we will see, due to land overuse, an increase in the number of workers in intensive agriculture leads to a loss of production capacity in the long term, and subsequently to a demographic decline.

If the food available per capita is high, then a part of the swidden workers move into monument construction. Monuments are built in proportion to the number of builders available, but they also decay slowly in time. If the harvest has poor yield, builders go back to practicing agriculture to compensate. Thus, a higher agricultural yield leads to a higher population and to a higher rate of monument building. The building of monuments does not have a direct effect on the population within the scope of our model.

We next outline the features of the model more precisely. The first three equations of model (3.1) dictate the population dynamics. The β parameter sets the scale for the first two terms, which represent the natality (birth and death) rates. The first term in each of these equations represents the crude birth rate, which we assume is proportional to: the total population x, the available food per capita n and the parameters p_s, p_i, which represent the proportion of each new generation that go into the respective occupations. Birth rates are often assumed in the literature to be proportional to the present population (Turchin, 2003a) and also to be monotonically increasing functions of the food per capita (Anderies, 1998; Motesharrei et al., 2014). The parameters p_s and p_i (which add up to 1) can be interpreted as the prevalence (or popularity) of swidden and intensive agricultural activities in the society.

In addition to these more conventional aspects, the birth rates feature the binary τ parameter, which is either set to 0 (before the onset of intensive agriculture) or to 1 (after the onset) and thus models a rapid change in the p_s, p_i parameters; see section 3.4 for more details.

The next term in the equations for the population dynamics is the death rate, which is also assumed to be proportional to population size. A natural candidate for the death rate's dependence on food availability is $n^{-\delta}$; this is because if there was no food, the population would quickly decline to zero, which means the death rate would grow very large (or even diverge) as $n \to 0$. For example, a death rate proportional to n^{-1} has been previously used in the World2 model by Forrester (1971).

The last term in the population equations is a diffusion term that models movement of people between two different specialisations: swidden agriculture and monument building. We assume that monument building will only take place if surplus production exists to support it. Specifically, if the food availability is high ($n > n_b = 2$) then enough surplus production exists to support non-agriculturally related activities and a shift of work

from purely subsistence based agriculture to monument building is modelled via the diffusion terms in Eq. (3.1). Once $n > n_b$, then $\theta(n) \simeq 1$ and people move (diffuse) from practicing swidden agriculture to building monuments. If $n < n_b$, then $\theta(n) \simeq 0$ then the opposite effect occurs. The σ parameter, which represents the diffusion coefficient, has an upper bound of 1 as we cannot have a population flow of over 100% within a year. We use a value of σ of 0.1 as determined by numerical optimisation (see section 3.4), implying that 10% of the population in a given specialisation changes to a different occupation within a year conditioned on the availability of food (as discussed above).

The movement between specialisations typically takes place much more rapidly (or on a shorter timescale) then the demographic growth of each specialisation. This has led us to make two simplifying assumptions in the model. First, the equation for x_b does not feature a birth rate term, and second, there is no movement (via diffusion) to intensive agriculture. Regarding the first simplification, it is possible to set the prevalence parameter of monument building activity to zero and not significantly affect the model dynamics. The birth rate term for the x_b variable (number of builders) would be dominated by the diffusion dynamics. Because of this, we chose to eliminate one parameter (the prevalence of monument building) and set it to zero. The second simplification is justified because the movement to intensive agriculture requires a large initial investment to be undertaken (allocation of land, building of terraces etc.). Therefore, it is unlikely that intensive practices can be picked up quickly. Due to sunk-costs effects (Janssen et al., 2003), once such a large investment is made, it is unlikely that the activity will be immediately abandoned for alternatives. Hence, we decided not to implement a diffusion mechanism towards or away from intensive agriculture.

The fourth equation of (3.1) models the resource dynamics. The first term follows the usual logistic dynamics and describes how resources recover over time while the second term captures the harvesting activity of the population. The production capacity y is a renewable resource that regenerates with a characteristic timescale of $1/r = 22$ years, which is consistent with the typical time between harvests in swidden agriculture (Turner, 1976). Left unexploited, resources will return to their maximum values within a matter of decades. This is likely what also happened in reality after the collapse, with the Maya environment today in good condition (Turner and Sabloff, 2012).

The Maya employed a wide range of agricultural techniques (Turner, 1974) and we do not attempt to capture the full complexity of their endeavours. The work of Turner (1976) suggests that agricultural practices are polarised into two categories, with short (up to two years) and long (1-2 decades) cycles. Thus, for simplicity, we distinguish two categories: swidden agriculture with a full harvesting cycle of 20 years and intensive practices with a cycle of 1 year. Intensive practice is not equated to short-fallow swidden agriculture, but represents an aggregated activity of the diverse types of methods that were used. The average amount of land per year that a person requires to fulfil their caloric needs is 0.5 hectares (Turner, 1976). Hence, we can measure the food production

capacity of the land y in hectares and set its initial value to $K = 100,000$ hectares, which is the size of the region we are modelling.

In the presence of a human population, the production capacity y decreases in proportion to the number of agricultural workers and their productivity. We take the productivity per capita of swidden agriculture to be $s = 0.5$ ha/yr/pers., which is the minimum value it can have to meet subsistence needs. For intensive agriculture, the harvest takes place annually, which is reflected in the model by assigning a productivity that is $\alpha = 20$ times higher than that for swidden practice. The depletion parameter d is chosen such that the average number of consecutive times a piece of land can be re-harvested until it is completely depleted by intensive practices is $1/(\alpha d) \simeq 7$ times. Soils of high productivity and less prone to erosion than the ones found in the Yucatan peninsula can be re-harvested for a maximum of 7 consecutive years, while still giving good yields (USDA Survey, 1962, pp. 20-21). Our choice of d thus reflects an optimistic lower bound on depletion rates of the Maya environment. Wilk (1997, p. 84) highlights the fact that even with good soil quality, such as enjoyed by the Mopan community of San Antonio, serious problems start to emerge once fallow cycles are shortened to five years or less. Depletion in our case refers only to the amount of food that can be produced (e.g., crops that can be harvested) and does not strictly refer to the state of the soil. Soil depletion varies widely throughout the Lowlands (Beach and Dunning, 2006) and its variation is too complex of an issue to capture in such a simple model.

When production capacity y is high, the resource extracted per worker is roughly constant (but depends on the type of agricultural activity). This assumption has been previously used in models of Easter Island (Basener and Ross, 2004; Basener et al., 2008) and warfare dynamics (Turchin, 2009). Nevertheless, once the production capacity of the land decreases below the threshold of $c = 20\%$ of the maximum K, productive land becomes increasingly sparse, which leads to a decrease in food production per capita. This dynamic is implemented through the exponential term in the definition of the food availability per capita n, see equations (3.2). When $y \to 0$, the extraction term of natural resources becomes, to first order, a predator-prey term as found in the Lotka-Volterra model (i.e., type I functional response). Because the c parameter signals scarcity of food, we expect it to be below 40% and through numerical optimisation the value $c = 20\%$ was determined.

A particular feature of the resource dynamics is the effect of precipitation. The absolute levels of rainfall are not relevant to the model; what is important is only how the relative variation of the amount of water impacts the different parameters in the model. There are three aspects directly related to rainfall: (i) the rate of resource regeneration r, (ii) the maximum amount of productive land K and (iii) the extraction term of natural/agricultural resources. Reductions in the amount of available water will reduce the rate of regeneration of the environment, only allowing for recovery to a smaller carrying capacity and also impede efforts to exploit it. The proposed model accounts

for all three effects. For simplicity, we assumed the effects to be linearly proportional to w_t, which is the relative amount of precipitation at time t. Thus, normal precipitation conditions correspond to $w_t = 1$. Deviations from this assumption are explored in Appendix E, Fig. E.1(e). Different areas of the Lowlands were subject to different exogenous factors, which, besides precipitation, also include volcanic ash (Tankersley et al., 2011). The effect of an exogenous contribution to environmental recovery, such as volcanic ash, can be incorporated in the model a similar way to precipitation. We can thus interpret the precipitation scaling factor w_t as an aggregate of external effects on resource recovery and use.

For clarity, the variable y is interpreted as the agricultural production capacity of the land, but the logistic equation for the growth of y only represents the dynamics of a renewable resource, which could equally represent forest resources. Also, the terms of the model dictating resource exploitation are not univocal in regard to their interpretation. Strictly, we can only say that we distinguish between low intensity and high intensity resource extraction. For concreteness, we associated the low intensity activity with swidden agriculture and the high intensity activity with intensive agriculture. The factor of $\alpha = 20$ between the intensities of the extraction activities is taken to match the relative difference between annual harvesting and swidden practice, but this might be seen as only one instance of a wider variety of low and high impact environmental activity. Thus, the variable y can more generally be interpreted as an aggregate of renewable resources, which can include output of agriculture, forestry and fishing. Then, the extraction activity can be seen as the exploitation of a set of resources, which has a positive effect on birth rates. As food security studies on modern agricultural Amazonian societies (Ivanova, 2010; Piperata et al., 2011) explain, the primary source of energy (caloric intake) is from agricultural products. Dietary diversity increases the nutritional content of an individual's intake, but does not contribute greatly to the overall caloric quantity. Because of this, and the important role energy has in societal development, we emphasise this agricultural interpretation of the stocks and parameters.

The last equation of (3.1) describes the dynamics underlying monument building. Monuments are constructed at a rate proportional to the number of builders. The productivity b of a builder is chosen such that 1000 people working for ~ 17 years would build on average one medium-sized monument. The monuments decay at a rate $m = 0.00015$, which implies a half-life of approximately 5000 years. The half-life is estimated based on observed weathering rates of 0.2 millimeters per century for Maya buildings of the Uxmal site in Yucatan (Roussel and André, 2013) and the assumption that a cumulated weathering of ~ 1 centimeter would compromise the structural integrity of a monument. In addition to our proposed equation for monument building, we have also considered another option that implements a minimum threshold of workers required to start construction, with increasing returns to scale. But, the output of the model does not change significantly, see Appendix D.

The model omits several features of the Maya society amenable to dynamical system modelling, e.g., war (Webster, 2000; Martin and Grube, 1995), water management (Lucero et al., 2011), and finer details of agricultural intensification (Johnston, 2003). The time period we model covers over 1000 years, so we strive to capture feedback mechanisms persisting over the longest timescales. Our assumptions prove sufficient for the model to reproduce historical patterns and so, the simplified treatment can be justified in the interest of parsimony.

The above specifications outline the model's main assumptions and dynamics. While they likely leave out some aspects of the real world's complexity, it is important to start from the simplest formulation that remains faithful to reality, namely one that captures the elements at play in long-term feedback and that also proves sufficient at explaining the data.

3.4 Methodology and results

We search for a calibration of the model proposed in section 3.3 that can give a good match to empirical data. More specifically, we determine the parameters that minimise the deviation of the model output with respect to the empirical time series for the population levels, birth rates (Folan et al., 2000), and monument building rates (Erickson, 1973). Depending on the model structure, deviations will not necessarily be small, hence, even with a optimal choice of parameter values the actual fit to the historical time series might be very poor. Also, even if the fit to the time series is excellent, there is no certainty that the numerically optimised parameters are realistic or match archaeologically determined values. Thus, we can validate the model by comparing the optimal parameter values with archaeological estimates as well as performing sensitivity testing. Thus, if the model predictions fit the empirical data well, with results largely insensitive to changes in parameters, and if parameter choices are consistent with archaeological estimates, then we can conclude that that proposed model is partially validated and is a viable theory for the historical processes it aims to capture.

More specifically, we aim to reproduce the historical evolution of: (i) the crude growth rates and population levels reconstructed by Folan et al. (2000) from Santley (1990), and (ii) the data on monument building rates from Erickson (1973). We refer to the time series in the data as reference modes. The scope of the model is dictated by the reference modes we wish to reproduce. Thus, the temporal limits are set between 0-1400 CE with regard to population dynamics, while for the monument building activity we focus on the time span between 400-900 CE (when most monuments are dated).

We can see in the time series of Folan et al. (2000) that the demographic evolution at many sites followed a similar pattern. Thus, instead of focusing on one specific region, we aimed at developing an abstract model that captures demographic commonalities of

several regions. The dynamical system model (3.1) we propose is intended to capture this prototypical dynamics that occurred in different regions. The reference mode for the population in Fig. 3.2(b) was generated using the reference mode for the overall crude growth rate observed in the south-central Maya lowlands in Fig. 3.2(a) (Folan et al., 2000, p. 13) and matches well to population development seen at Tikal and Calakmul (Folan et al., 2000, p. 12).

When analysing the data for the crude growth rate, see Fig. 3.2(a) (solid line), we can distinguish two regimes: an early regime where the birth rate was decreasing, indicating convergence towards an equilibrium (a sustainable outcome); and a later boom-bust regime, when the birth rate increased dramatically and subsequently crashed. We take the initial conditions such that the total population is 10,000, and the Maya had 90% of the population working in swidden agriculture and 10% in intensive agriculture. We assume that initially, because food requirements were met and intensive agriculture meant more effort, no new people would go into intensive practices, which means $p_i = 0$ and the extent of those activities was gradually declining. This leads to an initial decrease in the available food per capita and hence also of the birth rates, which corresponds to the first regime in the reference mode of Figs. 3.2 (a), (b). If this pattern had continued we would see only a modest rise in the population levels of the Classic Maya, see Fig. 3.2(b) (dotted line). Hence, we assume that the transition between the two regimes corresponds to a change in the occupations and agricultural practices of the society. Thus, from a certain time (t_T) a fraction (p_i) of each new generation starts practicing intensive agriculture.

We can numerically determine the optimal values of t_T and p_i that minimises the deviation of the model output from the historical data. We measure the deviation of model output from historical data as follows. Let $x = x_s + x_i + x_b$ be the total population, and let x_{ref} be the total population of the reference mode of Fig. 3.2(b). We define the following distance function to determine how far apart the total population from the model output is from the reference mode for the population (where $T = 1340$ years):

$$D(x, x_{ref}) = \frac{\int_0^T |x(t) - x_{ref}(t)|dt}{\int_0^T x_{ref}(t)dt} \tag{3.3}$$

The distance (3.3) is the L_1 metric divided by the area under the reference mode. The numerator of (3.3) measures the sum of all the areas where the curves of the model output and the reference mode differ. So, if $D(x, x_{ref}) = 0$, we would see a perfect fit between model predictions and historical data. A distance function similar to (3.3) can be defined between the building rate of monuments and the reference mode in Fig. 3.3(a).

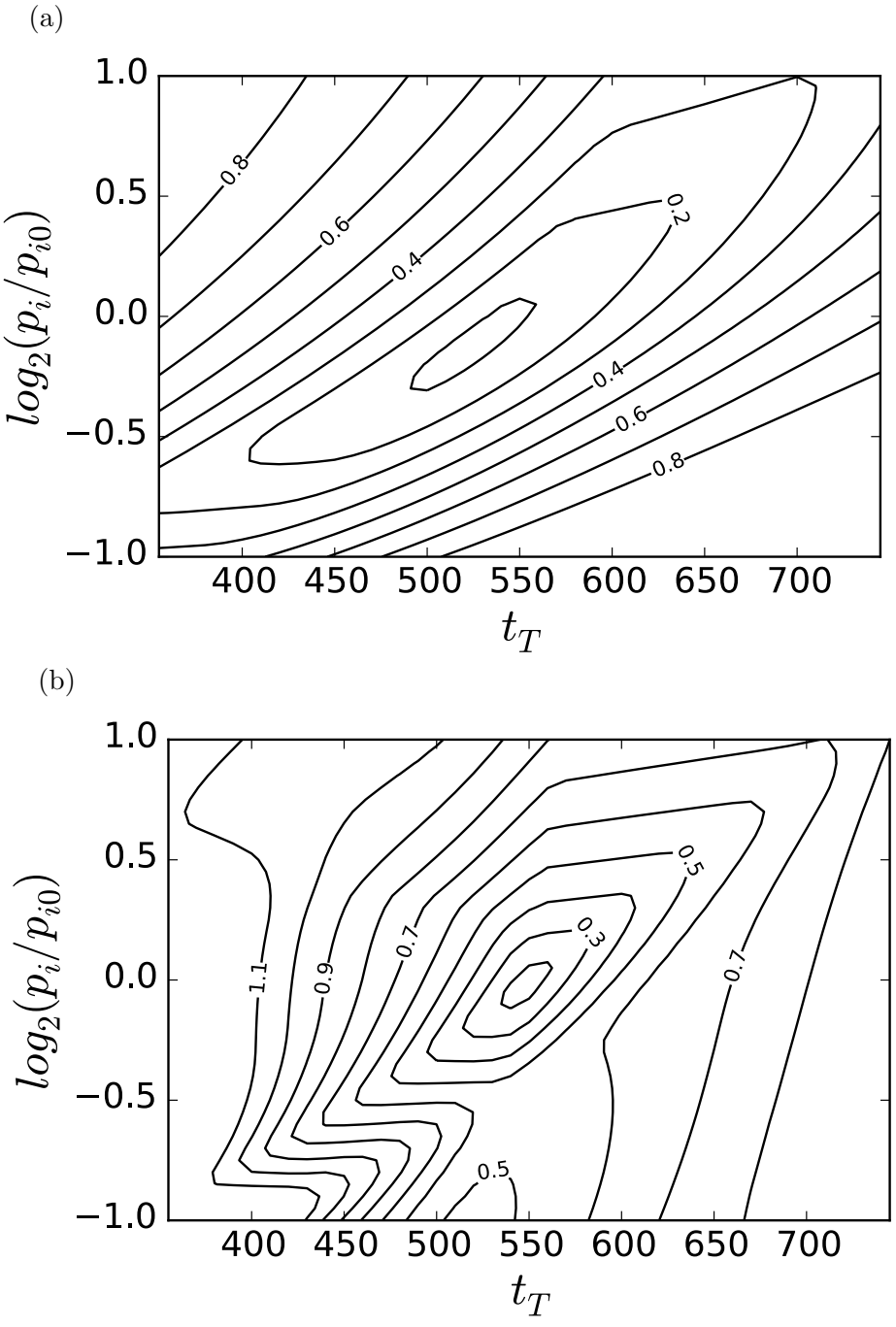

Figure 3.1: Level sets corresponding to the deviation of: (a) simulated total population (3.1) and the reference data from Fig. 3.2(b), (b) monument building predicted by model (3.1) and the reference data of Fig. 3.3(a). For p_{i0} cf. Table 3.1.

If we vary p_i by a factor of two above and below the entry in Table 3.1 and similarly vary t_T in the range of $350 - 750$ CE, and then plot the distances from the reference modes for the population levels and monument building rates, we obtain the contour plots visualised in Figs. 3.1(a), (b). We see that the parameter values in Table 3.1, namely $t_T = 550$ and $p_i = 73\%$, achieve a global minimum for the distance of the model output

from both the population levels at $\simeq 10\%$ and monument building rates at $\simeq 15\%$. All other neighbouring values show an increased deviation from either the population or monument data.

Hence, historical data cannot be reproduced, unless a change in agricultural preferences around the year $t_T = 550$ CE is assumed (which we model by changing the parameter τ from 0 to 1).

Thus, to explain the sudden rise in birth rates, assumptions about a dramatic change of the prevalence (or popularity) of intensive agricultural practices are required. This is reflected in the model by a shift of the initial prevalences $(p_s, p_i) = (1, 0)$ to $(0.27, 0.73)$ from the year 550 CE onwards; by attracting a larger share of new workers, intensive agriculture gradually became more widely used to the detriment of swidden practice. This leads to an increase in food production, which allows for an increase in the population.

With the optimal values for t_T and p_i, the model reproduces the population levels and (relative) crude growth rates very well, as seen in Figs. 3.2(a), (b). The maximum population density reached is around $100/\text{km}^2$, which is consistent with the estimates of (Turner, 1974). In addition to good agreement with the population reference modes, the model is also in good agreement with the data on monument building rates from Erickson (1973), especially in the time range of 600-850 CE, shown in Fig. 3.3(b). Moreover, the final density of monuments obtained in the model is consistent with the observed density in areas such as Tikal, see Fig. 3.3(b).

Furthermore, the values we obtain for p_i and t_T are consistent with the literature on the Maya. We know that at least 70% of the Maya were involved in agricultural production (Diamond, 2005), which is consistent with our estimate of p_i of 73%. The agreement between our result $p_i = 73\%$ and Diamond (2005)'s estimate can be attributed to the fact that intensive agricultural techniques are more likely to have a lasting environmental impact (Turner, 1974), and hence any estimate of the farming population is more likely to be more representative of the fraction involved in intensive practices. The year $t_T = 550$ corresponds to the start of the Late Classic period according to Lucero (1999, p. 212) and Estrada-Belli (2010, p. 3).

The change in the prevalence of activities (p_s, p_i) during the transition leads to changes in the population stocks, as Fig. 3.4(a) shows. A much larger fraction of the population becomes involved in intensive agriculture, reaching 63%, while the fraction practising swidden falls to 37%, see Fig. 3.4(b). The final fractions shown in Fig. 3.4(b) approach the prevalence parameters p_s, p_i.

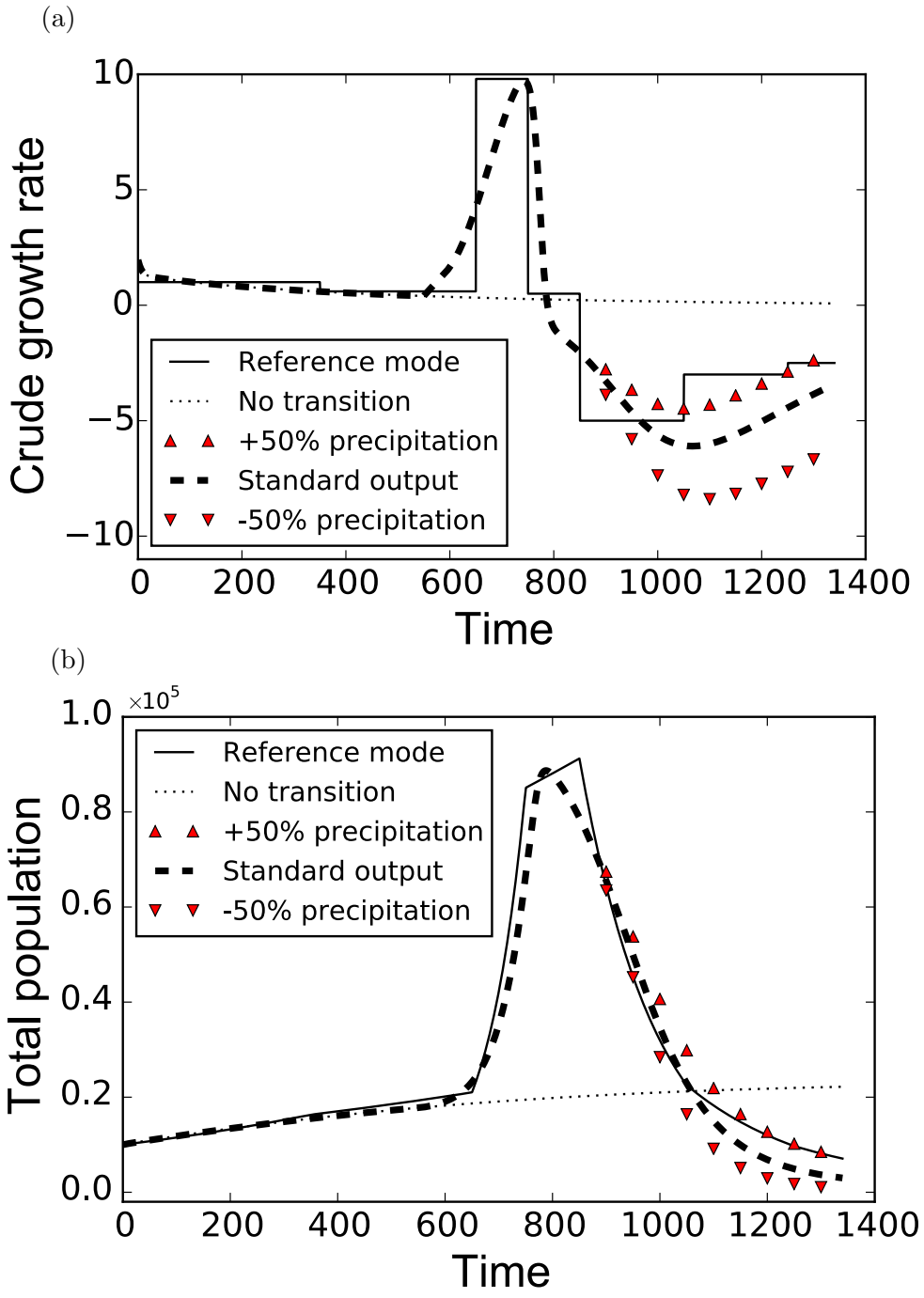

Figure 3.2: Model predictions for (a) relative crude growth rates and (b) total population when precipitation is: normal (dashed line), enhanced by 50% (triangles) and reduced by 50% (inverted triangles). The standard output in (a) is fitted to the historical reference (continuous line) for crude growth rates from Fig. 1.3 of (Folan et al., 2000, p. 13), reconstructed from (Santley, 1990, p. 343). The population reference (continuous line) in (b) is generated from the crude growth rates in (a). Population levels are similar to those seen at Tikal and Calakmul from Fig. 1.2 of (Folan et al., 2000, p. 12), reconstructed from (Santley, 1990, p. 342). For comparison we also show the (simulated) case under the assumption of no shift in agricultural activity and normal precipitation (dotted line).

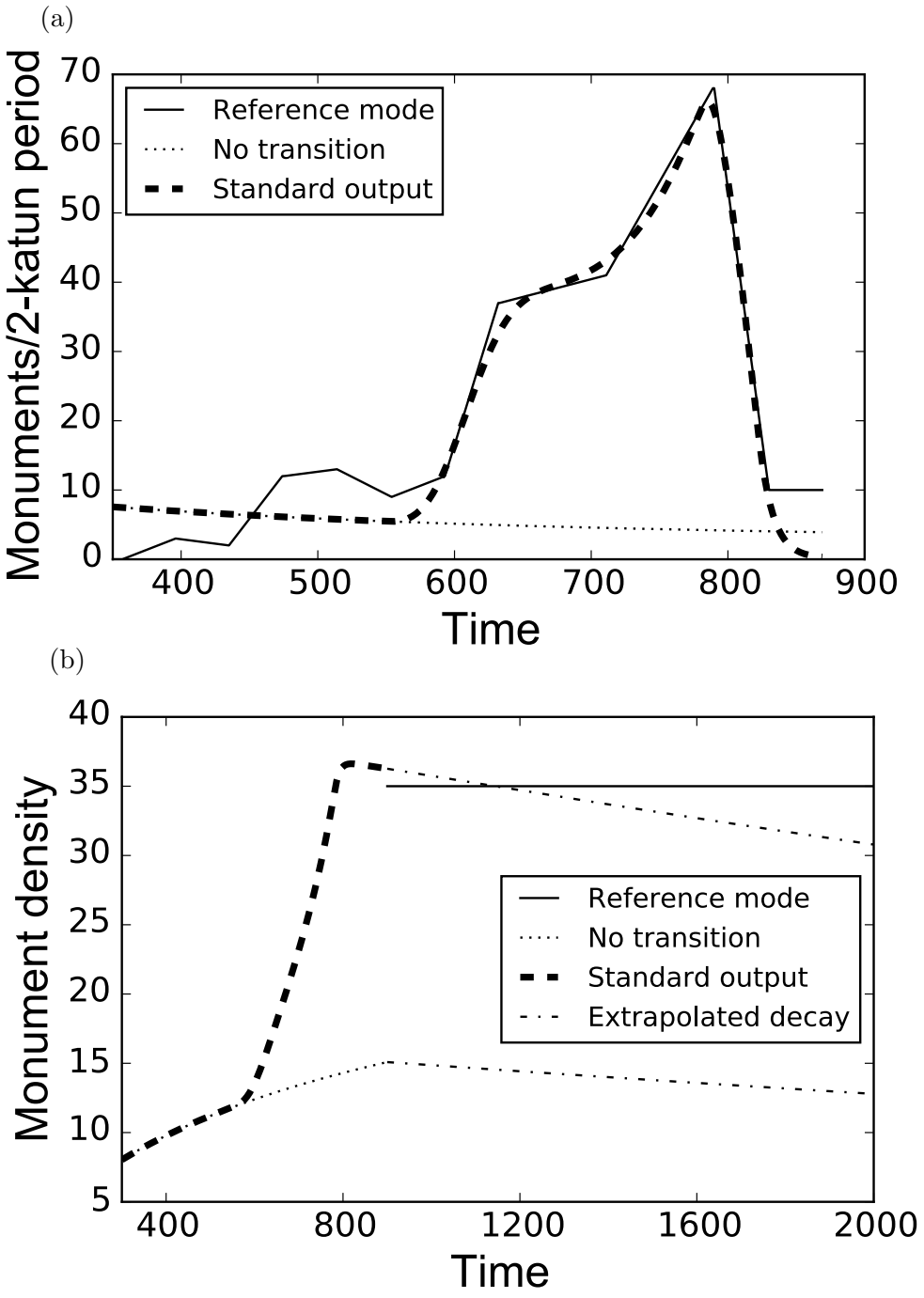

Figure 3.3: Model predictions for (a) monument building rates and (b) monument density in the case of normal precipitation with agricultural transition (dashed line) and without (dotted line). From 900 CE onward no significant building activity was undertaken and monuments only decay exponentially with constant rate (dash-dot line). The standard output in (a) is fitted to building rate data (continuous line) from (Erickson, 1973, p. 151). A 2-katun period is equal to 39 years. The simulated monument density over time in (b) is compared to the presently observed density in areas such as Tikal, which has approximately 200 monuments (Webster, 2002) over an area of 570km^2, corresponding roughly to 35 monuments per 100km^2 (continuous line).

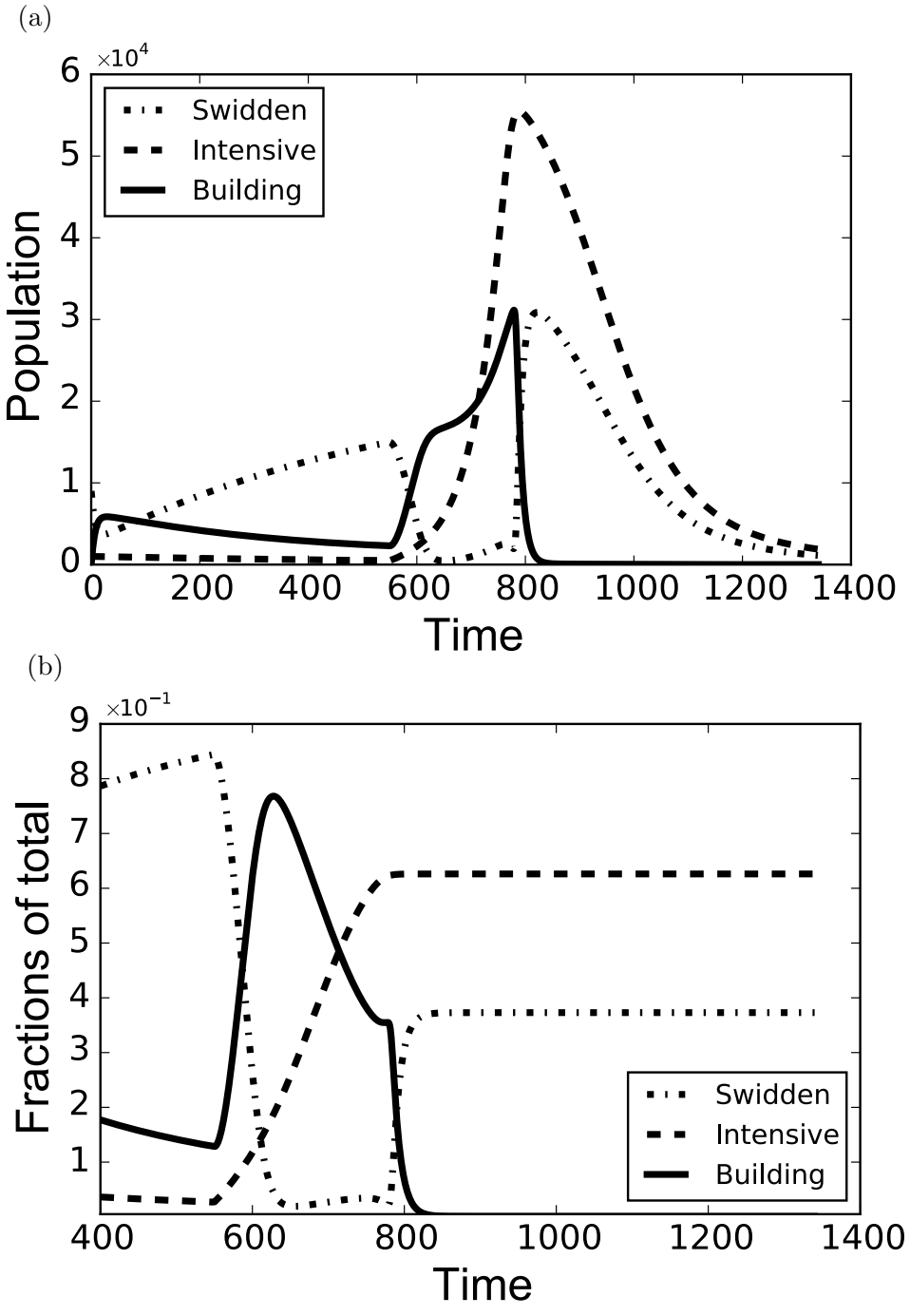

Figure 3.4: Simulated (best fit) model output for (a) the population level and (b) the fraction of the total population for each specialisation: swidden agriculture (dash-dot line), intensive agriculture (dashed line), and monument building (continuous line).

In the long term, the fraction of the population in intensive agriculture does equilibrate to the value of the popularity p_i, as the following calculation shows:

$$\frac{d}{dt}\left(\frac{x_i}{x_s+x_i+x_b}\right)=0 \rightarrow \frac{x_i}{x_s+x_i+x_b}=\frac{\dot{x}_i}{\dot{x}_s+\dot{x}_i+\dot{x}_b} \rightarrow \frac{x_i}{x_s+x_i+x_b}=p_i \qquad (3.4)$$

The approximate values we obtain in Fig. 3.4(b) are due to the transient nature of the dynamics. Hence, it is reasonable to compare p_i with the fraction of the population involved in intensive practices.

In Appendix D, we vary the prevalence parameter p_i and relativity productivity of intensive agriculture α to see how the behaviour of the model changes. When $\alpha \simeq 1$, all the stocks in the model equilibrate to stationary values, which is in line with what we would expect for a society with low, sustainable harvesting rates of swidden agriculture (Nigh and Diemont, 2013). If α exceeds a certain threshold, the system (3.1) undergoes a critical transition that leads to large oscillations in the population levels. Phrased more generally, when the harvesting rate increases beyond a certain point a (Hopf) bifurcation takes place that leads to large amplitude oscillations in the system. A similar conclusion has been reached for another model of a society that has collapsed, namely Easter Island (Roman et al., 2017). The findings here lend support to a more general thesis that societal collapse can be modelled as a certain type of critical transition (supercritical Hopf bifurcation).

A detailed mathematical treatment of the critical transition for a simplified version (without specialisations or monument building) of model (3.1) is also presented in Appendix D and exhibits very similar behaviour to the complete model when varying the α parameter.

In Appendix E, we use the distance function (3.3) for the population and a similarly defined function for the monument building rates to perform a thorough sensitivity analysis for the key parameters in the model, namely all the parameters except β and K (which set the scales in the model). What we find is that with respect to the deviation from the reference modes for the population levels and monument building rates, the model (with the parameters in Table 3.1) lies at a minimum in the subspace of population and resource related parameters $(\delta, r, c, d, \alpha, w_t)$ and close to a minimum in the subspace of monument related parameters (σ, b, k, n_b). The sensitivity analysis also indicates that similar output is obtained for a range of parameters around the standard values in Table 3.1. For changes in the parameters δ, r, c, d, α and water availability w_t, the deviation from the minimum is gradual and quasi-parabolic, while for σ, b, k, n_b, the shallowness of the optima also indicates robustness of the findings to parameter changes.

Furthermore, the optimal values of several important parameters in the model show good agreement of the values with the literature, as is the case with p_i, t_T, α, d. The fact that the model reproduces empirical time series well with optimal parameter values that are consistent with the real measurements indicates that the model structure and the choice of parameter values is viable. Therefore, model (3.1) is partially validated.

Given its critical role in the model, further comments are in order regarding the α parameter. The value of the relatively productivity of intensive agriculture is $\alpha = 20$, which was chosen because the harvesting period of intensive agriculture is on average 20

times less than that of swidden agriculture. For example, swidden agriculture employed different methods with cycles between 5-20 years, whereas intensive techniques ranged between 0.5 to 1 year (Turner, 1976, p. 80). But, as Fig. D.1(a) in appendix D shows, any value for α in the range $2 - 20$ can prove consistent with the archaeological record provided the initial population and land are re-scaled appropriately. Such re-scaling is necessary given the different land requirements and expected population densities for the different agricultural methods (Turner, 1976, p. 80). Fig. E.1(f) does not take such re-scaling into consideration and so, shows an increasing deviation from the reference modes for values of the relative productivity different from $\alpha = 20$.

Model (3.1) also allows us to study the impact of changes in precipitation. A reduction (-50%) (Medina-Elizalde et al., 2010) or increase ($+50\%$) in the available amount of water starting from the year $t_P = 800$ (Haug et al., 2003; Medina-Elizalde and Rohling, 2012) does not impact the population levels to a large extent. As detailed in section 3.3, we have assumed that precipitation directly affects the parameters r and K and the food available per capita n. If a smaller set of possible effects that precipitation can have is considered, then the model output is largely unchanged compared to Figs. 3.2(a), (b). Strictly speaking, a time lag should be included for the impact of precipitation, but we observe that lags (even up to a few years) have little effect on the system trajectory, and we have left them out for simplicity's sake.

It is important to note that in the sensitivity analysis in Appendix E, Fig. E.1(e), we vary the amount of precipitation w_t throughout the entire time span of the model such that we take the year that precipitation changes to be $t_P = 0$. If we consider any other starting time t_P for the precipitation change, the deviation in the model output from the reference mode would be comparable or smaller than that shown in Fig. E.1(e). Hence, irrespective of when the precipitation level changes (e.g., drought occurs), we expect to see either similar results to those discussed above or a larger deviation from the reference mode.

In formulating the model we have not addressed the issue property rights. Wilk (1997, p. 87-88) states that when population density in low, common access is favoured while, when the density is high, private property emerges as the dominant institution. Thus, the population pressure determines the assignment of property rights. Our model then suggests that prior to 550 CE common access was likely used and after, once the population grew, that private land become widespread. As such, property rights emerge from the output of our model and do not have to be explicitly considered in its formulation, which is in contrast to previous literature on the topic that considers it a foundational issue (Anderies, 2000; Reuveny and Decker, 2000; Dalton and Coats, 2000).

While we have assumed that, based on data of Folan et al. (2000), many Maya regions had similar population trajectories, there was, nevertheless, variation in demographic,

geographic and cultural elements occurring both spatially and temporally throughout the many regions (Aimers, 2007; Iannone, 2013). This also leads to asynchronous development and decline of the societies in the different areas (Wahl et al., 2007). For example, the Late Preclassic Maya in the Mirador Basin built some of the largest Maya structures (Dunning et al., 2012; Hansen et al., 2002). In addition to this, evidence of multiple intensive agricultural systems has been found in several Maya regions (Dunning and Beach, 2010). Hence, certain sites show deviations from our modelling assumptions, and hence, also from the model output. Note that our main goal was to reproduce aggregate patterns and that a more integrated multi-regional model would require verification against substantially more fine-grained temporal data of regional interactions (such as trade, warfare etc.).

3.5 Discussion and conclusion

In this study, we presented a low dimensional model with the aim of describing the evolution of population sizes, farming activities and monument building of the Classic Maya society. What insights do we gain? First, we show that a low dimensional model can indeed robustly reproduce demographic and monument building data. To the best of our knowledge, this is the first model of its type that has been validated by direct comparison with historical data and it is worth emphasizing that reproduction of the historical data is possible using a low dimensional model that only captures the most basic feedbacks between population, resources, and monument building activities. More generally, our modelling exercise suggests that, instead of building very detailed models that incorporate complex explanations of collapse, a better methodological practice is to attempt a simpler explanation or model as we have done here.

Second, the model indicates that a change in the practice of intensive agriculture in the Maya society around the year 550 CE is an important contributing factor to the collapse. It is important to note that our model formulation allows for a change in agricultural practices. However, the precise location of this shift in time is a direct result of optimization and shows that (within the scope of this class of low dimensional models) reproducing demographic and monument building dynamics is only possible if such a shift occurred at 550 CE. The year 550 CE is around the beginning of the Late Classic (Lucero, 1999; Estrada-Belli, 2010), a period which saw unprecedented expansion of the Maya, not only demographically, but also culturally. The model thus provides a mechanism by which this Golden Age and its later collapse can be explained.

The shift to intensive agriculture does not mean that the Maya forfeited their knowledge of environmental management, as most areas continued to adapt to their local conditions by using different techniques (Dunning and Beach, 2003), but a change large enough to forgo the established equilibrium is likely to have taken place. Why would this occur?

Most individuals would not typically pursue intensive forms of agriculture (Russell, 1988), despite being more productive, due to its taxing and time consuming nature (Boserup, 1965). Additional drivers are needed for the activity to become commonplace. We can only speculate on the likely reasons: (i) governing policy (e.g., in case of war), (ii) higher real or perceived degree of wealth in neighbouring regions, (iii) trading benefits and (iv) ideological (religious, political etc.) determinants, of similar nature to those described by Demarest (1992).

Third, the model brings into question the role drought played in the collapse. Drought is often named as the cause or a major contributing factor of the Maya collapse with recent estimates indicating up to a $40-50\%$ reduction in annual precipitation (Medina-Elizalde et al., 2010; Medina-Elizalde and Rohling, 2012). Our results indicate that a 50% reduction in rainfall does not significantly alter the outcome of the simulation with respect to the population levels, see Fig. 3.2(b). What the model is showing is that the land's production capacity might have already been severely exhausted and a reduction in crops might have been unavoidable even in the absence of drought. A fall in crop production is consistent with evidence from skeletal remains that show signs of progressive nutritional disease (Folan and Hyde, 1985; Sharer and Traxler, 2006), while at the same time, there are no mass graves discovered that might indicate large scale epidemics or warfare (Folan et al., 2000). Our research cannot be taken as proof, but it does suggest that drought, though important, played a smaller role than previously thought (Hodell et al., 2001; Haug et al., 2003; Gill et al., 2007; Webster et al., 2007; Kennett et al., 2012; Douglas et al., 2015).

Lastly, from a mathematical perspective the shift to intensive agriculture can be seen as a type of critical transition (a supercritical Hopf bifurcation). Specifically, when the harvesting rate of natural resources exceeds a this threshold, the dynamics of the system changes from a stationary state to a situation where large amplitude oscillations in the population are experienced, resulting in a collapse once the amplitude of the oscillations becomes too large and population numbers become too low. This echoes a similar finding for Easter Island (Roman et al., 2017).

The model developed in this study reproduces the general demographic trend seen in many regions of the Lowlands (Folan et al., 2000) by making minimum assumptions regarding changes in agricultural practices. In addition, the model predicts monument building rates that fit well with the time series of Erickson (1973). The model is initialised with the assumption that the society was in a sustainable regime but changes to a much more resource intensive regime to explain the rapid demographic rise. The nature of the transition that the society underwent is consistent with previous finding regarding the dynamics of societal collapse (Roman et al., 2017) and, thus, points to a more general mechanism by which collapse can be understood, namely, as a type of critical transition (supercritical Hopf bifurcation).

In addition, the methodology we employed could be adopted elsewhere and provide similar insights for other historical cases. Our methodology in exploring the parameter space led to a careful alignment of the model parameters with empirical data that has not been achieved before and our sensitivity analysis is more comprehensive than previous literature in this context. The behaviour of the model under changes in parameters shows that it achieves a local minimum in parameter space while staying consistent with estimates provided in the literature.

Prominent explanations of societal collapse throughout time often fall into the trap of preferring one cause, where that cause reflects the current dominant social problem or issue (Tainter, 2006), e.g., climate change or environmental degradation (Diamond, 2005). The case made for climatic variations leading to the collapse of the Classic Maya is in line with modern climate change concerns and highlights a common bias throughout time to single out current problems, project them into the past to function as cautionary tales (Tainter, 2008). On the other hand, if common lessons can be generalised from past cases of collapse, as we have done in this and previous work (Roman et al., 2017), this can provide a valuable insight into our present condition (Tainter, 1988).

We have not tried to single out any one cause for the collapse of the Classic Maya but aimed at identifying a set of interlocking mechanisms that could spur a positive feedback in population growth and monument building. Also, we do not claim to have settled the long-standing problem of the Classic Maya collapse but rather hope to re-balance the discussion regarding the role of drought and socio-cultural factors.

Acknowledgements

This work was supported by an EPSRC Doctoral Training Centre Grant (EP/G03690X/1). The model was implemented and all results were obtained using the Python programming language. No new data was collected by this research.

Chapter 4

Topology-dependent rationality and quantal response equilibria in structured populations

Abstract

Given that the assumption of perfect rationality is rarely met in the real world, we explore a graded notion of rationality in socioecological systems of networked actors. We parametrize an actors' rationality via their place in a social network and quantify system rationality via the average Jensen-Shannon divergence between the games Nash and logit quantal response equilibria. Previous work has argued that scale-free topologies maximize a system's overall rationality in this setup. Here we show that while, for certain games, it is true that increasing degree heterogeneity of complex networks enhances rationality, rationality-optimal configurations are not scale-free. For the Prisoner's Dilemma and Stag Hunt games, we provide analytic arguments complemented by numerical optimization experiments to demonstrate that core-periphery networks composed of a few dominant hub nodes surrounded by a periphery of very low degree nodes give strikingly smaller overall deviations from rationality than scale-free networks. Similarly, for the Battle of the Sexes and the Matching Pennies games, we find that the optimal network structure is also a core-periphery graph but with a smaller difference in the average degrees of the core and the periphery. These results provide insight on the interplay between the topological structure of socioecological systems and their collective cognitive behavior, with potential applications to understanding wealth inequality and the structural features of the network of global corporate control.

4.1 Introduction

Game theory has been a popular tool for modelling decision making scenarios, with applications that vary from understanding economic market forces (Cardell et al., 1997), to evolutionary biology (Nowak and Sigmund, 2004), to political science and considerations of warfare (De Mesquita, 2006). The identification of equilibrium states is a primary concern in the field, a key notion being that of Nash equilibria (Nash, 1950), which represent fully rational outcomes in strategy selection. Nevertheless, actors in the real world deviate from rational behaviour (Nell and Errouaki, 2013).

As a consequence, extended notions of equilibrium are needed to deal with the discrepancies between real and perfectly rational behaviour, and to precisely quantify such bounded rationality. One alternative equilibrium concept is the notion of quantal response equilibrium (QRE), which is given by statistical reaction functions that satisfy certain monotony properties with respect to the payoffs of possible strategies (McKelvey and Palfrey, 1995, p. 10). One possible class of parametric class of functions, which relate to the study of individual choice behaviour (Luce, 2005), define the logit quantal response equilibrium (LQRE). In LQRE a rationality parameter is used to interpolate between Nash equilibria and a uniform distribution over all the possible strategies (McKelvey and Palfrey, 1995). An early use of LQRE was to account for experimentally observed behaviour in choosing strategies when playing the Matching Pennies game (Ochs, 1995; McKelvey and Palfrey, 1995). Since then, the LQRE has found applications in the traditional areas of game theory, including auction theory (Goeree et al., 2002), participation games, e.g., voting (Enriqueta and Thomas, 2004; McKelvey and Patty, 2006), and theories of social learning (Rogers et al., 2009; Choi et al., 2012). Here, we will make use of the LQRE in conjuncture with network theory.

Games on networks have had a rich history, with early research started by considering propagation of strategic behaviour in spatial settings, e.g, on lattices by considering the Prisoner's Dilemma (Nowak and May, 1992) or, recently, the more general case of potential games (Szabó and Borsos, 2016). In recent times, evolutionary games on networks have been a topic of growing interest, see, e.g., (Szabó and Fath, 2007; Perc et al., 2013) for reviews.

Topology can have a significant effect on equilibria of the system, e.g., scale-free networks have been found to promote cooperation in the Prisoner's Dilemma, provided that pairwise imitation is used with the probability of imitation proportional to the difference in total payoffs (Santos and Pacheco, 2005). Other research has investigated the coevolution of internal states and topological features of networks where players are able to modify the structure by rewiring links, leading to a highly cooperative stationary state (Zimmermann et al., 2004), or, if cooperation is to be maintained as a viable strategy in the Prisoner's Dilemma then the network tends to acquire an exponential degree distribution (Szolnoki et al., 2008).

Also investigating the topological evolution of networks, Kasthurirathna and Piraveenan (2015) account for the fact that individuals are known to be influenced and biased by their social connections and thus consider LQREs for games played between agents connected via a social network. As more highly connected players are assumed to be in a better position to gather information, the rationality of players is modelled as an increasing function of node degree. The network structure is then optimised to minimise the overall deviation from perfect rationality (i.e., the Nash equilibrium), and the general result arrived at by Kasthurirathna and Piraveenan (2015) is that scale-free networks realise an optimum. More precisely, Kasthurirathna and Piraveenan (2015) employ two notions of rationality: the rationality of a node, which is given by a monotonic function of the degree, and system rationality ρ, which is equal to the average Nash-LQRE divergence (discussed below) but with opposite sign. Due to our close methodological alignment to Kasthurirathna and Piraveenan (2015), we use the same terminology.

Furthermore, the scale-free topology seems to emerge independently of the games considered by Kasthurirathna and Piraveenan (2015). Since then, the framework and results of Kasthurirathna and Piraveenan (2015) have been used in problems relating to internet routing (Kasthurirathna et al., 2016b) and optimising influence in social networks (Kasthurirathna et al., 2016a). Here, we argue that the optimal topology to maximise rational behaviour among all players depends on the games under consideration, and in no case does it correspond to a scale-free network.

Below we show that for the Prisoner's Dilemma and the Stag Hunt games the optimum topology is a core-periphery network, where the core consists of a low number of high degree hubs and the periphery is made up of many low degree nodes. For the Battle of the Sexes and Matching Pennies games, the optimum topology is also of core-periphery type, but there are differences in the number of hubs, as well as in the average degree of the nodes in the core and in the periphery. In all cases we provide analytic treatment and perform computational experiments to support our claims. In Section 4.2 we outline our methodology, which is closely aligned to that of Kasthurirathna and Piraveenan (2015). In Section 4.3 we present results, with Subsection 4.3.1 containing the treatment of the Prisoner's Dilemma and Stag Hunt games and Subsection 4.3.2 dealing with the Battles of the Sexes and Matching pennies. Section 4.4 concludes the paper.

4.2 Methodology

4.2.1 Logit Quantal Response Equilibrium

In this section we briefly revisit the framework of (Kasthurirathna and Piraveenan, 2015). Parameter choices and the nature of the equilibria we analyse in the rest of the paper are closely aligned with (Kasthurirathna and Piraveenan, 2015) to facilitate comparison.

Game	P2	
P1	u_{11}^1, u_{11}^2	u_{12}^1, u_{12}^2
	u_{21}^1, u_{21}^2	u_{22}^1, u_{22}^2

Table 4.1: Payoffs in the general form of two-person game.

Given a network, every node i is assigned a rationality $\lambda_i = f(d_i)$ which is a function of the nodes' degree d_i. The rationality function is an increasing function of the degree, which implies that higher degree nodes have higher rationality. We consider the cases in which the function f is: linear, where $f(d) = rd$ and $r = 0.2$, convex, where $f(d) = rd^2$ and $r = 0.002$ or concave, where $f(d) = r\sqrt{d}$ and $r = 0.5$.

A two-person game is played on every edge of the network, where the nodes represent the players and links denote the games. The payoffs for any two person game can be written as in Table 4.1. We will be considering games such as the Prisoner's Dilemma and we are interested in determining the Logit Quantal Response Equilibrium (LQRE) of the games, rather than their Nash equilibrium. Each edge has two players, labeled 1 and 2, with rationality λ_1 and λ_2, respectively. We consider mixed strategies, where each player has two available pure strategies, labeled cooperation and defection. Player 1 cooperates with probability p_c^1 and defects with probability $1 - p_c^1$, and similarly for player 2. Following McKelvey and Palfrey (1995) the LQRE is determined by solving the system of equations

$$\begin{aligned} p_c^1 &= \frac{e^{\lambda_1(p_c^2 u_{11}^1 + (1-p_c^2)u_{12}^1)}}{e^{\lambda_1(p_c^2 u_{11}^1 + (1-p_c^2)u_{12}^1)} + e^{\lambda_1(p_c^2 u_{21}^1 + (1-p_c^2)u_{22}^1)}} \\ p_c^2 &= \frac{e^{\lambda_2(p_c^1 u_{11}^2 + (1-p_c^1)u_{21}^2)}}{e^{\lambda_2(p_c^1 u_{11}^2 + (1-p_c^1)u_{21}^1)} + e^{\lambda_2(p_c^2 u_{12}^2 + (1-p_c^2)u_{22}^2)}} \end{aligned} \tag{4.1}$$

Alternatively, Eq.'s (4.1) can be written as:

$$\begin{aligned} p_c^1(1 + a_1 b_1^{p_c^2}) &= 1 \\ p_c^2(1 + a_2 b_2^{p_c^1}) &= 1 \end{aligned} \tag{4.2}$$

where

$$\begin{aligned} a_1 &= \exp(\lambda_1(u_{22}^1 - u_{12}^1)) \\ b_1 &= \exp(\lambda_1(u_{12}^1 + u_{21}^1 - u_{11}^1 - u_{22}^1)) \\ a_2 &= \exp(\lambda_2(u_{22}^2 - u_{21}^2)) \\ b_2 &= \exp(\lambda_2(u_{12}^2 + u_{21}^2 - u_{11}^2 - u_{22}^2)) \end{aligned} \tag{4.3}$$

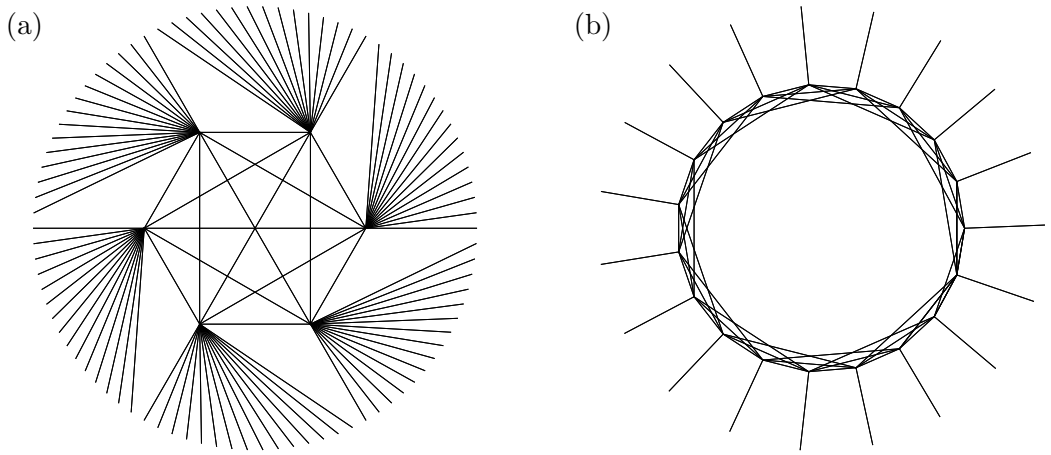

Figure 4.1: Illustrative example of a core-periphery topology that minimises the average divergence (while avoiding isolated nodes) in the case of the: (a) Prisoner's Dilemma and Stag hunt games, where the hubs form a complete subgraph and each has a high degree and (b) Battle of the Sexes, where the hubs for a regular subgraph. For the Matching Pennies the optimal topology is similar to (b) but the periphery consists of isolated K_2 graphs.

Eq. (4.2) will be helpful when solving for different games. In case of the Prisoner's Dilemma, if $\lambda_1, \lambda_2 \to \infty$, then $p_c^1, p_c^2 \to 0$, which corresponds to the Nash equilibrium, i.e., a rational outcome. For an edge k we write the probability distribution associated to player 1 as $P_k^1 = (p_c^1, 1-p_c^1)$, and likewise for player 2. We write Q^1, Q^2 for the probability distribution of the Nash equilibrium for players 1 and 2, respectively. For the Prisoner's Dilemma $Q^1 = Q^2 = (0, 1)$, i.e., the rational outcome in which no cooperation occurs.

We want to quantify the extent to which the players on the network play rationally. For this, we measure the average Jensen-Shannon divergence from the Nash equilibrium over the edges:

$$-\rho = \frac{1}{M}\sum_{k=1}^{M} Div(P_k^1||Q^1) + Div(P_k^2||Q^2), \tag{4.4}$$

where

$$Div(P||Q) = \frac{1}{2}\left(\sum_i P(i)\ln\frac{P(i)}{R(i)} + \sum_i Q(i)\ln\frac{Q(i)}{R(i)}\right) \tag{4.5}$$

is the Jensen-Shannon divergence and $R = (P+Q)/2$ is the average of the probability distributions P and Q and M is the number of edges in the network. We refer to $-\rho$ as the average Nash-LQRE divergence and to ρ as the system rationality.

4.2.2 Optimisation algorithm

What is the network topology that maximises the system rationality as measured by ρ or, equivalently, minimises $-\rho$? This is the question Kasthurirathna and Piraveenan (2015) posed, and the authors also suggested that scale-free graphs realise the optimum. More specifically, Kasthurirathna and Piraveenan (2015) showed that scale-free graphs have lower $-\rho$ than random graphs with the same number of nodes and edges. Furthermore, an optimisation procedure that rewired a random graph to minimise $-\rho$ gave rise to a network with a degree distribution that fitted a power-law with a R^2 correlation of 90%. There are at least two weaknesses in the argument: firstly, the optimisation run by Kasthurirathna and Piraveenan (2015) does not indicate convergence to a minimum, i.e., no plateau is visibly reached and secondly, checking through linear regression that the degree distribution fits a power-law is a poor test to verify that a scale-free topology is present, and it is more robust to perform linear regression on the rank distribution (Li et al., 2005).

In the next section we propose an alternative topology that minimises $-\rho$, and give computational and analytic support for this. To numerically obtain a network with minimum $-\rho$ we consider the following numerical scheme. The scheme, which is similar to other optimisation schemes previously employed in the context of path-length optimisation (Brede, 2010a) or optimal synchronisation (Brede, 2010b) essentially implements a random hillclimber. Start from a random graph and repeat the following operations:

1. Randomly select a node A, and one of its neighbors B.
2. The edge that links from A to B is rewired to connect A and a randomly selected node C which is not a neighbour of A. If we wish to prevent the appearance of isolated nodes, then we do not rewire away from nodes of degree one, i.e., we require $d(B) > 1$ when selecting B.
3. We calculate the divergence on each edge, according to (4.5), in the new neighborhood of C and sum them. We compare this sum to the analogous sum computed for the old neighborhood of B.
4. If there is a decrease in the value of the sum, the rewiring is kept. Otherwise, the original position of the edge is restored and the entire procedure is repeated.
5. If we allow isolated nodes to form during the optimisation, then we regularly remove them and randomly rewire the links between the remaining nodes (akin to simulated annealing). Afterwards, the optimisation proceeds as above.

The above algorithm implies that, after a re-wiring, the rationalities of a node and its neighbours are updated simultaneously. Note that, once a node becomes isolated, it will

PD	P2	
P1	1, 1	0, β
	β, 0	0, 0

SH	P2	
P1	β, β	0, 1
	1, 0	0, 0

Table 4.2: Payoffs for the Prisoner's Dilemma (PD) and Stag Hunt (SH) games.

never reconnect to the rest of network through the hill-climbing part of the optimisation. This is because a zero degree node will always increase the average divergence if reconnected to the rest of graph through an edge.

In the following section we reproduce the results of (Kasthurirathna and Piraveenan, 2015) for random and scale-free networks, and also consider two additional topologies, regular random graphs and what we refer to as core-periphery networks. The core-periphery network we explore can be described as having a bipartite subgraph, but, in addition, the high degree nodes, i.e., hubs, form a regular (or even complete) subgraph. See Fig. 4.1 for a illustration of the types of core-periphery networks we find when maximising system rationality.

4.3 Results

We analyse four games: the Prisoner's Dilemma, the Stag Hunt, the Battle of the Sexes and the Matching Pennies game. The network topologies we investigate are: core-periphery, scale-free networks, regular and Erdős-Rényi random graphs. The scale-free networks are generated using preferential attachment, according to the Barabási-Albert model (Barabási and Albert, 1999). Tables 4.3 and 4.5 show the average divergence in the case of the four games on networks that have $N = 1000$ nodes and $M = 2000$ edges. The results for the random and scale-free graphs are averaged over 100 instances, and likewise for the core-periphery topology in the case of the Prisoner's Dilemma and Stag Hunt games. The 'game parameter' is set to $\beta = 1.33$. The choice of games, network parameters and β parameter are again consistent with (Kasthurirathna and Piraveenan, 2015). We deviate from (Kasthurirathna and Piraveenan, 2015) by considering a more common form of the Matching Pennies that is employed in experimental setups (Ochs, 1995). In the case of the asymmetric games, namely the Battles of the Sexes and Matching Pennies, the game on each edge is played twice with players interchanging roles. This amounts to solving equations (4.1) once with rationalities (λ_1, λ_2) and once with (λ_2, λ_1), and then taking the average of the two divergences.

Game with $\beta = 1.33$	Prisoner's Dilemma					Stag Hunt				
Graph type	Core-periphery ($K = 13$)		Scale-free	Random	Regular	Core-periphery ($K = 18$)		Scale-free	Random	Regular
	Computed	Analytic				Computed	Analytic			
Linear	0.2149(2)	0.2135	0.361(2)	0.3914(3)	0.3982	0.1532(6)	0.1485	0.337(7)	0.311(1)	0.3377
Convex	0.2112(2)	0.2108	0.407(4)	0.4290(1)	0.4300	0.1988(1)	0.1983	0.395(4)	0.4263(1)	0.4286
Concave	0.3082(1)	0.2890	0.377(1)	0.3876(2)	0.3907	0.2435(5)	0.3817	0.284(3)	0.2930(7)	0.3067

Table 4.3: The average Nash-LQRE divergence ($-\rho$) in the case of the Prisoner's Dilemma and Stag Hunt games for the different network topologies and rationality functions. The numerical results for the core-periphery, scale-free and random networks are averaged over 100 instances. The core-periphery nodes have K hubs.

4.3.1 Symmetric games

4.3.1.1 Prisoner's Dilemma

Our results for the Prisoner's Dilemma on random networks closely match with (Kasthurirathna and Piraveenan, 2015), while the results for scale-free networks are consistent but show a larger decrease than reported by Kasthurirathna and Piraveenan (2015) compared to the random case, see Table 4.3. Next we consider rationality-optimised networks. Figure 4.2(a) shows the evolution of the divergence during optimisation. The numerical computations indicate that the topology of the random graph is evolving towards a core-periphery graph with a complete subgraph of $K = 13$ hubs, cf. Fig. 4.1 for a qualitative visualisation. To complement these simulations with analytic arguments we approximate the solutions to equations (4.1).

The network obtained through the optimisation procedure has a divergence within 2% of the analytic estimate, as Fig. 4.2(a) shows. The core-periphery networks that were generated to compute the entries in Table 4.3 have a divergence that deviates less than 0.5% from the analytic estimate (in the case of linear rationality). Hence, the difference between the numerical result and the analytic estimate in Fig. 4.2(a) likely stems from the optimisation getting stuck in a local optimum. Selective re-wirings of a few edges could further reduce the divergence but the global network topology would still be of core-periphery type with $K = 13$ hubs.

The payoffs for the Prisoner's Dilemma are shown in Table 4.2. In this case we have that $a_1 = 1, b_1 = e^{\lambda_1(\beta-1)}, a_2 = 1, b_2 = e^{\lambda_2(\beta-1)}$ and equations (4.1) take the form:

$$\begin{aligned} p_c^1(1 + e^{\lambda_1(\beta-1)p_c^2}) &= 1 \\ p_c^2(1 + e^{\lambda_2(\beta-1)p_c^1}) &= 1 \end{aligned} \tag{4.6}$$

We can obtain analytic results for regular graphs in which all players are characterised by the same rationality. Let p_r be the probability of cooperation on a regular graph.

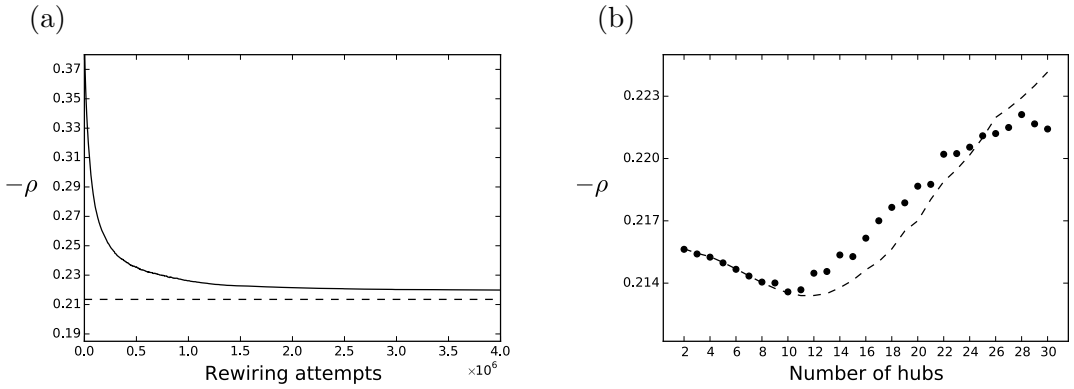

Figure 4.2: (a) The evolution of $-\rho$, the average Jensen-Shannon divergence between Nash and LQR equilibria, for the Prisoner's Dilemma ($\beta = 1.33$) with linear rationality, of an initially random network ($N = 1000$ nodes and $M = 2000$ edges) as a function of attempted edge rewirings, while not allowing isolated nodes. The optimisation gets within 2% of the estimated minimum (dashed line). (b) The divergence of a core-periphery graph with $N = 1000, M = 2000$ as a function of the number of hubs according to numerical calculations (dots) and analytic estimates (dashed line) using equation (4.12) for core-periphery graphs.

Then, in the case of the Prisoner's Dilemma, p_r satisfies the equation:

$$p_r(1 + e^{\lambda(\beta-1)p_r}) = 1, \tag{4.7}$$

where λ is the rationality of a node. The divergence $-\rho_r$ for a regular graph with N nodes and M edges is thus given by:

$$-\rho_r = p_r \ln 2 + (1 - p_r) \ln \frac{1 - p_r}{1 - p_r/2} + \ln \frac{1}{1 - p_r/2}. \tag{4.8}$$

The results of applying equation (4.8) for the different rationality functions match precisely with the entries for regular random graphs in Table 4.3. The degree distribution for the random graph has an average and mode of $\langle d \rangle = 4$, and we see that results for the random and regular topologies are close (within 2%), i.e., the regular random graph can be seen as a zero order approximation of the random graph.

Analytic results are also possible for the core-periphery graph, where the core consists of hubs with high degree (high rationality) and the periphery contains nodes of low degree (low rationality). Let p_h be the probability of cooperation for a hub and p_f the same quantity but for a periphery (fringe) node. For the Prisoner's Dilemma, the equations p_h and p_f satisfy are

$$\begin{aligned} p_h(1 + e^{\lambda_h p_f(\beta-1)}) &= 1 \\ p_f(1 + e^{\lambda_f p_h(\beta-1)}) &= 1 \end{aligned} \tag{4.9}$$

where λ_h and λ_f are the rationalities of the two types of nodes. If $\lambda_f > 0$ and $\lambda_h \gg 1$, then $p_h \simeq 0$ and this implies that $p_f = 0.5$. So, we can approximate the probability of cooperation of a periphery node with a hub to zero order by $p_f^{(0)} = 1/2$, while hubs do not cooperate, i.e., $p_h^{(0)} = 0$. The contribution of the edges between the high connectivity nodes in a core-periphery graph leaves the divergence -ρ largely unchanged, because the hubs are highly rational (due to their large degree). The divergence of a connected core-periphery graph with a finite number of hubs but infinite number of periphery nodes is thus given by $\mu = 3/4 \ln 4/3 = 0.216$, independent of the choice of rationality function is long as it is an increasing function of the degree.

For a more accurate picture we consider first order corrections and obtain

$$\begin{aligned} p_h &= \frac{1}{1+e^{\lambda_h(\beta-1)/2}} \simeq e^{-\lambda_h(\beta-1)/2} = p_h^{(1)} \\ p_f &= \frac{1}{1+e^{\lambda_f(\beta-1)p_c^1}} \simeq \frac{1}{2(1+\lambda_f(\beta-1)p_c^1/2)} \\ &\simeq \frac{1}{2} - \frac{\lambda_f(\beta-1)p_c^1}{4} = p_f^{(0)} + p_f^{(1)} \end{aligned} \tag{4.10}$$

In a core-periphery network with K hubs each each hub has degree $M/K + K - 1$ and the periphery nodes have average degree d that satisfies

$$\frac{K(K-1)}{2} + d(N-K) = M. \tag{4.11}$$

If the hubs are of high enough degree such that the first order corrections $p_h^{(1)}, p_f^{(1)}$ are small, then the divergence -ρ of the core-periphery graph with N nodes and K hubs can be approximated as follows:

$$\begin{aligned} -\rho_{cp} \simeq &\left(1 - \frac{K(K-1)}{2M}\right)\left(\mu + \frac{p_h^{(1)} \ln 2 + p_f^{(1)} \ln 3}{2}\right) \\ &- \frac{K(K-1)}{2M}\rho_c, \end{aligned} \tag{4.12}$$

where $-\rho_c$ is the average divergence over the edges between the hubs, which form a complete subgraph. The average divergence of the core-periphery network with $K = 13$ hubs for linear rationality is $-\rho_{cp} = 0.2135$. This result is close but slightly lower than the numerically computed entries in Table 4.3. As one would expect, the approximation is better for the convex rationality function (because it extends the region in which the approximation (4.10) holds), whereas the analytic estimate is poor for the concave case (due to the opposite effect).

Making use of Eq. (4.12) Fig. 4.2(b) shows the dependence of the Nash-LQRE divergence as a function of the number of hubs in the core-periphery network. We can understand the dependence by noting the two competing factors in equation (4.12).

With increasing numbers of hubs, the number of edges in the core increases which tends to lower the average divergence. On the other hand in a finite graph, an increasing number of hubs leads to a decrease of the average degree of a hub, which makes hubs less rational, and so the divergence tends to increase. For a graph with $N = 1000$ nodes and $M = 2000$ edges the minimum of (4.12) is obtained in the neighbourhood of 12 hubs, in good agreement with the numerical optimisation in Fig. 4.2(a) that tends toward a graph with 13 hubs.

As Table 4.3 shows, the results for the average divergence of the core-periphery graph are notably smaller than results obtained for all other topologies. Furthermore, it is easy to see that the core-periphery networks lie at local minima (in the space of possible graphs) with respect to the value of the Nash-LQRE divergence. This can be seen by exploring the effects of possible rewirings. Moving an edge that connects two nodes in the core (a *cc* edge) to connect another two nodes in core does not change the average divergence. Also, moving an edge that connects a core node to a periphery node (a *cp* edge) to connect another core-periphery pair has no effect. A rewiring that does affect the divergence involves moving an edge that lies between:

(a) two hubs, so that it connects a hub and a periphery node, i.e., moving from a *cc* edge to a *cp* edge

(b) two hubs, so that it connects two periphery nodes, i.e., moving from a *cc* edge to a *pp* edge

(c) a hub and a periphery node, so that it connects two periphery nodes, i.e., moving from a *cp* edge to a *pp* edge

Due to the high rationality of hub nodes, an edge between two hubs has a near zero contribution to the divergence. The low degree nodes are associated with low rationality, hence they will a have quantal response equilibria that differ significantly from the Nash equilibrium. Hence, moving an edge that lies between two hubs so that it now connects to one or two periphery nodes will lead to an increase the in the average divergence.

Moving an edge that connects a hub and a periphery node to connect two periphery nodes, will also lead to an increase in the divergence, which we can quantify. After rewiring an edge that connected a hub to the periphery to now connect two periphery nodes, the divergence is:

$$\begin{aligned} -\rho_w \simeq & \left(1 - \frac{K(K-1)/2 - 1}{M}\right)\left(\mu + \frac{p_h^{(1)} \ln 2 + p_f^{(1)} \ln 3}{2}\right) \\ & - \frac{K(K-1)}{2M}\rho_c + \frac{1}{M} p_{d+1} \ln 2 \\ & + \frac{1}{M}\left((1 - p_{d+1}) \ln \frac{1 - p_{d+1}}{1 - p_{d+1}/2} + \ln \frac{1}{1 - p_{d+1}/2}\right) \end{aligned} \tag{4.13}$$

where p_{d+1} is the probability of cooperation for a node in a regular graph of average degree $d+1$. If $p_{d+1} \simeq 0.5$, then the last three terms are approximately $2\mu/M$, which is larger than the term it is replacing that is approximately μ/M. Thus, $-\rho_w \geq -\rho_{cp}$. In summary, any rewiring either does not change the average divergence, or increases it. So, the core-periphery topology achieves a local minimum for the average divergence in the space of possible graph topologies.

4.3.1.2 Stag Hunt

The results for the Stag Hunt game are largely analogous to the Prisoner's Dilemma. The payoff matrix for the Stag Hunt is also in Table 4.2. We have that $a_1 = e^{\lambda_1}, b_1 = e^{-\lambda_1\beta}, a_2 = e^{\lambda_2}, b_2 = e^{-\lambda_2\beta}$ and equations (4.1) take the form:

$$\begin{aligned} p_c^1(1 + e^{\lambda_1(1-\beta p_c^2)}) &= 1 \\ p_c^2(1 + e^{\lambda_2(1-\beta p_c^1)}) &= 1 \end{aligned} \tag{4.14}$$

For a regular graph the equations reduce to:

$$p_r(1 + e^{\lambda(1-\beta p_r)}) = 1 \tag{4.15}$$

Applying Eq. (4.8) for the average divergence of a regular graph to the solution of (4.15) again matches with the numerical computations in Table 4.3.

If λ_h is large and λ_f is small then we can approximate to zero order $p_h = 0$ and $p_f = 1/(1 + e^{\lambda_f})$. If $\beta < 1 + e^{\lambda_2}$, then the first order approximations are:

$$\begin{aligned} p_h &= \frac{1}{1 + e^{(\lambda_h(1-\beta/(1+e^{\lambda_f})))}} \simeq e^{-\lambda_1(1-\beta/(1+e^{\lambda_f}))} \\ p_f &= \frac{1}{1 + e^{\lambda_f(1-\beta p_h)}} \simeq \frac{1}{2(1 - \lambda_f(1-\beta p_h)/2)} \\ &\simeq \frac{1}{2} - \frac{\lambda_f(1-\beta p_h)}{4} \end{aligned} \tag{4.16}$$

The optimum network that minimises $-\rho$ is a core-periphery network with $K = 18$ hubs that form a complete subgraph. For linear rationality, equation (4.12) gives an average divergence of $-\rho_{cp} = 0.1485$ which is in reasonable agreement with the numerical calculation in Table 4.3, while a close match is found for convex rationality. A large difference is observed between the numerical result and analytic estimate for the concave case, due to the square root function decreasing the rationality of the hubs and, thus, approximation (4.16) failing.

Above we have considered rewirings in which isolated nodes were prevented. However, the observation of the emergence of a strong core-periphery structure makes one wonder

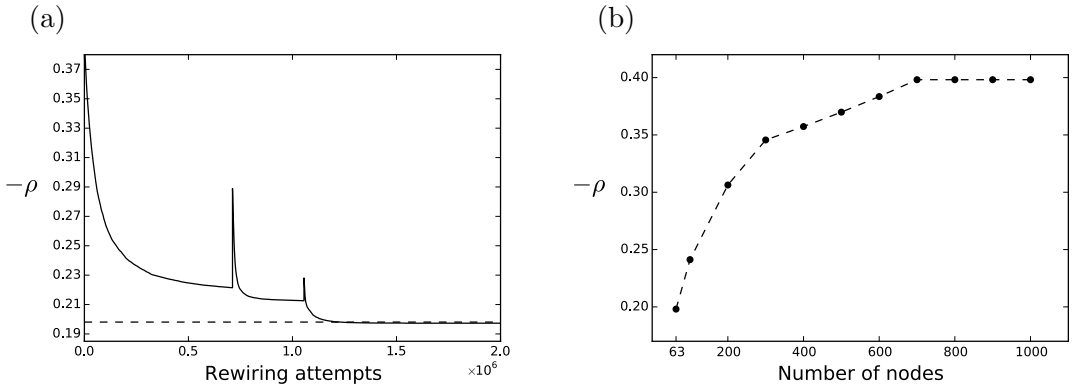

Figure 4.3: (a) The evolution of $-\rho$, the average Jensen-Shannon divergence between Nash and LQR equilibria, for the Prisoner's Dilemma ($\beta = 1.33$) with linear rationality, starting with an initially random network ($N = 1000$ nodes and $M = 2000$ edges) as a function of the number of attempted edge rewirings, allowing isolated nodes. The optimisation reaches the theoretical minimum (dashed line), which is achieved for a complete graph with 63 nodes. (b) Numerical (dots) and analytical (dashed line) results for the divergence of regular graphs with $M = 2000$ edges in the case of the Prisoner's Dilemma. Analytic values calculated according to equation (4.8).

if optimal networks would actually become disconnected when this constraint is removed. Hence, we consider again the Prisoner's Dilemma and relax the optimisation conditions in the rewiring of the network to allow for isolated nodes. Figure 4.3(a) shows the results of a variant of simulated annealing performed to optimise the network. The numerical results indicate that a majority of nodes become isolated and a certain number of hub nodes end up sharing the edges between them. If we approximate the remaining subgraph of hubs as a complete graph, then the number of hubs is given by

$$K = \frac{1 + \sqrt{1 + 8M}}{2} \tag{4.17}$$

The average divergence for a complete graph with K nodes is given by equation (4.8) for a regular graph when the average degree is $K - 1$. For $M = 2000$ the number of hubs is $K = 63$ and gives a divergence of $-\rho = 0.197$, which matches with the numerical optimisation in Fig. 4.3(a). Of all regular graphs with $M = 2000$ edges the complete graph with 63 nodes has minimum divergence, which is indicated in Fig. 4.3(b). For the Stag Hunt game the unconstrained optimisation leads to regular graph with $N = 400$ nodes and average degree $2M/N = 10$.

4.3.2 Asymmetric games

4.3.2.1 Battle of the Sexes

We now consider the asymmetric games: the Battle of the Sexes and the Matching Pennies, with payoffs given in Table 4.4. In the cases of these two games we compute

BS	P2	
P1	β, 1	0, 0
	0, 0	1, β

MP	P2	
P1	β, 0	0, 1
	0, 1	1, 0

Table 4.4: Payoffs for the Battle of the Sexes (BS) and Matching Pennies (MP) games.

the average Nash-LQRE divergence with respect to the mixed strategy Nash equilibria. For the Battle of the Sexes, we find that the average divergence with respect to the mixed Nash equilibrium, $Q^1 = (\beta/(1+\beta), 1/(1+\beta))$ and $Q^2 = 1 - Q^1$, is much closer to zero than for the pure strategy $Q^1 = Q^2 = (0, 1)$. In the case of the Matching Pennies games, there is no pure Nash equilibrium.

We first analyse the Battle of the Sexes for which $a_1 = e^{\lambda_1}, b_1 = e^{-\lambda_1(1+\beta)}, a_2 = e^{\lambda_2\beta}, b_2 = e^{-\lambda_2(1+\beta)}$. Equations (4.1) take the form:

$$\begin{aligned} p_c^1(1 + e^{\lambda_1(1-(1+\beta)p_c^2)}) &= 1 \\ p_c^2(1 + e^{\lambda_2(\beta-(1+\beta)p_c^1)}) &= 1 \end{aligned} \tag{4.18}$$

As equations (4.18) are not symmetric when exchanging players, the game is played twice on each edge, once solving equations (4.1) with the rationalities (λ_1, λ_2), and once with the rationalities interchanged, i.e, (λ_2, λ_1).

If λ_1 and λ_2 are small then we can approximate to zero order and obtain $p_c^1 = 1/2$ and $p_c^2 = 1/2$. The approximations to first order are given by:

$$\begin{aligned} p_c^1 &= \frac{1}{1 + e^{\frac{\lambda_1(1-\beta)}{2}}} \simeq \frac{1}{2\left(1 + \frac{\lambda_1(1-\beta)}{4}\right)} \simeq \frac{1}{2} + \frac{\lambda_1(\beta-1)}{8} \\ p_c^2 &= \frac{1}{1 + e^{\frac{\lambda_2(\beta-1)}{2}}} \simeq \frac{1}{2\left(1 + \frac{\lambda_2(\beta-1)}{4}\right)} \simeq \frac{1}{2} - \frac{\lambda_2(\beta-1)}{8} \end{aligned} \tag{4.19}$$

The average divergence for different topologies is found in Table 4.5. By optimising the network topology to minimise $-\rho$, as we did for the Prisoner's Dilemma game, we obtain the results in Fig. 4.4. The divergence is minimised for a core-periphery network where the core consist of $N/2 = 500$ nodes that form a regular graph, and each node in the core links to a single periphery node. The degree of a node in the core is $d_h = 7$, while in the periphery it is $d_f = 1$. A qualitative illustration of the network topology can be seen in Fig. 4.1(b).

If we optimise the network topology to minimise the divergence with respect to the pure strategy Nash equilibrium $Q^1 = Q^2 = (0, 1)$, we obtain a regular graph of average degree $2M/N = 4$ and $-\rho = 2\mu = 0.432$ for all rationality functions. As Table 4.5

Game with $\beta = 1.33$	Battle of the Sexes ($-\rho \times 10^2$)				Matching Pennies ($-\rho \times 10^2$)			
Graph type	Core-periphery (K=1500)	Scale-free	Random	Regular	Core-periphery (K=168)	Scale-free	Random	Regular
Linear	0.178	2.9(3)	0.25(1)	0.236	0.096	0.47(3)	0.215(1)	0.218
Convex	0.458	1.0(4)	0.473(1)	0.486	0.230	0.8(3)	0.252(1)	0.252
Concave	0.180	1.1(1)	0.200(1)	0.202	0.142	0.26(1)	0.200(1)	0.203

Table 4.5: The average Nash-LQRE divergence ($-\rho$) in the case of the Battle of the Sexes and Matching Pennies games for the different network topologies and different choices of rationality functions. The numerical results for the scale-free and random networks are averaged over 100 instances. The core-periphery nodes have K hubs.

shows, optimising with respect to the mixed strategy Nash equilibrium gives a much lower value for the average divergence $-\rho$, which is why we focus on this case.

We can gain analytic insight into the results presented in Table 4.5 by writing the average divergence as:

$$-\rho = \alpha(-\rho_c) + (1-\alpha)(-\rho_f) \tag{4.20}$$

where $-\rho_c$ is the average divergence of the core, i.e., that of a regular graph with average degree $d_h = 7$, and $-\rho_f$ is the average divergence of the periphery, i.e., the divergence for an edge connecting a degree $d_f = 1$ node with a node from the core. The value of α is the fraction of links that exist within the subgraph containing the core. Hence, $\alpha = N(d_h - 1)/(2M) = 75\%$. The rest of the links are part of the periphery. By numerically solving for the cooperation probabilities in (4.18) and using equation (4.20), we obtain an exact match to the numerically obtained entries in Table 4.5.

If we allow isolated nodes to form throughout the optimisation then, similar to the Prisoner's Dilemma and Stag Hunt games, the periphery nodes disconnect from the network but now a core with a strongly bi-modal degree distribution emerges. The core has $N_{c1} = 263$ nodes with degree $d_{h1} \simeq 8$, and $N_{c2} = 159$ nodes with degree $d_{h2} \simeq 12$. The average divergence is approximated well by (4.20), where the two contributions come from regular graphs with N_{c1}, N_{c2} nodes with average degrees 8 and, respectively, 12. Numerical and analytic results for regular graphs for the asymmetric games we consider are shown in Fig. 4.4(b).

4.3.2.2 Matching Pennies

Finally, we consider the Matching Pennies game with the more general payoff matrix shown in Table 4.4. In the case of the Matching Pennies we have that $a_1 = e^{\lambda_1}, b_1 =$

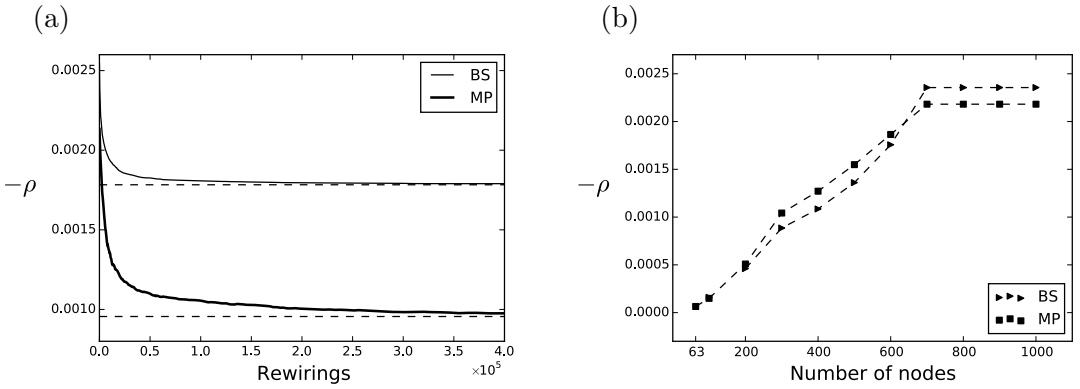

Figure 4.4: (a) The evolution of $-\rho$, the average Jensen-Shannon divergence between Nash and LQR equilibria, for the Battles of the Sexes (thin line) and Matching Pennies (thick line) ($\beta = 1.33$) with linear rationality, in the range of topologies between an initially random network ($N = 1000$ nodes and $M = 2000$ edges) as a function of attempted edge rewirings, while not allowing isolated nodes. The optimisations reaches the estimated minima (dashed lines). (b) The divergence for regular graphs with $M = 2000$ edges in the case of the Battle of the Sexes (triangular dots) and Matching Pennies (square dots), with analytic results shown by dashed lines.

$e^{-\lambda_1(1+\beta)}, a_2 = e^{-\lambda_2}, b_2 = e^{2\lambda_2}$ and equations (4.1) take the form:

$$\begin{aligned} p_c^1(1 + e^{\lambda_1(1-(1+\beta)p_c^2)}) &= 1 \\ p_c^2(1 + e^{\lambda_2(-1+2p_c^1)}) &= 1 \end{aligned} \tag{4.21}$$

Equations (4.21) are again not symmetric when exchanging players and so the game is played twice on each edge, as also done for the Battle of the Sexes. We can approximate the probabilities for strategy choice C to zero order by $p_c^1 = p_c^2 = 0.5$. If the rationalities are small then we can make the following first order approximations:

$$\begin{aligned} p_c^1 &\simeq \frac{1}{2} + \frac{\lambda_1(\beta - 1)}{8} \\ p_c^2 &\simeq \frac{1}{2} - \frac{\lambda_1\lambda_2(\beta - 1)}{16} \end{aligned} \tag{4.22}$$

Table 4.5 gives figures for the average divergence for different topologies and rationality functions, while Fig. 4.4(a) shows the results obtained numerically from an optimisation procedure to minimise $-\rho$. The results are largely analogous to the Battle of Sexes, with one exception: The core-periphery graph that minimises the divergence has a core consisting of a quasi-regular graph, with $N_c = 168$ nodes with average degree $d_h \simeq 19$, and the periphery nodes form $(N - N_c)/2 = 416$ pairs (K_2 graphs) completely disconnected from the core. Equation (4.20) can be applied with $\alpha = N_c d_h/(2M) \simeq 80\%$, and the results match with the entries in Table 4.5. If we allow isolated nodes to form during the optimisation, then the optimal network structure that minimises the average divergence is a quasi-regular graph with $N_c = 168$ and average degree $d_h \simeq 24$. Hence,

the core in both types of optimisation for the Matching Pennies game has the same number of nodes; it is only the number of edges within the core that varies due to the connectivity constraint.

4.4 Conclusion

Previous work has proposed that scale-free networks maximise the overall "rationality" of a networked system of players Kasthurirathna and Piraveenan (2015). Here we have shown that for the Prisoner's Dilemma game core-periphery graphs, composed of a core of connected hub nodes which each link to a single periphery node, have a significantly lower average Nash-LQRE divergence than scale-free networks. This result is supported by numerical experiments and also by an analytic approximation for the divergence of core-periphery graphs that reproduces numerical results well for all the different rationality functions considered. The accuracy of the analytic results can decrease due to the fact that in finite core-periphery graphs the hubs will always have a finite degree, and hence the approximations suffer. If no connectivity constraint is enforced during optimisation, optimal networks are found to consist of a core made up by a complete graph with all other nodes being isolated.

For the Stag Hunt game, an analogous analytic treatment of the connectivity constrained case yields qualitatively similar results to the Prisoner's Dilemma, while the connectivity unconstrained optimisation leads to a regular graph.

Further, in contrast to Kasthurirathna and Piraveenan (2015), we have demonstrated that highly heterogeneous degree distributions do not necessarily maximise system rationality for all classes of games. Analytic and simulation results show that, for the Battle of the Sexes and the Matching Pennies games, core-periphery graphs with cores that have a quasi-regular topology minimise the average Nash-LQRE divergence. If the connectivity of the network is not constrained in the optimisation procedure, then in the case of the Battle of the Sexes a graph with a strongly bi-modal degree distribution emerges, while for the Matching Pennies game we obtain a quasi-regular graph.

We can interpret the results for the Prisoners Dilemma or Stag Hunt games in a broader way. Cooperation is naturally associated with altruistic behaviour, whereas defection can be seen as a selfish course of action. Maximising system rationality, or minimising the difference between the probability distributions and the Nash equilibria, can thus be interpreted as promoting selfish behaviour within the system. The topology that emerges is one where a core consisting of roughly 1% of the nodes in the network are part of over 90% of the connections available, whereas each periphery node is as poorly connected as possible. If higher numbers of a node in a social network translates into greater influence/wealth, then we see that by maximising selfishness in a social network most of the power ends up concentrated in a very small set of players. This result echoes

present concerns regarding wealth inequality, and furthermore, a similar core-periphery structure has been found to underlie the network of global corporate control, wherein a "large portion of control flows to a small tightly-knit core of financial institutions" (Vitali et al., 2011). Our results elaborate a possible mechanism for the emergence of such highly concentrated core-periphery structures in social networks.

Acknowledgements

This work was supported by an EPSRC Doctoral Training Centre Grant (EP/G03690X/1). No new data was collected by this research.

Chapter 5

Conclusions and future work

Previous literature on the modelling of past societies, even work as prominent as Brander and Taylor (1998), has not aimed at reproducing the known historical time series for important data (Bahn and Flenley, 1992) that characterise the development of the society in question, such as the population size. Furthermore, most other work has either proposed models that are too complex, such as Hosler et al. (1977), or too simple, such as Hamblin and Pitcher (1980), to strike an adequate balance between the realistic features that should be captured and the tractability a model should posses to be insightful.

In our work, we have proposed a three stock model of Easter Island with similar calibration to the model proposed by Brander and Taylor (1998). In contrast to previous work, our model fits the archaeological record given by Flenley and Bahn (2003). Up to our best knowledge no other model has achieved such a fit. We have also built a model of the Maya civilisation that encapsulates the main specialisations of the population, the land dynamics and monument construction. Also for the case of the Maya, our model is the first to explicitly match archaeological data of population growth and monument building. Thus, the models capture sufficient features of the societies in question to adequately reproduce known historical trends. Nevertheless, simple socio-environmental feedbacks underlie the models and prove sufficient to reproduce the historical data regarding the collapse. This fact brings into question why more complicated hypotheses should be considered, such as those enumerated by Aimers (2007) for the Maya collapse.

Furthermore, the structure of the models allows for analytic insight into their dynamics. We can obtain a closed form analytic expression for the critical value of the harvesting rate, above which the Easter Island model undergoes a supercritical Hopf bifurcation. To the extent of our knowledge, no other model of a society that has collapsed has had a critical bifurcation parameter explicitly computed. Similarly, a bifurcation analysis for the model of Maya society shows that, when the harvesting rate exceeds a certain threshold, a supercritical Hopf bifurcation occurs. Thus, both the collapse on Easter

Island and the Classic Maya are modeled by the same type of critical transition. Hence, the models enjoy a level of tractability that allows us to derive useful, more general insights about the drivers of societal collapse.

Where comparison is possible, the model we built to describe the Classic Maya has a calibration consistent with the archaeological record. This, to the best of our knowledge, is unique in the literature on modelling societal development using low-dimensional dynamical systems. Furthermore, an extensive sensitivity analysis was performed on the model which shows that the calibration lies at a minimum in parameter space.

With the exception of the work by Anderies and Hegmon (2011), there has been little research on low dimensional systems that explores the dynamics of multiple coupled regions. Anderies and Hegmon (2011) does not find significant difference between the coupled and uncoupled regimes, possibly due to the specific coupling employed between the different regions. We have analysed the simplest scenario for possible couplings of societies, which is via diffusion. Each society is parametrised similar to Easter Island, with the exception of the extraction rate of resource per capita. We performed a bifurcation analysis of the diffusively coupled set of oscillators representing societies, where the critical parameters were the harvesting rates for the two societies.

In contrast to previous work (Anderies and Hegmon, 2011), we found that a simpler coupling makes a significant difference to the equilibrium states. Namely, as long as one society has a sufficiently low harvesting rate the overall system can achieve a stable state. Furthermore, we obtained an analytic derivation of the inner fixed point of the diffusively coupled system, which was used to numerically approximated the bifurcation boundary. In addition to the diffusive coupling, we proposed a model of wealth-driven diffusion between two societies and carried out a bifurcation analysis similar to the diffusive model, with similar results.

In our current research we have striven to develop models of intermediate complexity to understand the dynamics of ancient societies. The models aim to incorporate sufficient detail for a meaningful interpretation of the dynamics but also facilitate analytic understanding and communication. In future work an aim will be to develop a model in similar spirit for the mechanisms at play in an industrial society. It would be interesting to quantify macro-dynamical relationships and feedbacks in modern societies through dynamical systems models, such as we have done for the case of Easter Island (Roman et al., 2017) and the Classic Maya.

Most models that have been developed in this regard are either highly stylised (M. and J., 2013), aimed at analytic tractability or very detailed, large-scale and of unyielding complexity (Costanza et al., 2007b), but the mid-ground in-between has not been explored to a large extent. The starting point can be the Easter Island model which could be extended to incorporate some crucial, missing aspects, such as different industry

and energy sectors, so that the model can be calibrated and applied to modern societies. While other models exist that have incorporated such features, such as "Limits to Growth" (Meadows et al., 1972), these models have a large number of parameters which makes exploring their behaviour difficult and, as far as we know, the models are not adequate for analytic insights.

Another possible extension of the work is to consider multi-regional modelling of the Maya civilisation. Dynamical systems similar to the model we proposed can be set up to represent each of the Maya sites, which then can be coupled (diffusively or otherwise) to represent the relationship patterns among the Maya. The issue of societal connectivity has been under-explored (Roman et al., 2017) and a low dimensional dynamical system gives us a natural way of investigating the impact of connectivity on sustainability. Each node in the network could represent a Maya site, with the parameters calibrated specifically to it. Then, interaction between sites will be represented through the edges in the network. The interaction between nodes can include migration, trade, resource movement or warfare.

Thus, the framework of the proposed model would allow us to systematically look at the role of connectivity and analyse issues regarding trade, migration or warfare. This extension would provide a more comprehensive picture of the entire spatial distribution of the Maya civilisation and would allow us to track the historical evolution of different sites, thus also allowing for a greater degree of validation of the existing work.

Beyond the topic of dynamical system's modelling of societal structure and dynamics, we have provided contributions to the field of games on complex networks. We corrected numerical results of the work by Kasthurirathna and Piraveenan (2015) for a network model of agents interacting by playing symmetric games (Prisoner's Dilemma or Stag Hunt), according to strategies determined by the quantal response equilibrium. We have established that the minimum is not achieved by a scale free network as stated by Kasthurirathna and Piraveenan (2015), but by a type of core-periphery network. The core consists of a complete subgraph where the nodes have a high degree, while the periphery consists of nodes of degree one.

Furthermore, we obtained analytic results in the case of symmetric games for the optimal core-periphery topology and for the case of regular graphs. Zeroth and first order corrections for the quantal response equilibrium were determined, along with the corresponding value of the system rationality. Also, we arrived at numerical and analytic results for asymmetric games (Battle of the Sexes and Matching Pennies), with the optimal topology that maximises system rationality being a core-periphery topology with a core consisting of a regular subgraph. In contrast to Kasthurirathna and Piraveenan (2015), the specific features of optimal topology differ between symmetric and asymmetric games.

Within the wider context of the literature, our findings provide an alternative mechanism by which core-periphery structures can form. By accounting for a new factor, namely rationality of the players, our finding show that the emergence of core-periphery structure is more robust in the sense of occurring in a more diverse set of circumstances than previously considered.

Thus, we have provided some of the first accurate results that incorporate a graded notion of rationality in games played between agents on a network. The present model only considers a single layer network in which all relationships are treated as equal. There has been a growing interest in disaggregated network models (Gomez et al., 2013) and our model could also be extended in this regard by considering a multiplex network, wherein each level represents a different relationship between agents. For example, one level could determine the rationality of the agents, whereas another level can contain the neighbours against which the games are played. This extension of the model would differentiate between the cognitive plane, where rationality is computed, and the social aspect, which pertains to links to other nodes.

The thesis brings together several novel insights into the large-scale, long-term dynamics of societies and their structural organisation. In particular, the issue of rationality plays an important, unifying role in the present work, implicitly through the existence of sunk-costs effects in the societies we consider or explicitly in the modelling of agent's behaviour in networks. We hope to have achieved a notable advance compared to the existing literature on the subjects of societal dynamics and games on networks, and that our research inspires future work into these topics.

Appendix A

Common reasons for collapse

One common reason invoked for the collapse of complex societies is the gradual depletion of natural resources, e.g., deforestation, as argued in case of Easter Island (Diamond, 2005) or soil nutrient depletion in the case of the Maya (Webster, 2002). Alternatively, resources can be rapidly lost due to environmental change, most notably climatic shifts, e.g., high Nile floods that favoured soil crop parasites in the Middle Kingdom of Egypt (Butzer and Endfield, 2012) or drought in the case of the Maya (Kennett et al., 2012). Another possibility involves moving to a new resource base that lead to the loss of previously established social order (Harner, 1970). Natural resource arguments have the difficulty that societies develop administrative structure, and allocate labour and resources to deal with possible resource shortage and deteriorating environmental conditions (Isbell, 1978). Hence, these theories propose that societies collapse in conditions they have been adapting and dealing with since their formation.

Another category of explanations focuses on competition between societies, e.g., which might have led to the demise of the Huari and Tiahuanaco (Lanning, 1967). Similarly, intruders have been argued to have caused the collapse of different societies, such as in the case of the barbarian invasion of the Roman Empire (Manning and Trimmer, 2013), or the invasion of the Hittite Empire by seafaring nomads (Carpenter, 1966), or contact with Europeans for Easter Island (Stevenson et al., 2015). Catastrophes are also a frequently quoted cause of collapse, with examples including the volcanic eruptions and earthquakes for the Minoan Civilisation (Marinatos, 1939; Driessen and Macdonald, 1997), major epidemics for the Maya (Acuna-Soto et al., 2005) or rat infestation for Easter Island (Hunt, 2007). A related cause of collapse are contingent events, where a sequence of detrimental events led to the collapse. Catastrophes can also be considered as an extreme case of a contingent event. But, the explanation based on contingent events has no causal mechanism underlying it. Also, catastrophes, intruders and competition with other societies have been previously encountered by a given society but no collapse occurred, e.g. earthquakes in the Minoan civilisation, barbarian attacks on the Roman

front or competition between the Maya centres. These latter theories have the added difficulty of placing the drivers of the collapse outside of the society in question.

Conflict between social classes and elite mismanagement have been some of the earliest proposed causes for the collapse of civilisations. Their strength lie in placing the mechanism of collapse within the society in question. But, often, these explanations are accompanied by some mystical (vague, unmeasurable) factors underlying the collapse, e.g., a loss of social unity or of civic virtue.

An early theory of why societies decline and collapse was put forward by Khaldun (1377), who proposed a cyclical model for the rise and fall of civilisations. A key concept of Khaldun (1377) was that of "asabiyyah" which roughly translates to social cohesion and unity, which is strongly felt in the early stages of a society, but diminishes as the society grows and the leadership becomes too removed from the concerns of the majority of people. If a group at the periphery of the society enjoys a greater degree of social solidarity, this can eventually lead to a change in the leadership and a new cycle starts. The theory was applied by historians of the Ottoman Empire to understand its development, which started at the periphery of the Byzantine empire and grew to prominence (Lewis, 2006).

In the "Decline and fall of the Roman Empire" (Gibbon, 1776) it is argued that the "virtue" of the citizens degraded, as they were less willing to protect their borders and outsourced their military defences to barbarian mercenaries. Also, Gibbon argues that Christianity diminished the martial spirit of the Romans and belief in the afterlife made them reluctant to sacrifice themselves for the empire (Gibbon, 1776). We see in both Khaldun (1377) and Gibbon (1776) explanations based on the loss of social cohesion, either due to the leadership or the masses, and the subsequent invasion/replacement by an outside force.

After archeology developed as a scientific field, the explanations based on class conflicts gained new popularity. The first systematic study aimed at a comprehensive review and integration of historical knowledge on societal development and collapse was likely Toynbee's "A study of history" (Toynbee, 1961). Volumes IV-VI of (Toynbee, 1961) cover the "breakdown" and "disintegration" of civilisations. Toynbee (1961) does not consider environmental degradation or external invading forces as a root cause of the breakdown of a society. Rather, he argues the mechanism behind the collapse is internal to the society and develops a theory of how this unfolds: a "creative minority" is responsible for problem-solving within a society that leads to its growth and development, but eventually it ceases to be innovative, at which point it turns into a "dominant minority" which simply imposes rules and forces the majority into obedience. The majority is called the "proletariat" and further divided into internal and external categories. The internal proletariat is under direct subjugation of the dominant minority, whereas the external one is left in poverty and disorganised. This state of affairs creates a tension

that eventually leads to the disintegration of the social order. Toynbee (1961) applies the above theory to an extensive set of examples, including the Roman Empire, the Maya civilisation and Old Egyptian Kingdom.

Recent applications of the class conflict hypothesis include Easter Island (Pakandam, 2009) and the Maya (Hamblin and Pitcher, 1980; Chase and Chase, 2005). The main difficulty with theories of internal conflict and elite mismanagement is that these type of tensions and inefficiencies always exist in societies (Tuchman, 1984; Tainter, 1988). It is questionable that only at a certain point in a society's history did these recurrent themes cause the social structure to breakdown completely.

Another theory of collapse considers societies to be vulnerable and incapable of adaptation so, they cannot provide adequate and sufficient responses to their challenges and circumstances, e.g., the Aztec and Inca Empires (Conrad and Demarest, 1984). If a society could not find and implement effective solutions to its problems, what prevented it from doing so? While these type of theories postulate the natural implication that if a society is not able to respond adequately to problems it will collapse, they do not account for the state of fragility.

As seen above, most common theories of societal collapse either focus on factors that are not internal to the society in question, or in case the causes are intrinsic to the society, they refer to social conditions that have been characteristic to the society since its formation. Tainter (1988) proposes a theory that surpasses these difficulties, building upon the idea of diminishing returns to investments in problem solving. This is best exemplified by the Roman Empire (Tainter, 1988), whose early conquests were very profitable and allowed for the elimination of taxes for the citizens. With the expanding territory, the military and administrative costs grew as well. At a certain point, further conquests/conflicts proved less beneficial and even amounted to a loss of resources, like the wars with the German tribes. Maintenance of the empire ended up having larger costs then revenue, and territory was gradually lost. The Roman currency, the denarius was being debased to expand the money supply and cover the costs (at least temporarily) (Tainter, 2000). Throughout a period of 400 years these negative returns manifested as a collapse. Similar arguments have been forwarded regarding the Ottoman Empire (Lewis, 1958), the Chinese dynastic cycle (Lattimore, 1940), as well as the Maya (Culbert, 1991).

More generally, as was the case with the Roman Empire, the maintenance of a complex socio-political system requires resources and energy in various forms. Each new problem leads to an increase in the system's complexity due to the new institutions, more people and difference specialisations required to implement a solution. The increased complexity carries additional energy costs. The previously existing structures are not radically reformed but are expanded to incorporate new functionality or additional ones are created. So, the complexity tends to add in time and hence, also the costs of its maintenance. Furthermore, the benefits incurred in this enterprise suffer from the law of

diminishing returns (Tainter, 1996). As such, "investment in socio-political complexity as a problem-solving response reaches a point of declining marginal returns." (Tainter, 1988, p. 118). We see in Tainter's argument, besides the explanation of collapse, also a justification of why societies grow complex in the first place, namely to solve the problems they encounter.

At an advanced stage of socio-political growth, a society uses up most of its energy to maintain all the previously implemented solutions and has very low returns on solving new problems. Thus, it becomes increasingly sensitive and incapable to tackle internal or external threats and perturbations. In these conditions, collapse is a likely outcome irrespective of specific factors or circumstances.

We can see early seeds of the above argument in the work of Malthus (1798), who points out that population grows in exponential fashion, whereas agricultural production can only grow linearly. Eventually, the mismatch will cause population levels to return to sustainable levels. With increasing population density, the chances of wars breaking out increases, diseases are more easily transmitted, food becomes scarce and general livelihood become harsher which makes the bearing and raising of children more difficult. From the economic viewpoint, we can interpret this as saying that the costs of sustaining the population are growing faster than the capacity to sustain them.

With the industrial revolution, it became increasingly clear that technology could help eliminate, or at least delay the negative population pressure Malthus hypothesised. Eventually, an alternative theory appeared with the work of E. Boserup's "The Conditions of Agricultural Growth: The economics of agrarian change under population pressure" (Boserup, 1965) which argued that under conditions of rapid population growth and low land productivity, new, more intensive agricultural technology would be developed to provide sufficient food. Behind Boserup's thesis is the old tenet that "necessity is the mother of all invention." For example, the Maya civilization employed intensive agricultural practices (field raising, terrace forming etc.) and better irrigation and water management systems (e.g. building reservoirs) to cope with rainfall variability (including droughts) and their growing population (Turner, 1974).

The theories of Malthus and Boserup operate at different time-scales. When conventional farming methods prove insufficient, the short-term response is likely a diversification and intensification of agricultural practice to compensate any likely short-fall in production. But, as the Maya example shows, on much longer time scales, the (ultimately) finite carrying capacity of the environment would constrain population growth (assuming all other factors unchanged). Despite challenging Malthus (1798) by arguing that productivity per unit of land increases under intensification, Boserup (1965) argues that productivity per unit of labour actually decreases. Through factors such as preparation, fertilization and irrigation, human labour per unit of agricultural output increases but continues to be undertaken due to the growing population size. The work

of Boserup (1965) received quantitative support through the data compiled by Clark and Haswell (1966) and Wilkinson (1979), who show that the average and marginal return on agriculture does indeed decline with increasing labour.

Tainter (1988) generalises Boserup's observation to all problem solving endeavours, not just procurement of food. In particular, Tainter argues the same trend holds for technical innovation, e.g., to reach the same number of patent applications in 1958 as in 1946 the US required twice as many scientists and engineers, and three time as much investment then 12 years before (Machhup, 1962). Similar trends continue till today (Tainter and Patzek, 2011), e.g., Eroom's law in pharmaceutical discoveries that shows a decrease in R & D efficiency by a factor of 100 since 1950 to 2010 (Scannell et al., 2012).

Despite its strengths and empirical support, Tainter's theory does have a significant shortcoming that it does not precisely define what constitutes a societal problem. Also, the exact variables that indicate diminishing returns in human activity are not specified completely, but requires case by case checking for each society under study.

Appendix B

Easter Island model analysis

In the following we analyse system (2.1) by identifying the equilibrium points, discussing their stability and determining the critical transitions (bifurcations) of (2.1) under variations of the extraction rate of natural resources, namely the α parameter.

By equating the rates of change of the variables to 0, we find that the fixed points of the system (2.1) are given by:

1. The origin $O = (0, 0, 0)$.
2. The state with no human population and maximum amount of natural resources $N = (0, K, 0)$.
3. An interior equilibrium point $E = (x_e, y_e, z_e)$ where:

$$\begin{aligned} x_e &= \frac{r}{\alpha}\left(1 - \frac{y_e}{K}\right) \\ y_e &= \frac{1}{\alpha}\left(s\left(1 - \frac{b}{d}\right) + \rho c \log\frac{d}{b}\right) \\ z_e &= \rho x_e \log\frac{d}{b} \end{aligned} \tag{B.1}$$

Similar to the analysis by Motesharrei et al. (2014), we define an extraction rate at which $y_e = K$ which we call $\alpha_\star = (s(1 - b/d) + \rho c \log d/b)/K$. This value can be seen as a characteristic extraction rate for system (2.1) and sets a reference level for other values of the extraction rate. As such, we quote extraction rates by their relative value with respect to $\alpha_\star$.

To assess the stability of the fixed points of system (2.1), we look at the Jacobians which are given by:

1. At the origin O:

$$J_O = \begin{bmatrix} b-d & 0 & 0 \\ 0 & r & 0 \\ 0 & 0 & -c \end{bmatrix} \tag{B.2}$$

2. At the fixed point N:

$$J_N = \begin{bmatrix} b-d & 0 & 0 \\ -K\alpha & -r & 0 \\ K\alpha & 0 & -c \end{bmatrix} \tag{B.3}$$

3. At the interior equilibrium E:

$$J_E = \begin{bmatrix} -b\log\dfrac{d}{b} & 0 & \dfrac{b}{\rho} \\ -K\alpha_\star & -r\dfrac{\alpha_\star}{\alpha} & 0 \\ \dfrac{bs+cd\rho}{d}\log\dfrac{d}{b} & r-r\dfrac{\alpha_\star}{\alpha} & -c-\dfrac{bs}{d\rho} \end{bmatrix} \tag{B.4}$$

Thus, we can see that the origin O is a saddle node, while the state with maximum natural resources N is an attractive node. As we see in the bifurcation diagram shown in Fig. 2.2, the stability of E depends on the value of the relative extraction rate $\alpha/\alpha_\star$. Specifically, when varying α, we encounter three bifurcations:

(a) A transcritical bifurcation when $\alpha = \alpha_\star$. The fixed points E and N cross and E changes stability from a saddle node to an attractive one. No positive population exists for $\alpha < \alpha_\star$.

(b) A supercritical Hopf bifurcation at α_c which is given by:

$$\alpha_c = \frac{B+\sqrt{B^2+4AC}}{2A}\alpha_\star \tag{B.5}$$

where

$$\begin{aligned} A &= bdr\rho\left(ds - bs + cd\rho\log\frac{d}{b}\right) \\ B &= bdrs\rho(2c+d) + c^2d^2r\rho^2 + b^2rs(s-d\rho) \\ &\quad + bdr\rho(2bs+3cd\rho)\log\frac{d}{b} + b^2d^2r\rho^2\log^2\frac{d}{b} \\ C &= dr^2\rho\left(bs + cd\rho + bd\rho\log\frac{d}{b}\right). \end{aligned} \tag{B.6}$$

At the critical transition the fixed point E loses stability and a limit cycle is formed. The expression for α_c in (B.5) was obtained by applying the Routh-Hurwitz stability criterion to the characteristic polynomial of J_E in (3).

(c) A global heteroclinic bifurcation at a large extraction rate we call α_h. At this point the limit cycle and the N point intersect, which leads to the disappearance of the limit cycle and the formation of a heteroclinic orbit.

The term z/x in model (2.1) has a singularity at $x = 0$, but the fastest decrease the population variable x can exhibit is an exponential decay with rate $b - d$, meaning that if $x(0) > 0$ then for any finite time $x(t) > 0$. Numerically, the ratio z/x is regularised by adding a small positive quantity to the population, i.e., $x \to x + \epsilon$ where $\epsilon = 10^{-10}$. The system (2.1) was solved using a 4th order Runge-Kutta method.

Appendix C

Equilibria for diffusive coupled system

We can identify as fixed points of (2.6) the origin O, the state with maximum resources and an interior equilibrium point, which we denote E. We can estimate the bifurcation boundary by approximating the point E. Let $\boldsymbol{v} = (x_1, y_1, z_1, x_2, y_2, z_2)$ be the vector of state variables of (2.6), which we can then rewrite $\dot{\boldsymbol{v}} = \boldsymbol{f}(\boldsymbol{v})$. To compute the approximate equilibrium values, let $\boldsymbol{v}_0$ be the equilibrium when $\alpha_1 = \alpha_2$. We can expand $\boldsymbol{f}$ around $\boldsymbol{v}_0$:

$$\boldsymbol{f}(\boldsymbol{v}) = \boldsymbol{f}(\boldsymbol{v}_0) + (\boldsymbol{v} - \boldsymbol{v}_0)\boldsymbol{D}\boldsymbol{f}(\boldsymbol{v}_0) + \text{h.o.t.}$$

where $\boldsymbol{D}\boldsymbol{f}(\boldsymbol{v_0})$ is the Jacobian evaluated at $\boldsymbol{v_0}$. If we solve $\boldsymbol{f}(\boldsymbol{v}_0) + \boldsymbol{v}_1\boldsymbol{D}\boldsymbol{f}(\boldsymbol{v}_0) = 0$ for $\boldsymbol{v}_1$ then $\boldsymbol{v}_0 + \boldsymbol{v}_1$ is an $O(\Delta\alpha^2)$ approximation of the interior fixed point for the coupled system. The equilibrium populations for the uncoupled and coupled regime (obtained both analytically and numerically) are shown in Fig. B.1. By computing the eigenvalues of the Jacobian at $\boldsymbol{v}_0 + \boldsymbol{v}_1$ we can determine the bifurcation boundary for the system (2.6). The results are shown in the gray dotted curves of Figs. 2.4(a)- 2.4(d).

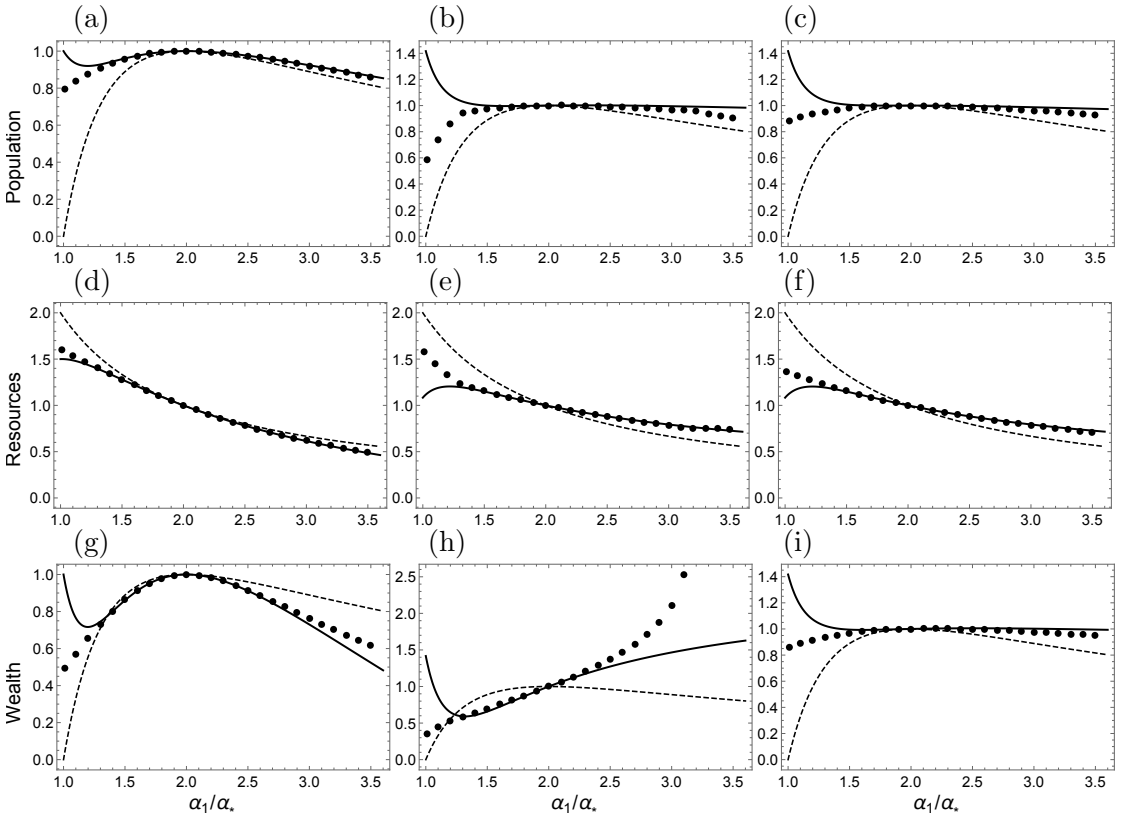

Figure B.1: Population, resource and wealth values at the stable, interior fixed point for society 1 when uncoupled (dashed line), or coupled via: migration alone (a), (d), (g), $(\sigma_x, \sigma_y, \sigma_z) = (0.1, 0, 0)$; migration and resource diffusion (b), (e), (h), $(\sigma_x, \sigma_y, \sigma_z) = (0.1, 0.01, 0)$; migration with wealth and resource diffusion (c), (f), (i), $(\sigma_x, \sigma_y, \sigma_z) = (0.1, 0.01, 0.1)$. In all cases we see a reasonable match between analytic (solid lines) and numerical results (dots). The results are quoted with respect to the equilibrium values for an isolated society with extraction rate $2\alpha_\star$, which is taken as a reference.

Appendix D

Analysis of critical transitions

Fig. D.1 shows the minimum and maximum population values that the Maya model (3.1) predicts in the long term. In Fig. D.1(a) we see that above a certain productivity the of intensive agriculture the system (3.1) shows a Hopf bifurcation. In Fig. D.1(b) a similar pattern is seen with respect to the fraction of people p_i working in intensive agriculture. In both case only the higher values for α and p_i are compatible with the archaeological record. To gain analytic insight into system (3.1) we first simplify it by considering only one specialisation x for the population who extract resources y at a relativity productivity α:

$$\begin{aligned} \dot{x} &= \beta(n - n^{-\delta})x \\ \dot{y} &= ry(1 - y/(wK)) - sdnx \end{aligned} \tag{D.1}$$

where n is the normalised food per capita:

$$n = w\alpha(1 - e^{-y/(wcK)}) \tag{D.2}$$

The equations (D.1) have two fixed points. One fixed point N is given by $(0, wK)$ and the other fixed point E is:

$$\begin{aligned} x_e &= ry_e(1 - y_e/(wK))/(sd) \\ y_e &= wcK \log\left(1 - \frac{1}{w\alpha}\right)^{-1} \end{aligned} \tag{D.3}$$

We denote the Jacobian at the fixed points by J_N and J_E. By applying the Routh-Hurwitz stability criterion to the characteristic polynomial of J_E we find that the fixed E changes from a stable spiral to an unstable one when the relative productivity α

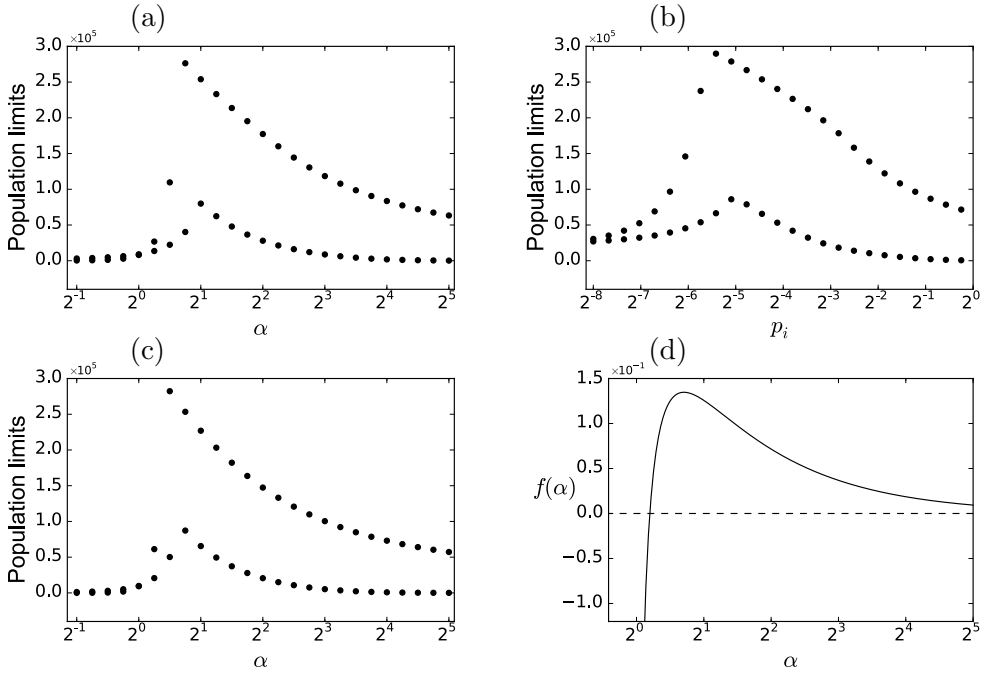

Figure D.1: Minimum and maximum values of the total population for the Maya model (3.1) when we vary (a) the relativity productivity α and (b) the fraction of people p_i that work in intensive agriculture. (c) is analogous to (a) but for the simplified system (D.1). (d) shows the point where $f(\alpha) = 0$ and the bifurcation in (c) occurs. When varying a parameter all other parameters are fixed at their standard value from Table 3.1.

exceeds the value given by:

$$f(\alpha) = 1 + \log\left(1 - \frac{\alpha}{w\alpha}\right)\left(-1 + 2c + w\alpha + c(w\alpha - 1)\log\left(1 - \frac{1}{w\alpha}\right)\right) = 0 \qquad \text{(D.4)}$$

In Fig. D.1(c) we see the maximum and minimum population determined by (D.1). In Fig. D.1(d) the plot of the function $f(\alpha)$ defined in (D.4) is shown. In Fig. D.1(c) the bifurcation of the simplified system (D.1) occurs when $\alpha_c = 1.15$, which is also when $f(\alpha) = 0$, as Fig. D.1(d) shows.

In addition to the main model considered in the paper, we have also analysed how a different formulation of monument construction. The following equation implements a minimum threshold of workers required for efficient monument building and describes the simplest form of increasing returns to scale:

$$\dot{z} = bx_b\theta_{build}(x_b) - mz \qquad \text{(D.5)}$$

where

$$\theta_{build}(x_b) = \frac{1}{1 + \exp 2k_{build}(x_{build} - x_b)} \qquad \text{(D.6)}$$

and x_{build} is the workforce threshold for monument construction to become efficient. We consider that a realistic range for x_{build} is between 100 and 500 people. We find that as long as k_{build} is large enough (above 5), then the value of x_{build} does not change the output significantly and the the consistency with the archaeological record is largely maintained, similar to Fig. 3.3(a).

Appendix E

Parameter sensitivity analysis

We refer to the model with the standard parameter values in Table 3.1 as the standard model and label quantities (parameters, population etc.) in this model with a 0 subscript. Let x_0 be the total population in the standard model. In Figs. E.1 (a)-(f) and E.2 (a)-(d) we vary all the key parameters in the model by a factor of 2 below and above the standard values from Table 3.1, and plot the two distance functions for the population level and building rate.

In Fig. E.1(a)-(f) the population and environmental parameters are varied. We see that the minimum value for the population distance is $D(x_0, x_{ref}) \simeq 10\%$, while for the building rate the distance is $\simeq 15\%$. Both minima are achieved by the standard parameter values. When varying the parameters related to monument building in Fig. E.2(a)-(d), we see that total population level is largely left unchanged. For the building rate, the minimum is achieved by the standard values. The deviation from the minimum is gradual in all cases, and so there is no sudden change in model behaviour under a change in parameter values.

Figs. E.1(a)-(f) and E.2(a)-(d) allows to conclude that standard model simultaneously minimises the distances from both reference modes with respect to all the key parameters. The standard values of parameters r, w_t, d, α, s, m were chosen to be aligned as much as possible with the literature. Hence, the model achieves a local minimum with values consistent with the literature (where available). This increases our confidence in the model's validity. Why define the distance function (3.3) with respect to the population levels and not the birth rates? The reference mode for the crude growth rate is discontinuous and likely less accurate than the total population levels. In case of the monuments, the building rate is sufficiently smooth and well known to define a distance function.

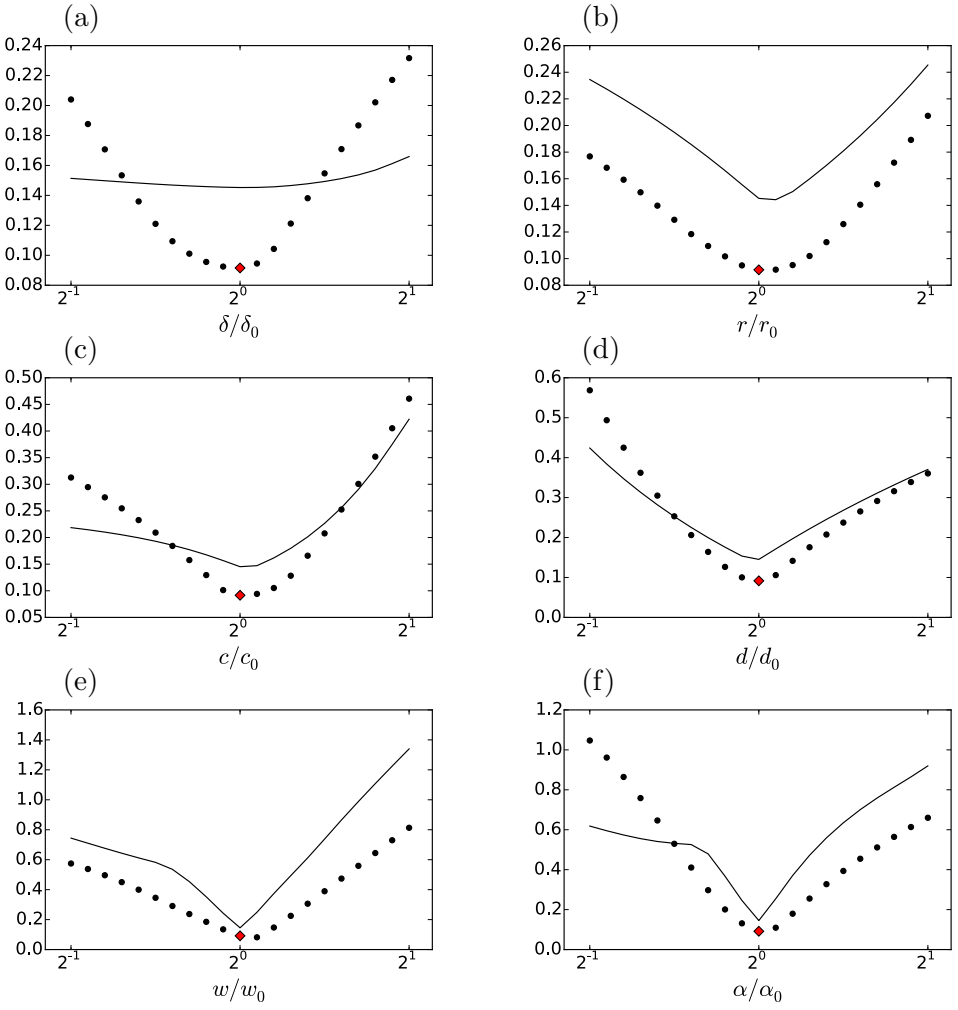

Figure E.1: Sensitivity analysis performed by varying the key population and environment parameters of the model with respect to the standard values (labeled with a 0 subscript) and measuring the distance by the formula (3.3) of the total population from the reference mode (dotted line). Also plotted is the distance of the building rate predicted by the model to the corresponding reference mode (solid line). The minimum distance from the reference mode (indicated by the red diamond for the population) is achieved by the standard value of the parameters from Table 3.1. The parameter axis is logarithmic in base 2. In analysing changes in water availability, see subfigure (e), we considered only constant functions $w_t = w$ throughout the entire time range.

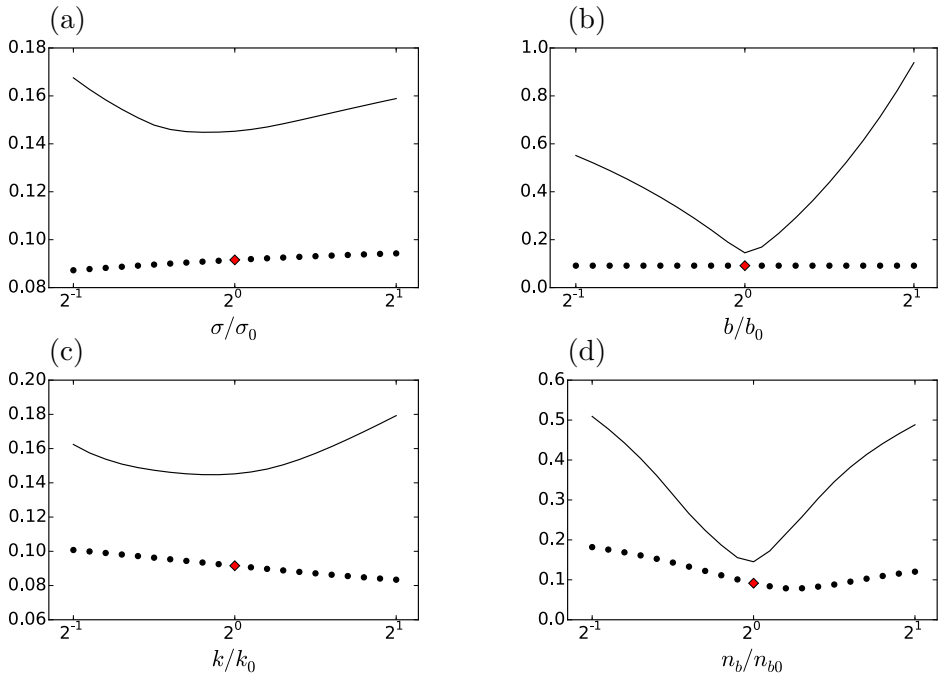

Figure E.2: Sensitivity analysis performed by varying the key monument related parameters of the model with respect to the standard values (labeled with a 0 subscript) and measuring the distance by the formula (3.3) of the total population from the reference mode. Also plotted is the distance of the building rate predicted by the model to the corresponding reference mode (solid line). The parameter axis is logarithmic in base 2.

References

Acuna-Soto, R., Stahle, D. W., Therrell, M. D., Chavez, S. G., and Cleaveland, M. K. (2005). Drought, epidemic disease, and the fall of classic period cultures in Mesoamerica (ad 750950). Hemorrhagic fevers as a cause of massive population loss. *Medical hypotheses*, 65(2):405–409.

Aimers, J. and Hodell, D. (2011). Societal collapse: Drought and the Maya. *Nature*, 479(7371):44–45.

Aimers, J. J. (2007). What Maya collapse? Terminal classic variation in the Maya lowlands. *Journal of archaeological research*, 15(4):329–377.

Alcamo, J., Leemans, R., and Kreileman, E. (1998). *Global change scenarios of the 21st century: Results from the IMAGE 2.1 model*. Elsevier.

Allahverdyan, A. and Galstyan, A. (2016). Emergence of leadership in communication. *PloS one*, 11(8):e0159301.

Anderies, J. M. (1998). Culture and human agro-ecosystem dynamics: the Tsembaga of New Guinea. *Journal of theoretical biology*, 192(4):515–530.

Anderies, J. M. (2000). On modeling human behavior and institutions in simple ecological economic systems. *Ecological Economics*, 35(3):393–412.

Anderies, J. M. (2003). Economic development, demographics, and renewable resources: a dynamical systems approach. *Environment and Development Economics*, 8(2):219–246.

Anderies, J. M. and Hegmon, M. (2011). Robustness and resilience across scales: migration and resource degradation in the prehistoric us southwest. *Ecology and Society*, 16(2):22. URL: http://www.ecologyandsociety.org/vol16/iss2/art22/.

Anghel, M., Toroczkai, Z., Bassler, K., and Korniss, G. (2004). Competition-driven network dynamics: Emergence of a scale-free leadership structure and collective efficiency. *Physical review letters*, 92(5):058701.

Anselmetti, F., Hodell, D., Ariztegui, D., Brenner, M., and Rosenmeier, M. (2007). Quantification of soil erosion rates related to ancient Maya deforestation. *Geology*, 35(10):915–918.

Axelrod, R. and Hamilton, W. D. (1981). The Evolution of Cooperation. *Science*, 211:1390–1396.

Axtell, R. L., Epstein, J. M., Dean, J. S., Gumerman, G. J., Swedlund, A. C., Harburger, J., Chakravarty, S., Hammond, R., Parker, J., and Parker, M. (2002). Population growth and collapse in a multiagent model of the Kayenta Anasazi in Long House Valley. *Proceedings of the National Academy of Sciences of the United States of America*, 99 Suppl 3:7275–7279.

Bahn, P. G. and Flenley, J. (1992). *Easter Island, Earth island*. Thames and Hudson, London, UK.

Barabási, A. and Albert, R. (1999). Emergence of scaling in random networks. *Science*, 286(5439):509–512.

Barceló, J. and Del Castillo, F., editors (2016). *Simulating Prehistoric and Ancient Worlds*. Springer International Publishing, Cham, Switzerland.

Bardi, U. (2011). *The Limits to Growth Revisited*. Springer Science + Business Media, New York, NY.

Barucca, P. and Lillo, F. (2016). Disentangling bipartite and core-periphery structure in financial networks. *Chaos, Solitons & Fractals*, 88:244–253.

Basener, B. and Ross, D. S. (2004). Booming and crashing populations and Easter Island. *SIAM Journal on Applied Mathematics*, 65(2):684–701.

Basener, W., Brooks, B., Radin, M., and Wiandt, T. (2008). Rat instigated human population collapse on Easter Island. *Nonlinear dynamics, psychology, and life sciences*, 12(3):227–240.

Beach, T. and Dunning, N. (2006). Impacts of the ancient Maya on soils and soil erosion in the central Maya Lowlands. *Catena*, 65(2):166–178.

Becker, M. J. (1973). Archaeological evidence for occupational specialization among the Classic period Maya at Tikal, Guatemala. *American Antiquity*, 38(4):396–406.

Bologna, M. and Flores, J. C. (2008). A simple mathematical model of society collapse applied to Easter Island. *Europhysics Letters*, 81:48006.

Borgatti, S. P. and Everett, M. G. (2000). Models of core/periphery structures. *Social networks*, 21(4):375–395.

Boserup, E. (1965). *The conditions of agricultural growth: The economics of agrarian change under population pressure*. Allen and Unwin, Crows Nest, New South Wales.

Boumans, R., Costanza, R., Farley, J., Wilson, M., Portela, R., Rotmans, J., Villa, F., and Grasso, M. (2002). Modeling the dynamics of the integrated earth system and

the value of global ecosystem services using the gumbo model. *Ecological Economics*, 41(3):529–560.

Bourgeois, M. and Friedkin, N. E. (2001). The distant core: social solidarity, social distance and interpersonal ties in coreperiphery structures. *Social networks*, 23(4):245–260.

Boyd, J. P., Fitzgerald, W. J., and Beck, R. J. (2006). Computing core/periphery structures and permutation tests for social relations data. *Social networks*, 28(2):165–178.

Brander, J. A. and Taylor, M. S. (1998). The simple economics of Easter Island: A Ricardo-Malthus model of renewable resource use. *The American Economic Review*, 88(1):119–138.

Brandt, G. and Merico, A. (2015). The slow demise of Easter Island: insights from a modeling investigation. *Frontiers in Ecology and Evolution*, 3(13).

Brede, M. (2010a). Coordinated and uncoordinated optimization of networks. *Physical Review E*, 81(6):066104.

Brede, M. (2010b). Optimal synchronization in space. *Physical Review E*, 81(2):025202.

Briggs, C. J. and Hoopes, M. F. (2004). Stabilizing effects in spatial parasitoid-host and predator-prey models: a review. *Theoretical population biology*, 65(3):299–315.

Bueno, N. P. (2011). A simple system dynamics model for the collapse of complex societies. In *The 29th International Conference of the System Dynamics Society*. The System Dynamics Society, Washington, DC.

Butzer, K. W. and Endfield, G. H. (2012). Critical perspectives on societal collapse. *Proceedings of the National Academy of Science*, 109(10):3628–3631.

Cardell, J., Hitt, C., and Hogan, W. (1997). Market power and strategic interaction in electricity networks. *Resource and energy economics*, 19(1):109–137.

Carleton, W., Campbell, D., and Collard, M. (2014). A reassessment of the impact of drought cycles on the Classic Maya. *Quaternary Science Reviews*, 105:151–161.

Carpenter, R. (1966). *Discontinuity in Greek civilization*. Cambridge University Press, Cambridge, UK.

Carson, R. (1962). *Silent Spring*. Houghton-Mifflin, Boston, MA.

Chakraborty, R. N. (2007). Sharing culture and resource conservation in hunter-gatherer societies. *Oxford economic papers*, 59(1):63–88.

Chase, A. F. and Chase, D. Z. (2005). Contextualizing the collapse: Hegemony and Terminal Classic ceramics from Caracol Belize. In López Varela, S. L. and Foias, A. E., editors, *Geographies of Power: Understanding the Nature of Terminal Classic Pottery in the Maya Lowlands*, pages 73–92. British Archaeological Reports, Oxford, UK.

Chesnais, J. C. (2001). *The demographic transition: Stages, patterns, and economic implications*. Oxford University Press, Oxford, UK.

Choi, S., Gale, D., and Kariv, S. (2012). Social learning in networks: a quantal response equilibrium analysis of experimental data. *Review of Economic Design*, 16(2–3):135–157.

Clark, C. and Haswell, M. (1966). *The Economics of Subsistence Agriculture*. Macmillan, London, UK.

Conrad, G. W. and Demarest, A. A. (1984). *Religion and empire: The dynamics of Aztec and Inca expansionism*. Cambridge University Press, Cambridge, UK.

Corning, P. A. (1998). "the synergism hypothesis": On the concept of synergy and its role in the evolution of complex system. *Journal of Social and Evolutionary Systems*, 21(2):133–172.

Costanza, R., Graumlich, L., Steffen, W., Crumley, C., Dearing, J., Hibbard, K., Leemans, R., Redman, C., and Schimel, D. (2007a). Sustainability or collapse: what can we learn from integrating the history of humans and the rest of nature? *AMBIO: A Journal of the Human Environment*, 36(7):522–527.

Costanza, R., Leemans, R., Boumans, R., and Gaddis, E. (2007b). Integrated global models. In Costanza, R., Graumlich, L., and Steffen, W., editors, *Sustainability or Collapse? An Integrated History and Future of People on Earth*, pages 417–446. MIT Press, Cambridge, MA.

Coyle, G. (2000). Qualitative and quantitative modelling in system dynamics: some research questions. *System Dynamics Review*, 16(3):225–244.

Crooks, A., Castle, C., and Batty, M. (2008). Key challenges in agent-based modelling for geo-spatial simulation. *Computers, Environment and Urban Systems*, 32(6):417–430.

Culbert, T. P. (1991). The collapse of the classic maya civilization. In Yoffee, N. and Cowgill, G. L., editors, *The Collapse of Ancient Civilizations*, pages 69–101. University of Arizona Press, Tucson, AZ.

D'Alessandro, S. (2007). Non-linear dynamics of population and natural resources: The emergence of different patterns of development. *Ecological Economics*, 62(2):473–481.

Dalton, T. R. and Coats, R. M. (2000). Could institutional reform have saved Easter Island? *Journal of Evolutionary Economics*, 10(5):489–505.

Dalton, T. R., Coats, R. M., and Asrabadi, B. R. (2005). Renewable resources, property-rights regimes and endogenous growth. *Ecological Economics*, 52(1):31–41.

de la Croix, D. and Dottori, D. (2008). Easter island's collapse: a tale of a population race. *Journal of Economic Growth*, 13:27–55.

De Mesquita, B. (2006). Game theory, political economy, and the evolving study of war and peace. *American Political Science Review*, 100(4):637–642.

Dean, J. S., Gumerman, G. J., Epstein, J. M., Axtell, R. L., Swedlund, A. C., Parker, M. T., and McCarroll, S. (2000). Understanding anasazi culture change through agent based modeling in dynamics. In Kohler, T. and Gumerman, G., editors, *Human and Primate Societies: Agent Based Modeling of Social and Spatial Processes*. Oxford University Press, New York & London.

Decker, C. S. and Reuveny, R. (2005). Endogenous technological progress and the malthusian trap: could simon and boserup have saved easter island? *Human Ecology*, 33(1):119–140.

Demarest, A. (1992). Ideology in ancient Maya cultural evolution: The dynamics of galactic polities. In Demarest, A. and Conrad, G., editors, *Ideology and pre-Columbian civilizations*, pages 135–157. School of American Research Press, Santa Fe, NM.

Demarest, A., Andrieu, C., Torres, P., Forné, M., Barrientos, T., and Wolf, M. (2014). Economy, Exchange, and Power: New evidence from the Late Classic Maya Port city of Cancuen. *Ancient Mesoamerica*, 25(1):187.

Diamond, J. (2002). Archaeology: Life with the artificial anasazi. *Nature*, 419:567–569.

Diamond, J. (2005). *Collapse: How Societies Choose to Fail or Succeed*. Penguin, London, UK.

Dornan, J. (2004). Beyond belief: religious experience, ritual, and cultural neuro-phenomenology in the interpretation of past religious systems. *Cambridge Archaeological Journal*, 14(01):25–36.

Douglas, P. M., Pagani, M., Canuto, M. A., Brenner, M., Hodell, D. A., Eglinton, T. I., and Curtis, J. H. (2015). Drought, agricultural adaptation, and sociopolitical collapse in the Maya Lowlands. *Proceedings of the National Academy of Sciences*, 112(18):5607–5612.

Dowdle, J. (1987). Road networks and Exchange Systems in the Aeduan Civitas, 300 b.c.-300 a.d. In Crumley, C. and Marquardt, W., editors, *Regional dynamics. Burgundian landscapes in historical perspective*, pages 265–294. Academic Press Inc.

Driessen, J. and Macdonald, C. F. (1997). *The troubled island: Minoan Crete before and after the Santorini eruption*. Aegaeum.

Dunning, N. P. and Beach, T. (2003). Noxious or nurturing nature? Maya civilization in environmental contexts. In Golden, C. and Borgstede, G., editors, *Continuity and change in Maya archaeology*, pages 125–141. Routledge Press, New York, NY.

Dunning, N. P. and Beach, T. (2010). Farms and forests: Spatial and temporal perspectives on ancient Maya landscapes. In *Landscapes and societies*, pages 369–389. Springer, Dordrecht, Netherlands.

Dunning, N. P., Beach, T. P., and Luzzadder-Beach, S. (2012). Kax and kol: Collapse and resilience in lowland Maya civilization. *Proceedings of the National Academy of Sciences*, 109(10):3652–3657.

Eguíluz, V. M., Zimmermann, M. G., Cela-Conde, C. J., and Miguel, M. S. (2005). Cooperation and the emergence of role differentiation in the dynamics of social networks. *American journal of sociology*, 110(4):977–1008.

Enriqueta, A. and Thomas, R. P. (2004). The effect of candidate quality on electoral equilibrium: An experimental study. *The American Political Science Review*, 98(1):77–90.

Epstein, J. M. (2008). Why model? *Journal of Artificial Societies and Social Simulation*, 11(4):12.

Epstein, J. M. and Axtell, R. L. (1996). *Growing Artificial Societies*. Brookings Institution Press MIT Press.

Erickson, E. E. (1973). The Life Cycle of Life Styles: Projecting the Course of Local Evolutionary Sequences. *Behavior Science Notes*, 8:135–160.

Erickson, J. D. and Gowdy, J. M. (2000). Resource use, Institutions, and Sustainability: A Tale of Two Pacific Island Cultures. *Land Economics*, 76(3):345–354.

Estrada-Belli, F. (2010). *The first Maya civilization: ritual and power before the Classic period*. Routledge, London, UK.

Faria, J. R. (2000). What happened to the neanderthals? the survival trap. *Kyklos*, 53(2):161–172.

Flato, G., Marotzke, J., Abiodun, B., Braconnot, P., Chou, S., Collins, W., Cox, P., Driouech, F., Emori, S., Eyring, V., and Forest, C. (2013). Evaluation of climate models. In *Climate Change 2013: The Physical Science Basis. Contribution of Working Group I to the Fifth Assessment Report of the Intergovernmental Panel on Climate Change*, pages 741–866. Cambridge University Press, Cambridge, UK.

Flenley, J. and Bahn, P. G. (2003). *The Enigmas of Easter Island*. Oxford University Press, New York, NY.

Folan, W. and Hyde, B. (1985). Climatic forecasting and recording among the ancient and historic Maya: an ethnohistoric approach to epistemological and paleoclimatological patterning. In Folan, W. J., editor, *Contributions to the Archaeology and Ethnohistory of Greater Mesoamerica*, pages 15–48. Southern Illinois University Press, Carbondale, IL.

Folan, W. J., Faust, B., Lutz, W., and Gunn, J. D. (2000). Social and environmental factors in the Classic Maya collapse. In Lutz, W., Priesto, L., and Sanderson, W., editors, *Population, Development and Environment on the Yucatan Peninsula: From Ancient Maya to 2030*, pages 2–32. International Institute for Applied Systems Analysis, Laxenburg, Austria.

Forest, T. (2007). Maya apocalypse: Warfare-punctuated equilibrium at the limit of growth. In *The 25th International Conference of the System Dynamics Society*. The System Dynamics Society, Boston, MA.

Forest, T. (2013). Maya apocalypse: Varying productivity, consumption, impacts, and results. In *The 31th International Conference of the System Dynamics Society*. The System Dynamics Society, Cambridge, MA.

Forrester, J. W. (1961). *Industrial Dynamics*. M. I. T. Press, Cambridge, MA.

Forrester, J. W. (1971). *World Dynamics*. Wright-Allen Press, Cambridge, MA.

Gailor, O. and Weil, D. N. (2000). Population, technology and growth: from malthusian stagnation to the demographic transition and beyond. *The American Economic Review*, 90:806–828.

Gibbon, E. (1776). *The History of the Decline and Fall of the Roman Empire*. Strahan & Cadell, London, UK.

Gill, R. and Keating, J. (2002). Volcanism and Mesoamerican archaeology. *Ancient Mesoamerica*, 13(01):125–140.

Gill, R., Mayewski, P., Nyberg, J., Haug, G., and Peterson, L. (2007). Drought and the Maya collapse. *Ancient Mesoamerica*, 18(2):283–302.

Goeree, J. K., Holt, C. A., and Palfrey, T. R. (2002). Quantal response equilibrium and overbidding in private-value auctions. *Journal of Economic Theory*, 104(1):247–272.

Goldstone, J. A. (1991). *Revolution and Rebellion in the Early Modern World*. University of California Press, Berkeley, CA.

Gomez, S., Diaz-Guilera, A., Gomez-Gardenes, J., Perez-Vicente, C., Moreno, Y., and Arenas, A. (2013). Diffusion dynamics on multiplex networks. *Physical Review Letters*, 110(2):028701.

Good, D. H. and Reuveny, R. (2006). The fate of easter island: The limits of resource management institutions. *Ecological Economics*, 58(3):473–490.

Good, D. H. and Reuveny, R. (2009). On the collapse of historical civilizations. *American Journal of Agricultural Economics*, 91(4):863–879.

Good, D. H. and Reuveny, R. (2012). Technical progress, foresight, and the collapse of historical societies.

Gross, T. and Blasius, B. (2008). Adaptive coevolutionary networks: a review. *Journal of the Royal Society Interface*, 5(20):259–271.

Gumerman, G. J., Swedlund, A. C., and Epstein, J. M. (2003). The evolution of social behavior in the prehistoric american southwest. *Artificial Life*, 9:435–444.

Guttenberg, N. and Goldenfeld, N. (2010). Emergence of heterogeneity and political organization in information exchange networks. *Physical Review E*, 81(4):046111.

Halsall, G. (2007). *Barbarian migrations and the Roman West, 376-568*. Cambridge University Press, Cambridge, UK.

Hamblin, R. L. and Pitcher, B. L. (1980). The Classic Maya collapse: Testing class conflict hypotheses. *American Antiquity*, pages 246–267.

Hansen, R. D., Bozarth, S., Jacob, J., Wahl, D., and Schreiner, T. (2002). Climatic and environmental variability in the rise of Maya civilization: A preliminary perspective from northern Petén. *Ancient Mesoamerica*, 13(2):273–295.

Harner, M. J. (1970). Population pressure and the social evolution of agriculturalists. *Southwestern Journal of Anthropology*, 26:67–86.

Haug, G. H., Günther, D., Peterson, L. C., Sigman, D. M., Hughen, K. A., and Aeschlimann, B. (2003). Climate and the collapse of Maya civilization. *Science*, 299(5613):1731–1735.

Heckbert, S. (2013). Mayasim: An agent-based model of the ancient Maya social-ecological system. *Journal of Artificial Societies and Social Simulation*, 16(4).

Hodell, D., Brenner, M., and Curtis, J. (2005). Terminal classic drought in the northern Maya lowlands inferred from multiple sediment cores in Lake Chichancanab (Mexico). *Quaternary Science Reviews*, 24(15):1413–1427.

Hodell, D. A., Brenner, M., Curtis, J. H., and Guilderson, T. (2001). Solar forcing of drought frequency in the Maya lowlands. *Science*, 292(5520):1367–1370.

Holme, P. (2005). Core-periphery organization of complex networks. *Physical Review E*, 72(4):046111.

Holme, P. and Ghoshal, G. (2006). Dynamics of networking agents competing for high centrality and low degree. *Physical review letters*, 96(9):098701.

Horan, D. R., Bulte, E., and Shogren, J. F. (2007). How trade saved humanity from biological exclusions: an economic theory of neanderthal extinction. *Journal of Economic Behavior & Organisation*, 58(1):1–29.

Hosler, D., Sabloff, J. A., and Runge, D. (1977). Simulation model development: a case study of the Classic Maya collapse. In Hammond, N., editor, *Social Process in Maya Pre-history*, pages 553–590. Academic Press, London, UK.

Hughes, B. B. (1993). *International futures: choices in the creation of a new world order*. Westview Press, Inc.

Hunt, T. L. (2007). Rethinking easter island's ecological catastrophe. *Journal of Archaeological Science*, 34(3):485–502.

i Cancho, R. and Solé, R. V. (2003). Optimization in complex networks. In Pastor-Satorras, R., Rubi, M., and Diaz-Guilera, A., editors, *Statistical mechanics of complex networks*, pages 114–126. Springer-Verlag, Berlin Heidelberg.

Iannone, G. (2013). *The great Maya droughts in cultural context: Case studies in resilience and vulnerability*. University Press of Colorado, Boulder, CO.

Inomata, T. (2008). *Warfare and the fall of a fortified center: Archaeological investigations at Aguateca*. Vanderbilt University Press, Nashville, TN.

Isbell, W. H. (1978). Environmental perturbations and the origin of the andean state. In Redman, C. L., Berman, M. J., Curtin, E. V., Langhorne, W. T., Versaggi, N. M., and Wanser, J. C., editors, *Social archeology: beyond subsistence and dating*, pages 303–313. Academic Press, New York, NY.

Ito, J. and Kaneko, K. (2001). Spontaneous structure formation in a network of chaotic units with variable connection strengths. *Physical Review Letters*, 88(2):028701.

Ito, J. and Kaneko, K. (2003). Spontaneous structure formation in a network of dynamic elements. *Physical Review E*, 67(4):046226.

Ivanova, S. A. (2010). *Dietary Change in Ribeirinha Women: Evidence of a Nutrition Transition in the Brazilian Amazon?* Ohio State University.

Jansen, V. A. (1995). Regulation of predator-prey systems through spatial interactions: a possible solution to the paradox of enrichment. *Oikos*, 74(3):384–390.

Janssen, M. A. (2009). Understanding artificial anasazi. *Journal of Artificial Societies and Social Simulation*, 12(4):13.

Janssen, M. A. (2010). Population aggregation in ancient arid environments. *Ecology and Society*, 15(2):19.

Janssen, M. A., Kohler, T. A., and Scheffer, M. (2003). Sunk-Cost Effects and Vulnerability to Collapse in Ancient Societies. *Current Anthropology*, 44:722–728.

Janssen, M. A. and Scheffer, M. (2004). Overexploitation of renewable resources by ancient societies and the role of sunk-cost effects. *Ecology and Society*, 9(1).

Johnston, K. J. (2003). The intensification of pre-industrial cereal agriculture in the tropics: Boserup, cultivation lengthening, and the Classic Maya. *Journal of Anthropological Archaeology*, 22(2):126–161.

Kasthurirathna, D., Harré, M., and Piraveenan, M. (2016a). Optimising influence in social networks using bounded rationality models. *Social Network Analysis and Mining*, 6(1):54.

Kasthurirathna, D. and Piraveenan, M. (2015). Emergence of scale-free characteristics in socio-ecological systems with bounded rationality. *Nature Scientific reports*, 5:10448.

Kasthurirathna, D., Piraveenan, M., and Uddin, S. (2016b). Modeling networked systems using the topologically distributed bounded rationality framework. *Complexity*, 21(S2):123–137.

Kennett, D. J., Breitenbach, S. F., Aquino, V. V., Asmerom, Y., Awe, J., Baldini, J. U., Bartlein, P., Culleton, B., Ebert, C., Jazwa, C., and Macri, M. J. (2012). Development and disintegration of Maya political systems in response to climate change. *Science*, 338(6108):788–791.

Khaldun, I. (1377). *Muqaddimah*.

Kianercy, A. and Galstyan, A. (2013). Coevolutionary networks of reinforcement-learning agents. *Physical Review E*, 88(1):012815.

Kirk, D. (1996). Demographic transition theory. *Population studies*, 50(3):361–387.

Kohler, T. A. and van der Leeuw, S. A., editors (2007). *The model-based archaeology of socionatural systems*. School for Advanced Research Press, Santa Fe, New Mexico, USA.

Kuil, L., Carr, G., Viglione, A., Prskawetz, A., and Blöschl, G. (2016). Conceptualizing socio-hydrological drought processes: The case of the Maya collapse. *Water Resources Research*, 52(8):6222–6242.

Kuznets, S. (1955). Economic growth and income inequality. *The American Economic Review*, 45(1):1–28.

Lancee, B. and Van de Werfhorst, H. G. (2012). Income inequality and participation: A comparison of 24 european countries. *Social Science Research*, 41(5):1166–1178.

Landry, A. (1934). *La révolution démographique: études et essais sur les problèmes de la population*. Sirey, Paris, France.

Lanning, E. P. (1967). *Peru Before the Incas*. Prentice-Hall, Upper Saddle River, NJ.

Lattimore, O. (1940). *Inner Asian Frontiers of China*. Beacon Press, Boston, MA.

Layte, R. and Whelan, C. (2014). Who feels inferior? a test of the status anxiety hypothesis of social inequalities in health. *European Sociological Review*, 30:525–535.

Levin, S. A. (1974). Dispersion and population interactions. *American Naturalist*, 108(960):207–228.

Lewis, B. (1958). Some reflections on the decline of the ottoman empire. *Studia islamica*, 9:111–127.

Lewis, B. (2006). Ibn khaldun in turkey. In *Ibn Khaldun: The Mediterranean in the 14th Century: Rise and Fall of Empires*, pages 376–380. Foundation El Legado Andalus.

Li, L., Alderson, D., Doyle, J. C., and Willinger, W. (2005). Towards a theory of scale-free graphs: Definition, properties, and implications. *Internet Mathematics*, 2(4):431–523.

Lipowski, A., Lipowska, D., and Ferreira, A. (2014). Emergence of social structures via preferential selection. *Physical Review E*, 90(3):032817.

Lowe, J. W. (1982). On mathematical models of the Classic Maya collapse: The class conflict hypothesis reexamined. *American Antiquity*, pages 643–652.

Luce, R. (2005). *Individual choice behavior: A theoretical analysis*. Dover, Mineola, NY.

Lucero, L. J. (1999). Classic lowland Maya political organization: A review. *Journal of World Prehistory*, 13(2):211–263.

Lucero, L. J., Gunn, J. D., and Scarborough, V. L. (2011). Climate change and Classic Maya water management. *Water*, 3(2):479–494.

Lux, T. (2015). Emergence of a core-periphery structure in a simple dynamic model of the interbank market. *Journal of Economic Dynamics and Control*, 52:A11–A23.

Luzzadder-Beach, S., Beach, T., and Dunning, N. (2012). Wetland fields as mirrors of drought and the Maya abandonment. *Proceedings of the National Academy of Sciences*, 109(10):3646–3651.

M., B. and J., D. V. B. (2013). The energy transition in a climate-constrained world: Regional vs. global optimization. *Environmental modelling & software*, 44:44–61.

Machhup, F. (1962). *The Production and Distribution of Knowledge in the United States*. Princeton University Press, Cambridge, MA.

Mahault, B., Saxena, A., and Nisoli, C. (2017). Emergent inequality and self-organized social classes in a network of power and frustration. *PloS one*, 12(2):e0171832.

Malthus, T. R. (1798). *An Essay on the Principle of Population as it Affects the Future Improvement of Society, with Remarks on the Speculations of Mr. Godwin, M. Condorcet, and Other Writers*. Johnson, London, UK.

Manning, P. and Trimmer, T. (2013). *Migration in world history*. Routledge, London, UK.

Marinatos, S. (1939). The volcanic destruction of Minoan Crete. *Antiquity*, 13(52):425–439.

Martin, S. and Grube, N. (1995). Maya superstates. *Archaeology*, 48(6):41–46.

Maxwell, J. W. and Reuveny, R. (2000). Resource scarcity and conflict in developing countries. *Journal of Peace Research*, 37(3):301–322.

Maxwell, J. W. and Reuveny, R. (2005). Continuing conflict. *Journal of Economic Behavior & Organisation*, 58(1):30–52.

McKelvey, R. D. and Palfrey, T. R. (1995). Quantal response equilibria for normal form games. *Game. Econ. Behav.*, 10(1):6–38.

McKelvey, R. D. and Patty, J. W. (2006). A theory of voting in large elections. *Games and Economic Behavior*, 57(1):155–180.

McKillop, H. (1996). Ancient maya trading ports and the integration of long-distance and regional economies: Wild cane cay in south-coastal belize. *Ancient Mesoamerica*, 7(1):49–62.

McNeil, C., Burney, D., and Burney, L. (2010). Evidence disputing deforestation as the cause for the collapse of the ancient Maya polity of Copan, Honduras. *Proceedings of the National Academy of Sciences*, 107(3):1017–1022.

Meadows, D., Randers, J., and Meadows, D. (2004). *Limits to growth: the 30-year update*. Chelsea Green Publishing, White River Junction, VT.

Meadows, D. H., Meadows, D. L., Randers, J., and Behrens, W. W. (1972). *The Limits to Growth*. Universe Books, New York, NY.

Medina-Elizalde, M., Burns, S., Lea, D., Asmerom, Y., von Gunten, L., Polyak, V., Vuille, M., and Karmalkar, A. (2010). High resolution stalagmite climate record from the Yucatán Peninsula spanning the Maya terminal classic period. *Earth and Planetary Science Letters*, 298(1):255–262.

Medina-Elizalde, M. and Rohling, E. J. (2012). Collapse of Classic Maya civilization related to modest reduction in precipitation. *Science*, 335(6071):956–959.

Mesarovic, M. and Pestel, E. (1974). *Mankind at the Turning Point: The Second Report to the Club of Rome*. Dutton, New York.

Moss, S. (2008). Alternative Approaches to the Empirical Validation of Agent-Based Models. *Journal of Artificial Societies and Social Simulation*, 11(1).

Motesharrei, S., Rivas, J., and Kalnay, E. (2014). Human and nature dynamics (HANDY): Modeling inequality and use of resources in the collapse or sustainability of societies. *Ecological Economics*, 101:90–102.

Murdoch, W. W., Briggs, C. J., Nisbet, R. M., Gurney, W. S., and Stewart-Oaten, A. (1992). Aggregation and stability in metapopulation models. *American Naturalist*, 140(1):41–58.

Murdoch, W. W. and Oaten, A. (1975). Predation and population stability. *Advances in ecological research*, 9:1–131.

Nagase, Y. and Mirza, T. (2006). Substitutability of resource use in production and consumption. In *Conference Proceedings, 3rd World Congress of Environmental and Resource Economics*.

Nagase, Y. and Uehara, T. (2011). Evolution of population-resource dynamics models. *Ecological Economics*, 72:9–17.

Nash, J. F. (1950). Equilibrium points in n-person games. *Proc. Natl. Acad. Sci.*, 36(1):48–49.

Nell, E. and Errouaki, K. (2013). *Rational econometric man: transforming structural econometrics*. Edward Elgar, Cheltenham, UK.

Neurath, P. (1994). *From Malthus to the Club of Rome and back: Problems of Limits to Growth, Population control, and Migrations*. M. E. Sharpe, Armonk, NY.

Nigh, R. and Diemont, S. (2013). The Maya milpa: fire and the legacy of living soil. *Frontiers in Ecology and the Environment*, 11(s1):e45e54.

Nisbet, R. M., Briggs, C. J., Gurney, W. S., Murdoch, W. W., and Stewart-Oaten, A. (1992). Two-patch metapopulation dynamics. In Levin, S. A., Steele, S. A., and Powell, J. H., editors, *Patch Dynamics in Terrestrial, Freshwater, and Marine Ecosystems*. Springer-Verlag, Berlin Heidelberg.

Nowak, M. and Sigmund, K. (2004). Evolutionary dynamics of biological games. *Science*, 303(5659):793–799.

Nowak, M. A. and May, R. M. (1992). Evolutionary games and spatial chaos. *Nature*, 359(6398):826–829.

Ochs, J. (1995). Games with unique, mixed strategy equilibria: An experimental study. *Games and Economic Behavior*, 10(1):202–217.

Oglesby, R., Sever, T., Saturno, W., Erickson, D., and Srikishen, J. (2010). Collapse of the Maya: Could deforestation have contributed? *Journal of Geophysical Research: Atmospheres*, 115(D12).

O'Mansky, M. and Dunning, N. (2004). Settlement and Late Classic political disintegration in the Petexbatun region, Guatemala. In Demarest, A., Rice, P. M., and Rice, D. S., editors, *The Terminal Classic in the Maya lowlands: collapse, transition, and transformation*, pages 83–101. University Press of Colorado, Boulder, CO.

Ozbekhan, H. (1976). The predicament of mankind. In Churchman, C. W. and Mason, R. O., editors, *World Modeling: A Dialogue*, volume 2, pages 11–26. American Elsevier, New York, NY.

Pakandam, B. (2009). Why easter island collapsed: an answer for an enduring question.

Peixoto, T. P. and Bornholdt, S. (2012). Evolution of robust network topologies: Emergence of central backbones. *Physical review letters*, 109(11):118703.

Perc, M., Gómez-Gardeñes, J., Szolnoki, A., Flora, L., and Moreno, Y. (2013). Evolutionary dynamics of group interactions on structured populations: a review. *Journal of The Royal Society Interface*, 10(80).

Perc, M. and Szolnoki, A. (2010). Coevolutionary games-a mini review. *BioSystems*, 99(2):109–125.

Pezzey, J. C. V. and Anderies, J. M. (2003). The effect of subsistence on collapse and institutional adaptation in population-resource societies. *Journal of Development Economics*, 72(1):299–320.

Piketty, T. (2014). *Capital in the Twenty-first Century*. Harvard University Press, Cambridge, MA.

Pikovsky, A., Rosenblum, M., and Kurths, J. (2001). *Synchronization:A universal concept in nonlinear sciences*. Cambridge University Press, Cambridge.

Piperata, B. A., Ivanova, S. A., Dagloria, P., Veiga, G., Polsky, A., Spence, J. E., and Murrieta, R. S. (2011). Nutrition in transition: dietary patterns of rural Amazonian women during a period of economic change. *American Journal of Human Biology*, 23(4):458–469.

Prskawetz, A., Gragnani, A., and Feichtinger, G. (2003). Reconsidering the dynamic interaction of renewable resources and population growth: a focus on long-run sustainability. *Environmental Modeling & Assessment*, 8(1):35–45.

Quirin, G. D., Sethi, S. P., and Todd, J. D. (1977). Market feedbacks and the Limits to Growth. *INFOR: Information Systems and Operational Research*, 15(1):1–21.

Reuveny, R. (2012). Taking stock of malthus: modeling the collapse of historical civilizations. *Annual Review of Resource Economics*, 4(1):303–329.

Reuveny, R. and Decker, C. S. (2000). Easter Island: Historical anecdote or warning for the future? *Ecological Economics*, 35(2):271–287.

Reuveny, R. and Maxwell, J. W. (2001). Conflict and renewable resources. *Journal of Conflict resolution*, 45(6):719–742.

Reuveny, R., Maxwell, J. W., and Davis, J. (2011). On conflict over natural resources. *Ecological Economics*, 70(4):698–712.

Reynolds, C. W. (1987). Flocks, herds and schools: A distributed behavioral model. *ACM SIGGRAPH Computer Graphics*, 21(4):25–34.

Robichaux, H. (2002). On the compatibility of epigraphic, geographic, and archaeological data, with a drought-based explanation for the Classic Maya collapse. *Ancient Mesoamerica*, 13(2):341–345.

Rockström, J., Steffen, W., Noone, K., Persson, A., Chapin, F. S. r., Lambin, E. F., Lenton, T. M., Scheffer, M., Folke, C., Schellnhuber, H. J., Nykvist, B., de Wit, C. A., T., H., van der Leeuw, S., Rodhe, H., Sörlin, S., K., S. P., Costanza, R., Svedin, U., Falkenmark, M., Karlberg, L., W., C. R., J., F. V., Hansen, J., Walker, B., Liverman, D., Richardson, K., Crutzen, P., and Foley, J. A. (2009). A safe operating space for humanity. *Nature*, 461:472–475.

Rogers, B. W., Palfrey, T. R., and Camerer, C. F. (2009). Heterogeneous quantal response equilibrium and cognitive hierarchies. *Journal of Economic Theory*, 144(4):1440–1467.

Roman, S., Bullock, S., and Brede, M. (2017). Coupled societies are more robust against collapse: A hypothetical look at Easter Island. *Ecological Economics*, 132:264–278.

Rombach, M., Porter, M., Fowler, J. H., and Mucha, P. (2014). Core-periphery structure in networks. *SIAM Journal on Applied mathematics*, 74(1):167–190.

Rosenmeier, M., Hodell, D., Brenner, M., Curtis, J., and Guilderson, T. (2002). A 4000-year lacustrine record of environmental change in the southern Maya lowlands, Petén, Guatemala. *Quaternary Research*, 57(2):183–190.

Rotmans, J. (1990). *IMAGE: an integrated model to assess the greenhouse effect*. Springer Science + Business Media, New York, NY.

Rotmans, J. and de Vries, B. (1997). *Perspectives on global change: The TARGETS approach*. Cambridge University Press, Cambridge, UK.

Roussel, E. and André, M. (2013). Quantitative assessment of pre-and post-restoration weathering rates of limestone Mayan temples (Uxmal, Yucatán). *Geografia Fisica e Dinamica Quaternaria*, 36:169–179.

Ruseski, G. and Quinn, J. (2007). Human fertility decisions and common property resources: a dynamic analysis. *Natural Resource Modeling*, 20(3):415–433.

Russell, J. C. (1972). Population in europe. In Cipolla, C. M., editor, *The Fontana Economic History of Europe, Vol. I: The Middle Ages*, pages 25–71. Collins/Fontana, Glasgow, UK.

Russell, W. M. S. (1988). Population, swidden farming and the tropical environment. *Population and Environment*, 10(2):77–94.

Santley, R. S. (1990). Demographic archaeology in the Maya lowlands. In Culbert, T. and Rice, D., editors, *Pre-Columbian population history in the Maya Lowlands*, pages 325–343. University of New Mexico Press, Albuquerque, NM.

Santos, F. C. and Pacheco, J. M. (2005). Scale-free networks provide a unifying framework for the emergence of cooperation. *Phys. Rev. Lett.*, 95(9):098104.

Scannell, J. W., Blanckley, A., Boldon, H., and Warrington, B. (2012). Diagnosing the decline in pharmaceutical r & d efficiency. *Nature reviews Drug discovery*, 11(3):191–200.

Scheffer, M., Carpenter, S., Foley, J. A., Folke, C., and Walkerk, B. (2001). Catastrophic shifts in ecosystems. *Nature*, 413:591–596.

Schelling, T. C. (1971). Dynamic models of segregation. *The Journal of Mathematical Sociology*, 1(2):143–186.

Sharer, R. and Traxler, L. (2006). *The Ancient Maya*. Stanford University Press, Redwood City, CA.

Sharer, R. J. (1977). The Maya collapse revisited. In Hammond, N., editor, *Social Process in Maya Pre-history*. Academic Press, London, UK.

Smith, C. M. (2001). Estimation of a genetically viable population for multigenerational interstellar voyaging: Review and data for project hyperion. *Acta Astronautica*, 97:16–29.

Sterman, J. D. (2000). *Business dynamics: systems thinking and modeling for a complex world*. Irwin/McGraw-Hill, New York, NY.

Stevenson, C. M., Puleston, C. O., Vitousek, P. M., Chadwick, O. A., Haoa, S., and Ladefoged, T. N. (2015). Variation in rapa nui (easter island) land use indicates production and population peaks prior to european contact. *Proceedings of the National Academy of Sciences of the United States of America*, 112(4):1025–1030.

Szabó, G. and Borsos, I. (2016). Evolutionary potential games on lattices. *Physics Reports*, 624:1–60.

Szabó, G. and Fath, G. (2007). Evolutionary games on graphs. *Physics reports*, 446(4):97–216.

Szolnoki, A., Perc, M., and Danku, Z. (2008). Making new connections towards cooperation in the prisoner's dilemma game. *EPL*, 84(5):50007.

Tainter, J. A. (1988). *The Collapse of Complex Societies*. Cambridge University Press, Cambridge, UK.

Tainter, J. A. (1996). Complexity, problem solving, and sustainable societies. In Costanza, R., Segura, O., and Martinez-Alier, J., editors, *Getting down to earth: practical applications of ecological economics*, page 17. Island Press, Washington, DC.

Tainter, J. A. (2000). Problem solving: Complexity, history, sustainability. *Population and Environment*, 22(1):3–41.

Tainter, J. A. (2004). Review of historical dynamics: Why states rise and fall by peter turchin. *Nature*, 427:488–489.

Tainter, J. A. (2006). Archaeology of overshoot and collapse. *Annual Review of Anthropology*, 35:59–74.

Tainter, J. A. (2008). Collapse, sustainability, and the environment: how authors choose to fail or succeed. *Reviews in Anthropology*, 37(4):342–371.

Tainter, J. A. and Patzek, T. W. (2011). *Drilling Down : The Gulf Oil Debacle and Our Energy Dilemma*. Springer Science + Business Media, New York, NY.

Tankersley, K. B., Scarborough, V. L., Dunning, N., Huff, W., Maynard, B., and Gerke, T. L. (2011). Evidence for volcanic ash fall in the Maya lowlands from a reservoir at Tikal, Guatemala. *Journal of Archaeological Science*, 38(11):2925–2938.

Taylor, M. S. (2009). Innis lecture: Environmental crises: past, present, and future. *Canadian Journal of Economics/Revue canadienne d'économique*, 42(4):1240–1275.

Toynbee, A. J. (1961). *A Study of History. In 12 Vols.* Oxford University Press, oxford, UK.

Tuchman, B. (1984). *The March of Folly*. Alfred A. Knopf, New York, NY.

Turchin, P. (2003a). *Complex population dynamics: A Theoretical/Empirical Synthesis*. Princeton University Press, Princeton, NJ.

Turchin, P. (2003b). *Historical dynamics: why states rise and fall*. Princeton University Press, Princeton, NJ.

Turchin, P. (2008). Arise 'cliodynamics'. *Nature*, 454(7200):34–35.

Turchin, P. (2009). Long-term population cycles in human societies. *Annals of the New York Academy of Sciences*, 1162:1–17.

Turchin, P., Currie, T. E., Turner, E. A., and Gavrilets, S. (2013). War, space, and the evolution of Old World complex societies. *Proceedings of the National Academy of Sciences*, 110(41):16384–16389.

Turchin, P. and Nefedov, S. A. (2009). *Secular cycles*. Princeton University Press, Princeton, NJ.

Turner, B. L. (1974). Prehistoric intensive agriculture in the Mayan Lowlands. *Science*, 185:118–124.

Turner, B. L. (1976). Population density in the Classic Maya Lowlands: New evidence for old approaches. *Geographical Review*, 66:73–82.

Turner, B. L. and Sabloff, J. A. (2012). Classic Period collapse of the Central Maya Lowlands: Insights about human–environment relationships for sustainability. *Proceedings of the National Academy of Sciences*, 109(35):13908–13914.

Turner, G. M. (2008). A comparison of The Limits to Growth with 30 years of reality. *Global Environmental Change*, 18(3):397–411.

Turner, G. M. (2012). On the cusp of global collapse? Updated comparison of The Limits to Growth with historical data. *GAIA-Ecological Perspectives for Science and Society*, 21(2):116–124.

Unruh, G. (2000). Understanding carbon lock-in. *Energy policy*, 28(12):817–830.

USDA Survey (June 1962). Soil survey, Kingfisher County, Oklahoma. US Department of Agriculture, Oklahoma Agricultural Experiment Station.

Van der Leeuw, S. and de Vries, B. (2003). Empire: the Romans in the Mediterranean. In de Vries, B. and Goudsblom, J., editors, *Mappae Mundi*, chapter 7, pages 209–256. Amsterdam University Press, Amsterdam, Netherlands.

Vitali, S., Glattfelder, J. B., and Battiston, S. (2011). The network of global corporate control. *PloS one*, 6(10):e25995.

Wahl, D., Byrne, R., Schreiner, T., and Hansen, R. (2007). Palaeolimnological evidence of late-Holocene settlement and abandonment in the Mirador Basin, Petén, Guatemala. *The Holocene*, 17(6):813–820.

Webster, D. L. (2000). The not so peaceful civilization: A review of Maya war. *Journal of World Prehistory*, 14(1):65–119.

Webster, D. L. (2002). *The fall of the ancient Maya: solving the mystery of the Maya collapse*. Thames & Hudson, London, UK.

Webster, J. W., Brook, G. A., Railsback, L. B., Cheng, H., Edwards, R. L., Alexander, C., and Reeder, P. P. (2007). Stalagmite evidence from Belize indicating significant droughts at the time of preclassic abandonment, the Maya hiatus, and the Classic Maya collapse. *Palaeogeography, Palaeoclimatology, Palaeoecology*, 250(1):1–17.

Wilk, R. (1997). *Household ecology: economic change and domestic life among the Kekchi Maya in Belize*. Northern Illinois University Press, DeKalb, IL.

Wilkinson, R. G. (1979). *Poverty and Progress: an Ecological Model of Economic Development*. Methuen, London, UK.

Wilkinson, R. G. (2002). *Unhealthy societies: the afflictions of inequality*. Routledge, London.

Wilkinson, R. G. and Pickett, K. E. (2017). The enemy between us: The psychological and social costs of inequality. *European Journal of Social Psychology*, 47(1):11–24.

Windrum, P., Fagiolo, G., and Moneta, A. (2007). Empirical validation of agent-based models: Alternatives and prospects. *Journal of Artificial Societies and Social Simulation*, 10(2).

Yang, J. and Leskovec, J. (2014). Overlapping communities explain coreperiphery organization of networks. *Proceedings of the IEEE*, 102(12):1892–1902.

Zelnio, R. (2012). Identifying the global core-periphery structure of science. *Scientometrics*, 91(2):601–615.

Zhang, J., Zhang, C., Cao, M., and Chu, T. (2014). Cooperation with potential leaders in evolutionary game study of networking agents. In *Evolutionary Computation*, pages 918–923. IEEE.

Zhang, X., Martin, T., and Newman, M. (2015). Identification of core-periphery structure in networks. *Physical Review E*, 91(3):032803.

Zimmermann, M. G. and Eguíluz, V. M. (2005). Cooperation, social networks, and the emergence of leadership in a prisoners dilemma with adaptive local interactions. *Physical Review E*, 75(5):056118.

Zimmermann, M. G., Eguíluz, V. M., and Miguel, M. S. (2001). Cooperation, adaptation and the emergence of leadership. In Kirman, A. and Zimmermann, J. B., editors, *Economics with heterogeneous interacting agents*, pages 73–86. Springer-Verlag, Berlin Heidelberg.

Zimmermann, M. G., Eguíluz, V. M., and San Miguel, M. (2004). Coevolution of dynamical states and interactions in dynamic networks. *Physical Review E*, 69(6):065102.

Zubrow, E. B. (1971). Carrying capacity and dynamic equilibrium in the prehistoric Southwest. *American Antiquity*, 36(2):127–138.